

University of Alberta

**DENDRITIC CELL-TARGETED NANOPARTICLES FOR THE
DELIVERY OF DNA AND PROTEIN VACCINES**

By

Dharmendra Raghuwanshi

A thesis submitted to the Faculty of Graduate Studies and Research
in partial fulfillment of the requirements for the degree of

DOCTOR OF PHILOSOPHY

in

Pharmaceutical Sciences

Faculty of Pharmacy and Pharmaceutical Sciences

© Dharmendra Raghuwanshi

Fall 2012

Edmonton, Alberta

Permission is hereby granted to the University of Alberta Libraries to reproduce single copies of this thesis and to lend or sell such copies for private, scholarly or scientific research purposes only. Where the thesis is converted to, or otherwise made available in digital form, the University of Alberta will advise potential users of the thesis of these terms.

The author reserves all other publication and other rights in association with the copyright in the thesis and, except as herein before provided, neither the thesis nor any substantial portion thereof may be printed or otherwise reproduced in any material form whatsoever without the author's prior written permission.

Dedication

I dedicate this thesis to my beloved Mother with all my love and respect. Your memories and affection will always be alive in my heart.

ABSTRACT

Dendritic cells (DCs) play a central role in shaping antigen-specific immune response. Antibody-mediated antigen targeting to DC-specific surface receptors is a promising approach to enhance vaccine efficacy. The objective of this thesis was to develop DC-targeted nanoparticulate formulations for the delivery of DNA and protein antigen using a novel strategy. The approach involved use of a two-component DC targeted delivery system for enhanced immune response. One component consisting of a recombinant bifunctional fusion protein (bfFp) was used for DC targeting, whereas, the other component made of biotinylated nanoparticles encapsulated antigen.

For DNA vaccines, two strategies were adapted. In the first strategy, bfFp functionalized biotinylated chitosan nanoparticles containing DNA-encoding for nucleocapsid (N) of severe acute respiratory syndrome coronavirus (SARS-CoV) or hemagglutinin (HA) of avian influenza virus was used for nasal delivery. Immune response studies in mice showed that intranasal administration of targeted formulation along with DC maturation stimuli (anti-CD40 mAb) enhanced magnitude of mucosal, humoral and cellular immune responses.

In the second strategy, a DNA (pDECN) vaccine encoding a fusion protein comprised of SARS CoV N antigen and anti-DEC-205 scFv was constructed. In vitro studies showed that expressed protein was able to bind with DCs. Vaccination of mice with pDECN-loaded chitosan nanoparticles induced significantly higher IgG and cytokine (IFN- γ and IL-2) response relative to SARS

CoV N DNA. Coadministration of anti-CD40 antibody further improved efficacy of nanoencapsulated DNA formulations.

For the delivery of a model antigen ovalbumin (OVA), biotinylated poly(D,L-lactic-*co*-glycolic acid) (PLGA) nanoparticles were formulated using biotin-PEG-PLGA polymer and were decorated with bfFp. In vitro uptake studies revealed one-fold higher uptake of targeted nanoparticles compared to non-targeted NPs. In vivo studies show targeted NPs in conjunction with anti-CD40 mAb enhanced OVA-specific IgG and IgG subclass responses. Splenocytes of these mice secreted significantly higher levels of IFN- γ and IL-2, indicating Th1 response.

In conclusion, these results demonstrate that bfFp based DC targeting is a versatile approach and vaccine efficacy can be enhanced via non-invasive DC targeting. The two-component DC targeting approach can serve as a viable alternative to conventional antibody-targeted vaccines that also precludes any post-formulation modification of the antigen-loaded NPs.

ACKNOWLEDGEMENTS

I wish to extend my sincere gratitude to the following people:

My supervisor Dr. Mavanur R. Suresh, whose expertise and knowledge added considerably to my graduate experience. His enthusiasm in the pursuit of knowledge seeded the curiosity within me and truly inspired me to pursue this work. I wish him good health and happiness.

My supervisor Dr. Kamaljit Kaur, for generously accepting responsibility to supervise me after Dr. Suresh. I am deeply indebted to her for assistance, guidance, and constructive advice. The completion of this thesis would have not been possible without her timely support.

My supervisor late Dr. John Samuel, for accepting me as a graduate student in his lab. He was a great mentor and always willing to walk the extra mile when needed. I salute you from the bottom of my heart for introducing me to the science and immunology.

I would like to extend special thanks to my supervisory committee members, Dr. Hasan Uludağ and Dr. Afsaneh Lavasanifar for continuous guidance, encouragement and constructive suggestions.

I am very thankful to Dr. Michael R. Doschak for encouragement and support during my Ph.D. program and Dr. Carlos A. Velázquez for serving on my defense committee.

I would like to acknowledge Dr. Vivek Mishra, Dr. Dipankar Das, Dr. Welson Wang and Dr. Palani for their kind support and suggestions.

Dr. Darwyn Kobasa, National Microbiology Laboratory, Public Health Agency of Canada, Winnipeg, Canada, for his kind help in avian influenza project and for performing hemagglutination inhibition assays.

A special thanks to all my friends Sai Kiran, Subodh, Jigar, Ballu, Rambabu, Shiv Verma, Advaita, and all members of Suresh's lab for continuous support.

Last but not the least; special thanks to my loving wife, Yogita, for her love, support and continuous encouragement without any complaint or regret, that has enabled me to complete this Ph.D. project.

Special thanks to my father, sisters and brothers, and family members for supporting me by all means, always believing in me and keeping me motivated.

Finally, I would like to thank to the following institutes:

- Canadian Commonwealth Scholarship Programs (CCSP) and Canadian Bureau for International Education (CBIE), for managing my tuition fees and academic expenses.
- The Alberta Glycomics Centre (formerly known as Alberta Ingenuity Centre for Carbohydrate Science, AICCS) for funding me during the last year of my graduation.
- The Faculty of Pharmacy and Pharmaceutical Sciences, University of Alberta, Edmonton, Canada, for accepting me in the graduate studies program and providing me with the facilities, training, and qualification.

TABLE OF CONTENTS

Chapter 1: Introduction	1
1.1 Dendritic cells	2
1.1.1 DC origin and subsets	2
1.1.2 Location in the periphery and lymph nodes	3
1.1.3 DC maturation/activation	5
1.1.4 Antigen processing, presentation and cross-presentation	6
1.1.5 Activation of T cells	7
1.2 Dendritic cell associated receptors	8
1.2.1 DEC-205/CD205 receptor	11
1.2.2 Other DC receptors	15
1.3 Dendritic cell targeting strategies	17
1.3.1 Dendritic cell targeted PLGA nanoparticles	19
1.4 DNA vaccines	22
1.4.1 Strategies to improve DNA vaccines	25
1.4.2 DC targeted DNA delivery	26
1.4.3 Strategies for DNA delivery	28
1.4.4 Chitosan as DNA carrier	28
1.5 Rationale	31
1.6 Hypothesis	33
1.7 Objectives	35
1.8 References	36

CHAPTER 2: Dendritic cell targeted chitosan nanoparticles for nasal DNA immunization against SARS CoV nucleocapsid protein	50
2.1 Introduction	51
2.2 Materials and methods	53
2.2.1 Materials.....	53
2.2.2 Plasmid DNA (pVAXN) construction and detection of SARS-N protein	54
2.2.3 Preparation of biotinylated chitosan and estimation of chitosan modification using fluorescamine assay	55
2.2.4 Formulation of pVAXN loaded biotinylated chitosan NPs	56
2.2.5 Physicochemical characterization of biotinylated chitosan NPs	56
2.2.6 Expression and purification of bfFp and SARS CoV N protein	57
2.2.7 Immunization studies	58
2.2.8 Statistical analysis	61
2.3. Results	61
2.3.1 Construction and expression of pVAXN DNA.....	61
2.3.2 Biotinylation of chitosan and formulation of pVAXN loaded NPs	63
2.3.3 Expression and medium-scale purification of bfFp and N Protein	67
2.3.4 Systemic N protein specific IgG antibody response	68
2.3.5 Mucosal N protein specific antibody response.....	71
2.3.6 Interferon-gamma profile	73
2.4 Discussion	75
2.5 References	78

CHAPTER 3: Dendritic cell targeted chitosan nanoparticles for mucosal and systemic genetic immunization against avian influenza 83

3.1 Introduction	84
3.2 Materials and Methods	86
3.2.1 Materials.....	86
3.2.2 Expression and purification of HA1.....	86
3.2.3 Plasmid DNA, biotinylated chitosan and bfFp.....	87
3.2.4 Formulation and characterization of pCAG α -HA loaded biotinylated chitosan nanoparticles	88
3.2.5 Mice and immunizations	89
3.3 Results	92
3.3.1 Formulation and characterization of chitosan NPs	92
3.3.2 Expression and purification of HA1 in E. coli.....	93
3.3.3 HA-specific systemic IgG response	95
3.3.4 HA-specific mucosal IgA response.....	97
3.3.5 Ex vivo cytokine production	99
3.4 Discussion	101
3.5 References	104

CHAPTER 4: Chitosan nanoparticle encapsulated fusion DNA vaccine for dendritic cell targeted delivery of SARS-coronavirus nucleocapsid protein108

4.1 Introduction	109
4.2 Materials and Methods	111
4.2.1 Materials.....	111
4.2.2 Plasmid DNA constructs and DNA preparation	112
4.2.3 Transfection and expression of antigens	113
4.2.4 In-vitro DC binding studies.....	113

4.2.5 Formulation of DNA loaded chitosan nanoparticles (NPs).....	114
4.2.6 In vitro transfection	115
4.2.7 Animals and immunization	115
4.2.8 Statistical analysis	117
4.3 Results	118
4.3.1 Construction and expression of pDECN DNA vaccine	118
4.3.2 Formulations and characterization of DNA loaded chitosan NPs.....	121
4.3.3 Antibody responses to SARS CoV N protein and fragments.....	124
4.3.4 SARS N protein specific cytokine responses	126
4.4 Discussion	128
4.5 References	131

CHAPTER 5: Ovalbumin encapsulated dendritic cell-targeted PLGA nanoparticles for enhanced immune responses.....	134
5.1 Introduction	135
5.2 Material and Methods.....	136
5.2.1 Materials.....	136
5.2.2 Synthesis of biotin-PEG-PLGA conjugate.....	137
5.2.3 Formulation of nanoparticles	137
5.2.4 Characterization of formulations.....	138
5.2.5 Bone-marrow derived dendritic cell (BMDCs) culture.....	140
5.2.6 BfFp decoration to nanoparticles	140
5.2.7 Uptake of nanoparticles by BMDCs	140
5.2.8 Cytokine secretion and maturation of BMDCs	141
5.2.9 Immunization experiments	142
5.2.10 Evaluation of humoral immune responses	143

5.2.11 Ex vivo cytokine assay	144
5.2.12 Statistical analysis	144
5.3 Results	145
5.3.1 Formulation of OVA-encapsulated biotinylated PLGA nanoparticles ..	145
5.3.2 DEC-205 receptor-mediated uptake of nanoparticles	150
5.3.3 Nanoparticle mediated DC maturation and cytokine secretion.....	152
5.3.4 Enhanced IgG and IgG isotype responses in the presence of costimulatory anti-CD40 mAb	157
5.3.5 Induction of ex-vivo cytokines.....	159
5.4 Discussion	161
5.5 References	165
Chapter 6: General discussion, conclusions, and future directions	169
6.1 General discussion.....	170
6.2 Conclusions	178
6.3 Future directions.....	179
6.4 References	181

LIST OF TABLES

Table 2.1	Different pVAXN formulations used for intranasal and intramuscular immunization in mice	59
Table 3.1	Immunization schedule and HA DNA vaccine formulations	90
Table 4.1	Characterization of pVAXN and pDECN loaded chitosan nanoparticles	122
Table 5.1	OVA and PLGA nanoparticle vaccine formulations	143
Table 5.2	Physico-chemical characterization of PLGA NPs	147

LIST OF FIGURES

Figure 1.1	Dendritic cell associated C-type lectin receptors	10
Figure 1.2	Methods for targeting antigens to DCs in vivo	18
Figure 1.3	Chemical Structure and biodegradation products of PLGA	20
Figure 1.4	Induction of cellular and humoral immunity by DNA vaccines	24
Figure 1.5	Chemical structure of chitosan	29
Figure 1.6	Research hypotheses	34
Figure 2.1	Detection of SARS N protein expression by Western blot	62
Figure 2.2	Synthesis and characterisation of biotinylated chitosan	64
Figure 2.3	Formulation of pVAXN loaded biotinylated chitosan NPs	66
Figure 2.4	IMAC purification profile of bifunctional fusion protein	67
Figure 2.5	IMAC purification profile of SARS CoV N protein	68
Figure 2.6	SARS CoV N protein specific IgG titers	70
Figure 2.7	SARS-CoV N protein specific IgA levels in the nasal washes	72
Figure 2.8	Analysis of IFN- γ levels in mice immunized with different pVAXN formulations	74
Figure 3.1	Optimization of pHA (pCAG α -HA) loaded biotinylated chitosan nanoparticles	92
Figure 3.2	Expression and purification of recombinant HA1 in E. coli	94
Figure 3.3	HA-specific systemic IgG response in mice vaccinated with various DNA vaccine formulations using intranasal (A) and intramuscular (B) route	96
Figure 3.4	HA-specific IgA responses in the nasal washes and vaginal washes	98
Figure 3.5	HA-specific IFN- γ and IL-4 responses	100

Figure 4.1	DNA vaccine constructs and dendritic cell targeting strategy	111
Figure 4.2	Cloning and expression of vaccine vectors	119
Figure 4.3	Dendritic cell binding study of expressed antigens	120
Figure 4.4	Formulation and nuclease digestion profile of chitosan nanoparticles	122
Figure 4.5	In vitro transfection efficiency of pEGFP-C1 loaded chitosan nanoparticles	123
Figure 4.6	Detection of SARS CoV N protein and N protein fragment-specific humoral immune response in the mice immunized with various DNA vaccine	125
Figure 4.7	SARS CoV N protein specific ex-vivo cytokines secretion profile	127
Figure 5.1	Synthesis and characterization of biotin-PEG-PLGA conjugate	145
Figure 5.2	Characterization of PLGA nanoparticles	148
Figure 5.3	Uptake of targeted and non-targeted nanoparticles using flow cytometry	151
Figure 5.4	Analysis of CD86 and CD40 expression on BMDCs treated with PLGA NPs	153
Figure 5.5	In vitro cytokine secretion profile of BMDCs treated with PLGA NPs	156
Figure 5.6	Analysis of OVA-specific IgG response	158
Figure 5.7	OVA-specific ex-vivo cytokine secretion profile	160

LIST OF ABBREVIATIONS

°C	degrees centigrade
µg	micro gram
µl	micro liter
Ag	antigen
ANOVA	analysis of variance
APCs	antigen presenting cells
ATCC	American type culture collection
BCA	bicinchoninic acid
B-chitosan	biotinylated chitosan
BfFp	bifunctional fusion protein
BMDC	bone-marrow-derived dendritic cells
BSA	bovine serum albumin
BsMAb	bispecific monoclonal antibody
CCL	chemokine ligand
CCR	chemokine receptor
CD	cluster of differentiation
CD40L	CD40 ligand
cDNA	complementary DNA
CFA	complete Freund's adjuvant
CLRs	c-type lectin receptors
ConA	concanavalin A
CpG	cytosine-phosphate-guanine
CRDs	carbohydrate recognition domains
CTL	cytotoxic T lymphocyte
DC	dendritic cells
DCM	dichloromethane
DC-SIGN	dendritic cell-specific intercellular adhesion molecule-3- grabbing non-integrin
DLS	dynamic-light scattering

DMEM	Dulbecco's modified eagle's medium
DNA	deoxyribonucleic acid
ELISA	Enzyme-Linked ImmunoSorbent Assay
FACS	fluorescent-activated cell sorting
FBS	fetal bovine serum
FDA	food and drug administration
FITC	fluorescein isothiocyanate
Flt3	fms-like tyrosine kinase receptor-3
GFP	green fluorescent protein
GM-CSF	granulocyte-macrophage colony stimulating factor
h	hour
HA	hemagglutinin
HBsAg	Hepatis B surface antigen
HCTU	2-(6-Chloro-1H-benzotriazole-1-yl)-1,1,3,3-tetramethylaminium hexafluorophosphate
His	histidine
HRPO	horseradish peroxidase
HSLAS	Health Sciences Laboratory Animals Services
HSP	heat shock protein
IFA	incomplete Freund's adjuvant
IFN- γ	interferon-gamma
IgA	immunoglobulin class A
IgG	immunoglobulin class G
IL	interleukin
IM	intramuscular
IMAC	immobilized metal affinity chromatography
IN	intranasal
IPTG	isopropyl β -D-thiogalactoside
ISCOMS	immune stimulating complexe
kDa	kilo Dalton

LPS	lipopolysaccharide
mAb	monoclonal antibody
MFI	mean florescence intensity
mg	milligram
MHC	major histocompatibility complex
min	minute
mL	milliliter
MMR	macrophage mannose receptor
mV	millivolt
MW	molecular weight
N protein	SARS CoV nucleocapsid protein
ng	nanogram
Ni-NTA	nickel-nitrilotriacetic acid
NK cells	natural killer cells
nm	nanometer
NMR	nuclear magnetic resonance
NPs	nanoparticles
OD	optical density
OVA	ovalbumin
PAGE	polyacrylamide gel electrophoresis
PAMPS	pathogen-associated molecular patterns
PBS	phosphate buffered saline
PBST	PBS with 0.1% Tween 20
PCR	polymerase chain reaction
pDECN	pVAX1 vector encoding for anti-DEC-205 scFv-SARS CoV nucleocapsid protein
pDNA	plasmid deoxyribonucleic acid
PEG	polyethylene glycol
PI	polydispersity index
PLGA	poly(D,L-lactic-co-glycolic acid)

Poly (I:C)	Polyinosinic-polycytidylic acid
PRRs	pattern recognition receptors
PSG	penicillin, streptomycin and L-glutamine
PVA	polyvinyl alcohol
pVAXN	pVAX1 vector encoding for SARS CoV nucleocapsid protein
PVDF	polyvinylidene fluoride
RMPI	roswell park memorial institute
RNA	ribonucleic acid
rpm	rounds per minute
RSV	respiratory syncytial virus
RT	room temperature
SARS CoV	Severe acute respiratory syndrome coronavirus
scFv	single chain antibody
SD	standard deviation
SDS	sodium dodecyl sulfate
SEM	scanning electron microscopy
Th	T helper
TLR	toll-like receptors
TMB	3, 3', 5, 5'-tetramethylbenzidine
TMRD	tetramethyl rhodamine dextran
Treg	T-regulatory cell
v/v	volume-to-volume ratio
w/o/w	water-in-oil-in-water
w/v	weight-to-volume ratio
w/w	weight-to-weight ratio
α CD40	anti-CD40 antibody
ζ	Zeta Potential

Chapter 1: Introduction

1.1 Dendritic cells

Dendritic cells (DCs) were discovered in 1973 by late Ralph M. Steinman and Zanvil Cohn [1]. During the last four-decades, these cells have been the focus of intensive research and emerged out as crucial link between innate and adaptive immune responses [2]. DCs are regarded as the most professional antigen presenting cells (APC) for their role in generation and maintenance of primary immune responses. Depending upon the nature of the antigen and the microenvironment during antigen capture and presentation, DCs dictate the outcome of the immune response, which can be either immune activation or tolerance [3]. Given the role DCs play in orchestrating the immune responses, harnessing DCs to create more effective vaccines has stimulated immense research efforts. To date, a number of DC based vaccines are evaluated at preclinical and clinical stages. Concomitantly, delivery of vaccine antigens in the particulate form has gained significant due to enhanced antigen uptake capability in this form. Various strategies have been adapted to achieve DC selective targeting of particulate vaccine delivery systems. This thesis explores and evaluates nanoparticulate delivery system for DC targeted delivery of DNA and protein antigens. This chapter elaborates on key features of DCs that are of relevance for developing vaccines and provides the rationale for targeting nanoparticulate vaccines to DCs.

1.1.1 DC origin and subsets

Dendritic cells represent a complex ‘immunological system’ comprised of heterogeneous population of cells with a dendritic shape, produced in the bone marrow by differentiation of precursor cells. In mouse and humans, DCs originate from myeloid or lymphoid pathways of development and represent two major subsets. The myeloid and lymphoid DC subsets differ in the phenotype, microenvironment localization and functional specialization [4]. In the steady state based on their function, tissue distribution, expression of surface markers, murine DCs can be further classified into six groups [5].

In steady state, DCs in the spleen and lymph nodes of mice are characterized by the expression of the CD11c and major histocompatibility complex (MHC) class II. In the spleens of mice, at least three subsets of DCs are present. They are CD8 α ⁺ lymphoid DCs (CD11c^{high} CD8 α ⁺ DEC205⁺), CD8 α ⁻ myeloid DCs (CD11c^{high}CD8 α ⁻CD11b⁺DEC205⁻), and plasmacytoid DCs (CD11c^{intermediate}CD8 α ^{+/-} CD11b⁻B220⁺ Gr-1⁺). In the lymph nodes of mice, in addition to the above mentioned phenotypes, at least two additional subsets: Langerhans cells (LCs) (CD11c^{high}CD8 α ^{dull}DEC205^{high}Langerin⁺) and dermal DCs (CD11c^{high}CD8 α ⁻ CD11b⁺ DEC205⁺) are present.

Different DC subsets have capacity to uptake, process, and present antigens to T cells. However, the type of immune response generated is often based on the functional specialization. The CD8 α ⁺ lymphoid DCs are positioned in the T cell rich areas of lymph nodes and have inherent capacity to secrete abundant quantities of IL-12 (p70) and prime Th1 helper T cell responses [6, 7]. The most important characteristic of CD8 α ⁺ lymphoid DCs is the ability to constitutively cross-present antigens in context of MHC class I molecules [8, 9]. The ability to cross-present antigens and induce CD8 T cell activation make them key subsets involved in the presentation of viral antigens [10]. These cells are also specialized to take up antigens from dead and dying cells and cross-present in the context of MHC class I [11].

In contrast, CD8 α ⁻ myeloid DCs are localized in the marginal zones of the spleen, and the subcapsular sinuses of the lymph nodes, secrete IL-10 and induce Th2 helper T cell responses. The plasmacytoid DCs (PDCs) are found in the spleen, thymus, and T cell rich areas of lymph node. PDCs are major producers of interferon-alpha (INF- α) and play a key role generation of innate and adaptive immune responses against viral infections.

1.1.2 Location in the periphery and lymph nodes

DCs have unique distribution pattern in the periphery and in the secondary lymphoid organs. They are abundantly located in the most of tissues and under the epithelium at the mucosal surfaces (i.e. respiratory and gastrointestinal system).

DCs continuously scan mucosal surfaces by extending their dendritic processes through the epithelial tight junctions [12].

The strategic location of DCs increases the capture of infectious or non-infectious and self antigens from the environment. After sampling antigens, DCs leave peripheral tissues and migrate to regional lymphoid organs through lymphatic vessels. The migration of DCs is controlled by chemokine-chemokine receptor interactions. Immature DCs respond to inflammatory chemokines through CCR1, CCR5 and CCR6 receptors. Specifically, DCs respond to CCL20 through CCR6 and this interaction is responsible for the localization of immature DCs at the skin and mucosal surfaces under homeostatic and inflammatory conditions.

In contrast, mature DCs downregulate CCR1, CCR5 and CCR6 and upregulate CCR7, this allows their migration into afferent lymphatic system. CCR7 is a chemokine receptor that responds to two chemokines: Epstein- Barr Virus-(EBV)-induced molecule (ELC/MIP-3 beta) and secondary lymphoid tissue chemokine (SLC/6CKine). ELC/MIP-3 beta is produced by the lymph node resident DCs in the T cell areas; whereas SLC/6CKine is produced in high endothelial venules (HEVs) and stromal cells in T cell area of lymph nodes. Both SLC and ELC play an important role in directing the migration of the antigen-loaded mature dendritic cells in the T cell area of lymph node for interaction with naïve T cells.

Beside peripheral tissues, a hallmark of DC location is their abundance in lymphoid tissues, particularly the T cell areas [13]. Numerically, DCs represent a small fraction of total cells in lymph nodes but the presence of many extensions “dendrites” allow them to form a vast and labyrinthine network and increase surface area. The large surface area equip DCs to interact with multiple T cells at a time and such a competent scanning sets stage for selection of rare antigen-specific T cell clones (1 in 10^5 - 10^6). The real-time two-photon microscopy of intact lymph node revealed that one DC can scan at least 500 different T cells per hour.

1.1.3 DC maturation/activation

DCs maturation is tightly linked with their migration from peripheral tissues to secondary lymph-node organs. Indeed, DC maturation is a continuous process that starts in periphery upon antigen encounter and ends during DC-T cell interaction. DCs mature in distinct ways in response to various types of microbial and host-derived stimuli. The pattern recognition receptors (PRRs) such as toll-like, NOD, RIG-1 and MDA5 receptors on DC surface, help them sense distinct pathogen associated molecular patterns (PAMPs) associated with the pathogens.

The maturation status of DCs helps to decide the outcome of innate and adaptive immune responses. In the steady state in the absence of maturation stimuli, DCs can induce antigen-specific tolerance when they capture self or environmental antigens [14]. However, maturation of DCs in response to microbial products ‘danger signals’ results in altered expression of a number of genes, leading to synthesis of number of cytokines such as type I interferons (IFN α and β) and IL-12 [15, 16]. The cytokine secretion pattern is influenced by the maturation stimuli and by the DC subset. These inflammatory cytokines can in turn provoke DC maturation; however direct maturation in the presence of the pathogen components results in fully immunologically active DCs that can promote T helper cell differentiation [17]. Upon exposure to pathogens, dendritic cells produce 3 waves of distinct chemokines to recruit different cells such as neutrophils, natural killer (NK) cells, memory T cells and naive T lymphocytes in succession to the site of DC maturation [18].

Immature DCs have small cytoplasmic processes called dendrites on their surface, which provide a large surface area for efficient pathogen uptake. Maturation induces distinct morphological changes through cytoskeletal reorganization and dendrites become longer, probably for simultaneous interaction with multiple T cells [19]. Furthermore, maturation process is also associated with down-regulation of endocytic/phagocytic machinery, shift in pH of lysosomal compartments with upregulation of DC-lysosomal-associated membrane protein (DC-LAMP) and transport of peptide-MHC complexes to the cell surface [20].

Importantly, maturing DCs remodel their surface and upregulate the expression of MHC class II and co-stimulatory molecules like CD86, CD83, CD80 and CD40 [21, 22]. The upregulation of these molecules helps in bidirectional signalling and contact between DCs and T cells.

The state of DC maturation plays a key role in shaping the outcome of immune responses. Particularly, CD4 T cell differentiation is significantly governed by the type of DC maturation stimuli DC encounter. Depending upon the type of maturation stimuli CD4 T cells differentiate in Th1, Th2, Th17 or Treg phenotypes.

The DC maturation is also influenced by vaccine adjuvants and this in turn shapes the resulting immune responses. Antigen delivery to DEC-205 positive DCs in the presence of a TLR3 ligand (synthetic double-stranded RNA, poly IC) skewed the CD4 T helper lymphocytes to a Th1 lineage by an IL-12-independent and CD70-dependent mechanism [23]. Furthermore, immunization of mice with nanoparticle containing antigens plus monophosphoryl lipid A and R837 adjuvants that signal through TLR4 and TLR7 respectively, induced synergistic increases in antigen-specific neutralizing antibodies compared to immunization with nanoparticles containing antigens plus a single TLR ligand [24].

1.1.4 Antigen processing, presentation and cross-presentation

Immature DCs are very efficient in antigen uptake and use several pathways. Depending on the source and form of antigen, DC use different endocytic processes. Macropinocytosis is major pathway for uptake of solutes, nutrient and large gulps, while phagocytosis for uptake of large particles (>500 nm), apoptotic and necrotic cell fragments. DCs are also highly specialized at receptor-mediated endocytosis (RME) via cell surface associated receptors. Most of the receptors involved in RME belong to the class of C-type lectin receptors (CLRs).

DCs display several unique features related to antigen loading and presentation that can be exploited for improved vaccination. These include (i) a low rate of antigen degradation as compared with macrophages [20], which in turn permits

antigen retention in lymphoid organs in vivo for extended periods for antigen presentation and development of T-cell immunity, (ii) a remarkable stability of peptide-MHC class II complexes on the cell membrane of mature DCs facilitates T cell receptor recognition [25], and (iii) the capacity to cross-present exogenous antigens on MHC class I molecules.

DCs are specialized cells that are capable of processing endogenous and exogenous antigens. DCs capture, process and subsequently display antigenic epitopes on their surface in association with major histocompatibility complex (MHC) class I and class II molecules to T cells. Typically, endogenous antigens are processed through cytosolic pathway and presented in association with MHC class I molecules to CD8+ T cells. In this model, antigen uptake into endosomes is followed by translocation of internalized antigens from endosomes to the cytosol of the DCs. In the cytosol, proteins get ubiquitinated, degraded into the peptides. These peptides are shuttled across endoplasmic reticulum (ER) membrane with the help of TAP (transporters of antigen presentation) proteins. In the ER, peptides get loaded into the groove of newly synthesized MHC class I molecule associated with the β -microglobulin for presentation at the cell surface. The majority of endogenous antigens (normal cell proteins, viral or tumor antigens) follow “classical” MHC-I pathway of presentation.

Alternatively, DCs sample exogenous antigens and route them through early or late acidic endosomal/lysosomal compartments for degradation by proteases. The degraded peptides then associate with the MHC class II molecules within the MHC class II compartments (MIIC) and translocate to cell surface. Thus, peptides displayed in context of MHC class II molecules and recognized by CD4+ T cells.

1.1.5 Activation of T cells

One of the most important features of DCs is their ability to activate immunologically naïve T cells. This exclusive ability of DCs is because of constitutive expression of MHC class I and class II as well as co-stimulatory molecules. Matured/activated DCs are capable of providing three signals required

for efficient priming of naïve T cells. Upon maturation, DCs down regulate their endocytic activity and upregulate surface expression of MHC class I and MHC class II molecules that present the processed peptides to the naïve CD8⁺ and CD4⁺ T cells, respectively (signal 1). Mature DCs also express high levels of accessory molecules, which help them interact with other receptors on T cells to augment adhesion and co-stimulation (signal 2). Adhesion molecules such as intercellular adhesion molecule (ICAM-1) displayed by DCs interacts with T cell's intercellular adhesion molecule lymphocyte function-associated antigen (LFA)-1. Beside this, upregulation of co-stimulatory molecules such as CD40, CD80, and CD86 DCs to efficiently interact with T cells and form a tight synapse. In addition mature DC also secret large amounts of IL-12, that provides the third signal required for the induction of efficient T cell activation.

1.2 Dendritic cell associated receptors

DCs express numerous pattern recognition receptors (PRRs) such as the toll-like receptors (TLRs), as well as non-TLRs such as intracellular nucleotide-binding domain and leucine-rich-repeat-containing family (NLRs), retinoic acid-inducible gene I (RIG-I)-like receptors and C-type lectin receptors (CLRs).

The immature DCs express a wide variety of C-type lectin receptors and these mediate specific recognition of both self-antigens and pathogens. The CLRs internalized antigens are degraded in lysosomal compartments, which ultimately results in antigen processing and presentation [26, 27].

The classical C-type lectins contain highly conserved carbohydrate recognition domains (CRDs) that bind sugar residues in a calcium (Ca⁺⁺)-dependent manner. The Ca⁺⁺ ions are necessary for both ligand recognition as well as maintaining structural integrity of the CRDs [26, 28]. However, CLR family now includes proteins that have one or more domains that are homologous to carbohydrate recognition domains but do not always bind carbohydrate structures. The C-type lectins contain a prototypic lectin fold, which consists of two anti-parallel β -

strands and two α -helices. C-type lectins form oligomers within the cell membrane to strengthen and limit binding to a specific structure with a certain carbohydrate density and spacing of ligands [29].

The C-type lectins are either secreted as soluble proteins or produced as trans-membrane proteins. Trans-membrane C-type lectins contain carbohydrate recognition domains, which are also capable of binding with protein or lipids and with carbohydrates in Ca^{++} -independent manner [30]. Ligands for C-type lectins and lectin-like receptors are poorly characterized, so the term C-type lectin is collectively applied to these proteins irrespective of whether they contain Ca^{++} -ligating elements or have a known carbohydrate-binding activity [31].

The transmembrane C-type lectins receptors on DCs can be further classified into two classes, namely, type I and type II depending on the orientation of their amino (N) terminus in their molecular structure [26]. The type I CLR has N-terminus located extracellularly, whereas type II CLR has its N-terminus located within the cytoplasm (**Figure 1.1**).

The type I CLR (also noted as mannose receptor family) has an N-terminal cysteine-rich (CR) domain, a fibronectin type II (FNII) domain, multiple C-type lectin-like domains (CTLDs) (eight or 10) in the extracellular domain, and a short cytoplasmic domain. Representatives of this type are macrophage mannose receptor (MMR) and DEC-205. The type II CLR is characterized by a short cytoplasmic tail, a transmembrane domain, an extracellular stalk region, and a Ca^{2+} carbohydrate binding CRD. The length of the stalk region varies among the different members and is involved in oligomerization. The classical members of type II CLR include DC-specific ICAM-3 grabbing non-integrin (DC-SIGN), Langerhans cell specific C-type lectin (Langerin), DC-associated C-type lectin-2 (Dectin-2), DC-immunoreceptor (DCIR) and Dectin-1.

Because of their restrictive expression by DC subsets and their function as uptake receptors, CLR has been prime candidates for in vivo targeted delivery of vaccine antigens to DCs. Therefore, various approaches to target CLR on DCs are under extensive investigation and several studies demonstrate that enhanced

immune responses can be induced by coupling CLR ligands to soluble or particulate antigens. The most-identified CLRs that are candidates for DC targeting include DEC-205, MMR and DC-SIGN.

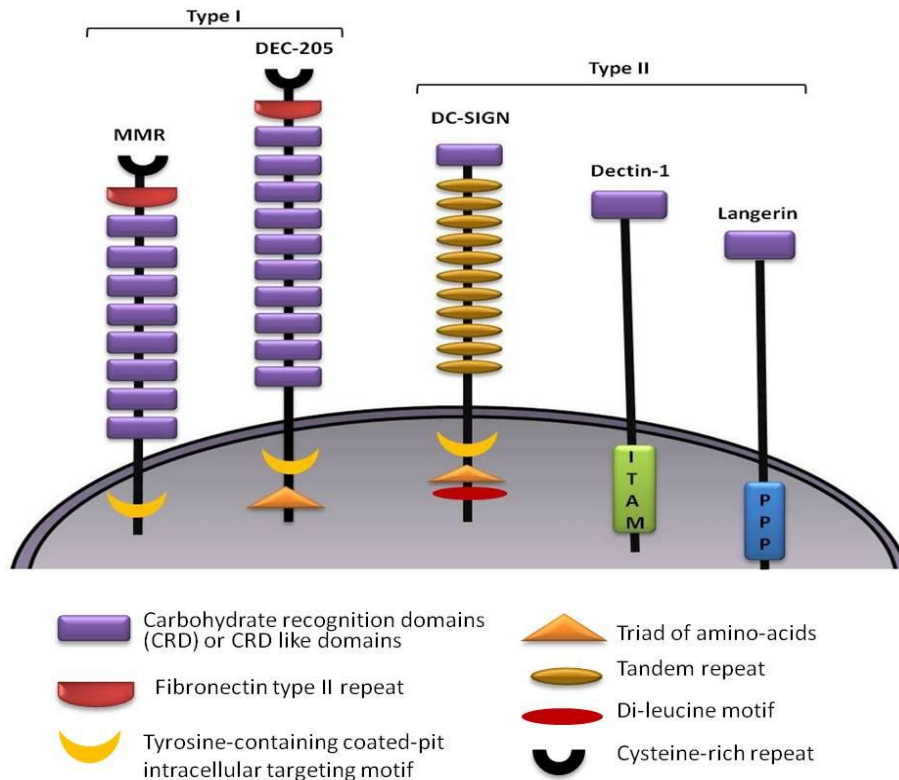


Figure 1.1 Dendritic cell associated C-type lectin receptors (CLRs). Type I C-type lectin receptors (MMR and DEC-205) contain an amino-terminal cysteine-rich repeat (S-S), a fibronectin type II repeat (FN) and 8 to 10 carbohydrate recognition domains (CRDs), which bind ligand in a Ca^{2+} -dependent manner. Type II C-type lectins contain only one CRD at their carboxy-terminal extracellular domain. The cytoplasmic domains of the CLRs are diverse and contain several conserved motifs that are important for antigen uptake: a tyrosine-containing coated-pit intracellular targeting motif, a triad of acidic amino acids and a dileucine motif. Other type II C-type lectins contain other potential signalling motifs such as immunoreceptor tyrosine-based activation motif (ITAM) and proline-rich regions (PPP). DC-SIGN, dendritic-cell specific ICAM-3 grabbing non-integrin; ITAM, immunoreceptor tyrosine-based activation motif; MMR, macrophage mannose receptor.

1.2.1 DEC-205/CD205 receptor

DEC-205 (CD205) is a second member of the macrophage mannose receptor family of type I C-type lectins. The murine DEC-205 receptor was first identified as the antigen recognized by monoclonal antibody obtained from NLDC-145 hybridoma [32, 33]. The natural ligand of DEC-205 and its carbohydrate specificity are currently unknown.

Structural characteristics: DEC-205 is a 205-kDa protein, consisting of a single polypeptide chain; extracellular N-terminal cysteine-rich domain, cytosolic domain consisting of tyrosine-based motif and a distal acidic EDE triad, a fibronectin type II domain, and ten carbohydrate recognition domains (CRDs) (**Figure 1.1**). Unlike MMR, none of its ten CRD domains seem to contain the consensus amino acid sequences required for the carbohydrate or Ca^{++} - binding [26].

Intracellular routing and recycling: DEC-205 is internalized by means of clathrin-coated pits and vesicles, and recycles through late endosome/early lysosome compartments that are rich in MHC class II molecules. A tyrosine containing FSSVRY motif is responsible for initial clathrin-coated pit-mediated endocytosis, while an acidic EDE triad motif targets DEC-205 to late endosomes/early lysosomes, allowing endocytosed antigen to reach the MHC class II loading compartment [32, 34]. Therefore, DEC-205 cytosolic domain mediates a distinct endocytosis pathway that entails efficient recycling through late endosomes and hence enhances efficiency of antigen presentation to CD4 T cells. It has been demonstrated that DEC-205 mediated routing to MHC class II compartments is 30–100 time more efficient compared to the MMR receptor, which doesn't have an acidic triad [34].

Importantly, the DEC-205 endocytic pathway is non-stimulatory and cross-linking of receptor with antibody does not maturate DCs and antigen delivery in the absence of maturational stimuli results in presentation of antigens by immature or 'semimature' DC leading to the induction of CD4 and CD8 T-cell tolerance.

However, tolerance induction can be overcome if the antigen is delivered with DC maturation stimuli [14, 35].

Expression pattern and up regulation on mature DCs: In mice, DEC-205 is expressed at high levels on thymic medullary DCs (CD11c⁺ CD8⁺), and subsets of peripheral DCs, such as CD11c⁺ CD8⁺ splenic/lymph node DCs, dermal/interstitial DCs, and Langerhans cells [32, 33]. In humans, it is highly expressed by BDCA1⁺ cDCs, monocytes and to low levels on B-cells, NK cells, plasmacytoid DCs and T cells [36, 37]. A distinguishing feature of DEC-205 is its high-level expression on the DCs in the T-cell areas of lymphoid organs, which suggest its role in the regulation of T-cell responses.

Unlike that of the MMR or other CLR, which tend to be down-regulated upon DC maturation, the DEC-205 is up-regulated upon DC maturation [37, 38]. DEC-205 expression pattern closely parallels to MHC class II molecules, which are mainly found in the intracellular compartments of immature DCs, but are redistributed to the cell surface upon maturation. The higher expression level of DEC-205 on the mature DCs is thought to be result of *de novo* synthesis as well as redistribution of molecules from endocytic compartments to the cell surface [39]. DEC-205 is highly conserved in mammals, and human and murine DEC-205 share ~90% amino acid homology [40]. Therefore, mouse can be used as a potential experimental model at preclinical stage.

Role in tolerance: The DEC-205 has been demonstrated as a recognition receptor for apoptotic and necrotic self [41, 42]. It has recently been implicated in the capture of apoptotic thymocytes by thymic epithelial cells. As thymic epithelial cells express DEC-205 capture of apoptotic thymocytes could provide the rich source of peptides required for positive and negative selection in the thymus [41]. These studies demonstrate that CRDs 3 + 4 and 9 + 10 of DEC-205, can recognise ligands on apoptotic and necrotic cells. Furthermore these ligand(s) were trypsin-sensitive and thus involved proteins. Both of these studies suggest a possible role of DEC-205 in the generation of tolerance against self antigens.

Antigen targeting: The field of DEC-205 receptor targeting has been pioneered by Nobel laureate late Dr. Steinman and colleagues at the Rockefeller University. Currently four types of DEC-205 targeting systems have been reported and all of them are based on the design of antibody-mediated antigen targeting systems. These systems are HB290 single chain (anti-DEC-205) antibody (scFv) coated liposomes [43], chemical conjugation of anti-DEC-205 mAb on the surface of pH-sensitive polymeric microparticles [44] or chemical conjugation of anti-DEC-205 mAb with antigen [38, 45], and the development of a anti-DEC-205 mAb fusion protein [14, 46, 47]. The antibody based DEC-205 receptor-mediated targeting of antigens to DCs has been shown to enhance antigen presentation in the context of MHC class I and II molecules, resulting in induction of robust CD8 and CD4 T cell responses.

In most of the systems studied thus far, induction of antigen-specific immunity with DEC-205-targeting is dependent on concomitant delivery of a DC activation/maturation stimulus (LPS, anti-CD40 antibody or TLR ligands etc.). Surprisingly, antigen targeting to DEC-205 receptor, in the absence of DC activation/maturation stimuli results in the generation of antigen-specific T-cell tolerance [14, 35, 43]. Therefore, DEC-205 targeting in the absence of activation/maturation stimuli can be exploited for the induction of antigen specific immune suppression for treating autoimmune diseases and preventing transplant rejection. In this context a recent study has shown that targeting of pancreatic β -cell antigens to DEC-205 receptor resulted in deletion of β -cell antigen-specific autoreactive CD8 T cells in a mouse model of type 1 diabetes [48]. Tolerance was induced even in the context of ongoing autoimmunity in non-obese diabetic (NOD) mouse model with known tolerance defects.

In vivo targeting of ovalbumin (OVA) to matured DCs via DEC-205 receptor has been shown to induce substantial antitumor effects, when mice were challenged with OVA expressing B16 melanoma [38]. The DEC-205 targeting also prolonged presentation of OVA peptide complexes in context of MHC class I molecules. Presentation of peptide-MHC class I complexes was found to persist

for at least 2 weeks, while peptide-MHC class II complexes were no longer detectable after seven days. Furthermore, subcutaneous injection of DEC-205 mAb conjugated OVA along with anti-CD40 mAb was found to provide protective immunity against mucosal challenge of OVA modified vaccinia virus. The mice vaccinated with DEC-205 targeted antigen had significantly reduced virus titers and symptoms compared to controls [38].

To demonstrate therapeutic efficacy of DEC-205 targeted antigen delivery, Mahnke and co-workers used a B16 melanoma model. In this study, DEC-205 antibody mediated targeting of two melanoma antigens (gp100 and tyrosinase-related protein 2) together with a DC maturation stimulus (unmethylated bacterial CpG motifs) was found to cure ~70% of the mice from existing tumors. The antitumor effects were found to be mediated by the induction of melanoma-antigen specific CD4 and CD8 T lymphocytes [45]. Furthermore, the maturation status of DCs was crucial for successful induction of immunity and when the DC maturation stimulus CpG was omitted, no protection against tumors was observed after immunization. Taken together, the results of these pioneering studies demonstrate that antigen targeting to DCs via DEC-205 receptor along with a DC maturation stimulus represents an efficient strategy for inducing long-lasting and effective anti-tumor immunity.

In one study, DC targeted delivery of a xenogenic form of self-antigen (survivin) via DEC-205 receptor together with anti-CD40 mAb and poly (I:C) as maturation stimuli has been shown to induce a CD4 T cell responses against non mutated over expressed murine survivin [49]. However, induction of murine survivin specific CD8 T cells was not observed despite using combination of stimuli and frequent dosing. Furthermore, a recent study has shown that DEC-205 antibody based delivery of LcrV virulence protein from *Yersinia pestis* to DCs can protect mice against pneumonic plague [50]. In this study LcrV antigen was genetically fused to carboxyl terminus of anti-mouse DEC-205 heavy chain. Immunization of mice with fusion protein in conjunction with poly (I:C) and anti-CD40 mAb was shown to induce antibody responses and broad Th1 immunity specific to several

LcrV peptides. DC targeting using this approach was found to protect mice against a virulent form of *Yersinia pestis* isolate from humans.

1.2.2 Other DC receptors

Macrophage mannose receptor (MMR): The MMR is a founding member of type I C-type lectin receptor family [51]. It is abundantly expressed on mouse BMDCs, human monocyte-derived DCs (mDCs) and interstitial DCs [28, 52]. The abundance of MMR on immature DCs and macrophages indicates a key role of this receptor in antigen recognition [53]. The MMR has been shown to mediate receptor mediated endocytosis of mannan conjugated antigens and facilitate presentation in context of MHC class II and MHC class I molecules [54]. A recent report has shown that uptake and cross-presentation of antigen by MMR depends on the form of antigen. In this study soluble, but not cell-associated form of ovalbumin (OVA) was found to be cross-presented by DC [55].

Ligand bound MMR recycles through early endosomal pathway and low pH of endosome leads to dissociation and recycling to the cell surface [56]. Endocytosis of MMR takes place in clathrin coated vesicles, and shortly thereafter, the MMR and its ligand appear in larger vesicles, followed by colocalization with MHC class II molecules in lysosomes [53].

Structurally MMR contains N-terminal extracellular cysteine-rich domain, a fibronectin type II-like repeat and eight C-type lectin CRDs, a single transmembrane domain, and a short cytoplasmic tail at the C terminus. The extracellular domain of MMR contains various ligand binding regions: an N-terminal cysteine-rich repeats (S-S) recognize carbohydrates, a fibronectin-type II repeat that binds to collagens and eight CRDs for carbohydrate binding. The MMR has been shown to bind with mannose, fucose or N-acetylglucosamine through two CRD domains, namely CRD4 and CRD5 [57, 58]. Specifically, the binding to mannose is predominantly through CRD4 and is Ca^{++} - dependent.

It has also been demonstrated that DC targeting using mannan conjugated tumor-associated antigen (MUC1) can induce either Th1 or Th2-type of immune responses, depending on the mode of conjugation [59, 60]. The reduced mannan

conjugated MUC1 induced Th2-type response accompanied with production of IgG1, IL-4, and low frequency cytotoxic CD8 T cells, and failed to protect mice against a tumor challenge. However, conjugation of MUC1 with oxidized mannan generated a potent Th1-type response, accompanied with high levels of cytotoxic CD8 T cells and IFN- γ production. More recently, DC targeting of melanoma-associated antigen pmel17 and model protein antigen OVA with the help of MMR antibody has been shown to improve magnitude of antigen-specific CD8 T cell responses and generate protective tumor immunity in a mouse model [61, 62].

Dendritic cell-specific ICAM-grabbing non-integrin (DC-SIGN): Dendritic cell-specific ICAM-grabbing non-integrin (DC-SIGN/CD209) is a member of type II CLR family and it is primarily expressed on immature DCs and at lower levels on macrophages and endothelial cells [63, 64]. In humans, DC-SIGN is abundantly expressed by DCs in lymphoid, dermal tissues and at mucosal surfaces. The mouse and human DC-SIGN counterparts have huge variation in structure and expression pattern and mouse DC-SIGN is expressed in multiple forms, and most of them are functionally unrelated to human counterpart [65, 66]. Moreover, carbohydrate specificity of murine DC-SIGN is similar to that of human counterpart and both bind to mannose-containing ligands and Lewis antigens Le(x/y) and Le (a/b) [67]. DC-SIGN recognizes various pathogens such as ebola virus, herpes viruses and *Neisseria gonorrhoeae* and meningitidis. Specifically, DC-SIGN has been shown to bind with human immunodeficiency virus (HIV) and contributes to the spread of HIV virus and plays a key role in pathogenesis [63, 68]. Similar to MMR and DEC-205, the DC-SIGN has been shown to mediate endocytic function and antigens targeted to DC-SIGN are routed to late endosomes/lysosomes, where they are efficiently presented by MHC class II pathway to CD4 T cells [69-71]. Furthermore, DC targeting of antigens with the help of DC-SIGN antibody has been shown to augment naïve and memory T cell responses, via MHC class II and class I mediated antigen

presentation [70]. The major advantage of targeting DC-SIGN over the other CLR is its restricted expression pattern on DCs.

1.3 Dendritic cell targeting strategies

Dendritic cells targeted delivery of vaccine antigens can be accomplished using, to broad strategies: ex vivo loading or in vivo targeting. Although ex vivo DC loading is elegant strategy that allows controlled DC maturation and activation of particular DC subset. It is a labour-intensive procedure, requires sophisticated techniques and need to be tailored for each individual [31]. As an alternative to this, numerous strategies are currently developed for in vivo targeted delivery of antigens to DCs (reviewed in [72-74]). The in vivo DC targeting strategies offer several benefits: lower production cost at large-scale production, good product quality and optimum antigen delivery within the physiological environment.

To achieve in vivo DC targeted delivery, vaccine antigens are coupled with natural carbohydrate ligands or antibodies against DC surface associated receptors. In vivo DC targeting with natural carbohydrate ligand-antigen conjugates is a viable option, since targeting ligand can be chemically synthesized in a cost effective manner on the large-scale. The carbohydrate ligands lack exclusive DC receptor-specificity and can be moped up by other cells. As an alternative to carbohydrate ligands, antibodies are increasingly used for in vivo DC targeting and in this regard different type of antibody-based DC strategies are being explored (**Figure 1.2**).

First and foremost strategy has been chemical conjugation of vaccine antigens to full-length DC-receptor specific antibody. Although antigen-antibody conjugates can be prepared within a short span of time using chemical cross-linker, the end product is not well-defined, non-stoichiometric and difficult to characterize. Moreover, chemical reaction can also hamper the receptor binding affinity of the antibody.

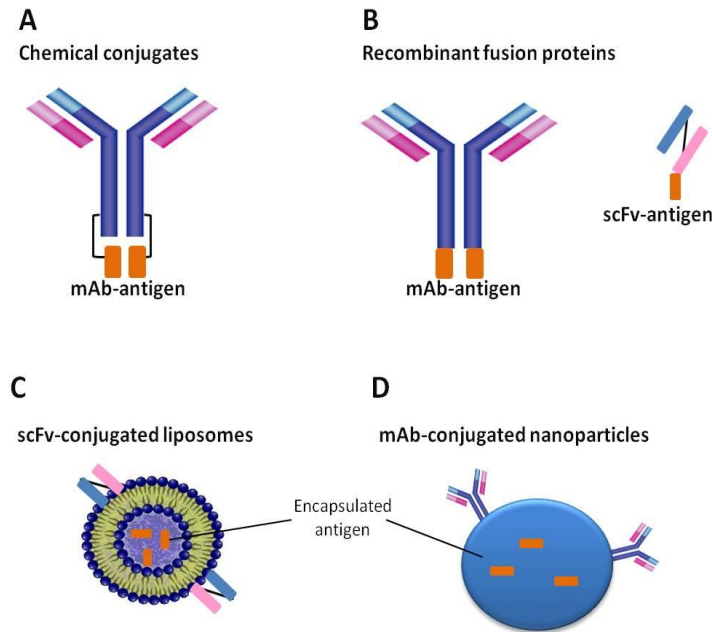


Figure 1.2 Strategies for targeting antigens to DCs in vivo. (A) Antigen is chemically conjugated to full-length mAb. (B) The heavy chain and light chain of the full-length mAb or the single chain variable fragment (scFv) are genetically engineered to carry antigen (Ag). (C) The scFv recognizing DC-specific receptor is conjugated onto surface of Ag and adjuvant carrying stealth-liposomes. (D) Nanoparticles carrying Ag-payload are surface modified to allow the attachment of DC receptor specific mAb.

To avoid this, genetic fusion approach was developed. In this approach, antigen is genetically fused to single chain antibody (scFv) or to the C-terminus region of heavy chain of full-length antibody. To date, fusion protein based approach is explored in most of the preclinical studies. Fusion protein based DC targeting has been shown to provoke augmented humoral and cellular immune response following in vivo DC targeted delivery. A number of DC associated CLR's such as DEC-205, MMR, DC-SIGN, CLEC9A and others have been explored (reviewed in [31, 72, 75]). The in vivo targeting using genetic fusion strategy has been shown to deliver targeted antigens to lymph-node resident DC subsets and provide enhanced immune responses and thus prove to be very promising. The genetic fusion protein based DC targeting strategy has its own limitations: this approach

requires tailoring and production of a separate construct for each antigen, which is laborious and costly process. Furthermore, only one molecule of antigen can be coupled with an antibody, this could result in less payload delivery to DCs. Furthermore, this strategy does not allow simultaneous delivery of multiple vaccine components (antigen and adjuvants) to same DC subset.

To overcome these drawbacks, more recently the antibody-targeted nanoparticulate antigen delivery systems are increasingly explored for designing improved vaccines. The particulate antigen delivery systems offer several advantages: one of the greatest benefits of particle based antigen delivery systems resides in their capacity to co-deliver antigens and adjuvants to the same DC [24, 76, 77]. Furthermore, DC targeted delivery of particulate vaccines can be achieved using passive approach based on the size (<200 nm) [78, 79] or active approach. Active-targeting involves functionalization of particles with DC receptor-ligand such as natural carbohydrates, monoclonal antibodies (mAb) or single chain antibody fragments (scFv) to obtain specific binding and uptake by receptor-mediated endocytosis. interactions to obtain Particulate vaccines may be formulated using different polymeric materials, but the majority of these systems fall into two general classes: vesicular systems (liposomes) or solid biodegradable systems composed of poly(lactic-co-glycolic acid) (PLGA) polymer. In this context application of PLGA based DC targeted vaccine delivery system is discussed below.

1.3.1 Dendritic cell targeted PLGA nanoparticles

The biodegradable poly(lactic-co-glycolic acid) PLGA polymer based systems have been extensively used for the delivery of various therapeutic agents and vaccine antigens. PLGA is a US FDA approved polymer and in the body PLGA is non-enzymatically hydrolyzed into lactic and glycolic acid monomers, which are natural metabolites (**Figure 1.3**).

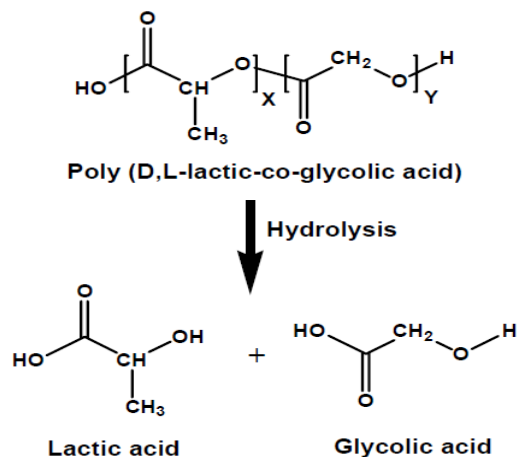


Figure 1.3 Chemical structure and biodegradation products of PLGA. PLGA is an aliphatic polyester composed of lactic and glycolic acid monomers. X and Y represent number of units of lactic and glycolic acid, respectively.

PLGA based vaccines delivery is a promising approach for augmenting immune responses against a range of antigens such as recombinant proteins, peptide and DNA. These systems offer several advantages over other antigen delivery systems (reviewed in [80-82]). First, they can be formulated in nanometer scale and thus facilitate efficient uptake by DCs. Second, they protect antigens against exacerbated degradation before reaching to DCs. Third, they allow co-delivery of antigens and adjuvants to the same DCs. Fourth, they can be designed to provide pulsatile Ag release and thus provide single dose formulation, which can serve the purpose of priming and booster dose. Finally, control over the particle surface chemistry can facilitate attachment of varying the density of targeting ligands to receptors on DCs.

Because of these properties, PLGA polymer based delivery systems have been extensively explored to design nanoparticulate vaccines [81, 83]. Many peptide and protein antigens have been successfully encapsulated within PLGA micro- and nanoparticles (NPs). Furthermore, co-encapsulation of antigen and TLR ligands within PLGA NPs has been shown to robustly improve antigen-specific

immune responses [76, 77, 84, 85]. Furthermore, a recent study has demonstrated that antigen and adjuvant delivery in two separate PLGA NPs induces robust antibody responses compared to co-delivery of antigen and adjuvant in the same particle [24]. These formulations also resulted in formation of germinal centre/memory B cells and afforded complete protection against lethal avian and swine influenza virus strains in mice.

To improve DC selective targeted delivery of model vaccine antigens, PLGA NP can be surface functionalized with DC-receptor specific antibodies. However, despite wealth of research conducted on PLGA based vaccines delivery systems, only a few studies have reported on antibody-based DC targeted delivery by PLGA NPs [86-88]. A study compared the DC targeting ability of anti-DC-SIGN antibody functionalized PLGA nanoparticles and microparticles, demonstrated that only targeted NPs specifically deliver antigens to human DCs [86]. Furthermore, targeted delivery of nanoparticle encapsulated antigen was found to enhance and provided T cell responses at 10-100 fold lower doses than non-targeted formulations.

A recent study performed to target PLGA NP coencapsulated antigen and TLR ligands to DEC-205 receptor on DCs in mice demonstrated that co-targeting can further improve the immune responses [88]. These results indicate that potent cytotoxic CD8 T cell responses can be induced at much lower doses of TLR ligands, when they are conencapsulated with antigen in NPs, instead of administering in soluble form. The DEC-205 targeted delivery of NP coencapsulating antigen and adjuvant also reduced serum levels of pro-inflammatory cytokine (IL-6, TNF- α , IFN- α and β) levels and related toxicity and provided a 100-fold reduction in dose of TLR ligands.

A study from Fahmy's group used avidin-biotin based approach to achieve DC-targeted delivery of PLGA NPs [87]. In this system antigen-loaded PLGA NPs were surface decorated with avidin and biotinylated anti-DEC-205 mAb was used to impart DC targeting. In the absence of DC maturation cross-linking DEC-205 receptor with antibody functionalized PLGA NPs induced secretion of IL-10. In

vivo studies in mice showed that mere DEC-205 targeted delivery induced antigen-specific antibody responses that were comparable with non-targeted formulations. However, authors have not reported whether coadministration of DC maturation stimuli with targeted formulations can enhanced immune response.

1.4 DNA vaccines

DNA vaccination or genetic immunization represents a novel strategy, which can serve as viable alternative to conventional vaccine approaches. The concept of DNA vaccination first came into the scientific limelight in the early 1990s, when it was recognized that intramuscular (IM) administration of recombinant DNA in mice resulted in the expression of the encoded protein [89]. Not soon after, it was shown that administration of DNA into the skin of mice could elicit antibody responses against encoded antigen [90] and then simultaneous studies by Ulmer et al. and Fyan et al. demonstrated that immunization with plasmid DNA could protect mice against a lethal influenza challenge [91, 92]. Furthermore, a study by Wang et al. showed that a plasmid DNA vaccine could provide protective immune responses against human immunodeficiency virus type I (HIV-1) [93]. Altogether, the implications of these studies provided evidence that DNA immunization could serve as an elegant vaccine platform. During the past two decades, the DNA vaccines have been tested and tried to induce immune responses against a range of infectious pathogens and tumor antigens (reviewed in [94]).

The novelty and usefulness of DNA vaccines stems from the several unique features, namely, they are conceptually safe, non-infectious and non-replicating, thereby overcome safety concern associated with live-attenuated vaccines. The DNA vaccine can be manufactured on large-scale with high purity and stability in a cost-effective manner and can be stored without the need for a cold chain (temperature range of 2-8°C) [95]. Furthermore, DNA vaccines can be promptly constructed based on pathogens genetic code and manufactured promptly,

something paramount with ongoing pandemic or bioterrorism threats. More importantly, DNA vaccine can induce antigen-specific mucosal (IgA), humoral (protective neutralizing antibodies) and cellular (cytotoxic T lymphocytes) immune responses. Despite the above mentioned advantages of DNA vaccines, their mechanism of action remains poorly understood.

Mechanism of action: DNA vaccines elicit strong and broad immune responses in many animal models, however, the precise mechanisms by which plasmid DNA (pDNA) vaccines induce antigen-specific immunity in vivo are complex and yet to be fully elucidated. At cellular level, it is thought that after optimized pDNA sequence is inoculated into the muscle or skin tissues (**Figure 1.4**), using the host cell machinery pDNA enters the nucleus of the transfected somatic cells (myocyte or keratinocyte), and small number of tissue-resident APCs such as DCs. Thereafter, pDNA encoded gene is transcribed and translated as foreign antigen. These host-synthesized antigens are then processed and presented to immune surveillance in the context of MHC class I and MHC class II molecules of DCs. Antigen-loaded DCs then travel to draining lymph nodes, where they interact with naive T cells via the peptide-loaded MHC complexes in combination with co-stimulatory molecules. This interaction provides secondary signals to prime an immune response, resulting in activation and expansion of antigen-specific T cells (cellular immune response). Alternatively, B cells acquire shed antigen with the help of immunoglobulin receptor and present it to CD4 T helper cells and get activated to produce antibodies (humoral immune response).

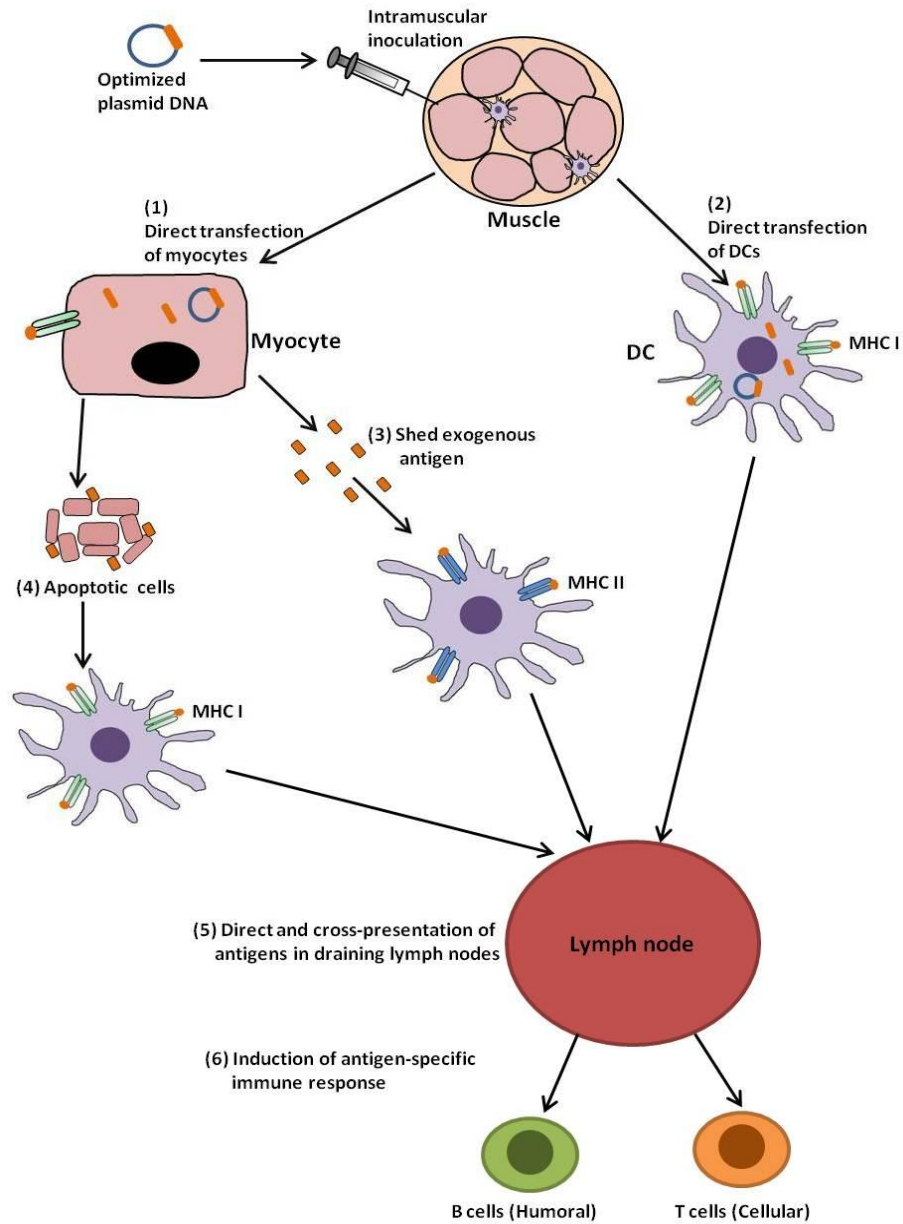


Figure 1.4 Induction of cellular and humoral immunity by DNA vaccines. The schematic diagrams details the key role played by DCs in induction of cellular and humoral immune response following intramuscular DNA immunization. The DCs are crucial for MHC class II-restricted presentation of exogenous antigens, secreted by the transfected myocytes; MHC class I-restricted cross-presentation of antigens that are released by the apoptotic transfected myocytes and MHC class I-restricted presentation of antigens that are produced endogenously in the transfected muscle-resident DCs.

Based on the mechanism of action delineated above, it is evident that following intramuscular and intradermal inoculation of plasmid DNA in mice, the myocytes and keratinocytes serve as antigen factories. These cells do not express MHC class II and costimulatory molecules required for effective priming and activation of naive immune cells and they do not have access to naive T cells as they do not migrate to lymphoid tissues. Therefore, it is speculated only a few transduced DCs play dominant role in priming immune responses, while the antigen secreted from transfected myocytes and keratinocytes then boost immune responses [96].

In general, DCs appear to play key role in priming antigen-specific immune response following DNA immunization via at least three mechanisms: (1) MHC class II-restricted presentation of exogenous antigens, secreted by the transfected somatic cells; (2) MHC class I-restricted presentation (direct priming) of antigens that are produced endogenously in the transfected DCs themselves; and (3) MHC class I-restricted, “cross-priming” of antigens that are released by the transfected somatic cells. All three mechanisms can be simultaneously involved in the processing and presentation of plasmid DNA encoded antigen [95, 96]. This is so because after delivery, pDNA can transfect different cell types and, depending on this, the antigen will be produced and presented differentially. However, the role played by direct or cross-priming in the induction of cytotoxic T cell (CTL) responses is still debatable. Nevertheless, based on mechanism of action, it is evident that DCs, most likely play a key role in initiating primary immune responses after DNA vaccination.

1.4.1 Strategies to improve DNA vaccines

A significant obstacle to successful development of DNA vaccine is their low immunogenicity in humans and in large animals. The DNA vaccines are often good at priming small animals (e.g. mice) but are less effective in larger animals. Numerous factors may contribute to their poor immunogenicity including: low transfection efficiency of naked DNA, insufficient antigen expression, and extra and intracellular barriers in the host [97].

Many strategies are currently explored to enhance the immunogenicity of DNA vaccines. These include optimization of plasmid DNA to improve antigen expression, use of cytokines and co-stimulatory molecules as adjuvant, use of proper delivery systems or formulations, use of next-generation delivery methods (e.g. electroporation), prime-boost strategies, and proper targeting of vaccine antigens to DCs (reviewed in [94-96, 98]). Among these approaches, targeting of DNA vaccines to DCs, and formulation and delivery of DNA vaccines using non-viral delivery systems is discussed here.

1.4.2 DC targeted DNA delivery

The potency of DNA vaccines can be enhanced by modifying the properties of antigen-expressing DCs and by targeting DNA or encoded antigen to DCs. Modification of properties of DC can be accomplished by the simultaneous delivery of DNA vaccine with that of plasmids encoding different types of immune-modulator molecules such as chemokines (MIP-1 α , SLC), cytokines (IL-2, IL-12, GM-CSF, flt-3 ligand) and DC costimulators (CD40L, CD86, CD80) (reviewed in [98, 99]). These immune modulator adjuvants act via promoting DC recruitment to the site of inoculation, promoting *in vivo* expansion of DCs, and activation and maturation of DCs. However, application of immune-modulators shows pleiotropic effects on many different types of cells. Therefore, more appropriate approach is to directly transfect DNA vaccines into DCs.

Many studies demonstrated that for DNA vaccine, direct transfection of DCs is indeed a very effective approach. Hattori and colleagues demonstrated that mannose-targeted liposomes carrying plasmid DNA were able to enhance *in vivo* DC transfection of encoded antigen and resulted in the induction of augmented antigen-specific CD4 Th1 cell and CTL responses [100-102].

DC-specific expression of encoded antigen can also be achieved using DC-specific promoters such as CD11c, DC-SIGN, Langerin, DC-STAMP (DC-specific transmembrane protein) [103] and fascin [104]. These promoters allow transcriptional targeting of DCs and avoid antigen expression by non-professional APCs. Moreover, the activity and length of promoter is critical determinant of

immune response to transfected antigens. Among all DC-associated promoters tested so far, fascin promoter appears the most promising because of its high activity in matured DCs [104]. Importantly, the length of promoter was also critical as a short mouse CD11c promoter (700-bp length) was shown to be optimum for DC selective antigen expression than the long one with 5.5-kb length. Immunization of mice with short CD11c promoter containing plasmid DNA induced antigen specific B- and T-cell responses and provided anti-tumor immunity comparable in strength to CMV promoter containing plasmid [105].

Beside directly transfecting DCs, targeting of DNA encoded antigen to DCs can also be realized by linkage of antigen to molecules capable of targeting receptors on DCs, e.g. MHC class II, cytotoxic T lymphocyte-associated antigen 4 (CTLA-4), IgG Fc fragments, CD40 ligand, and secreted form of heat shock protein 70 (HSP70). In one study, DNA vaccine encoding antigen linked to a secreted form of HSP70, which can bind with scavenger receptors such as CD91 on the surface of DCs was shown to enhance antigen specific CTL responses, antibody production and provided anti-tumor effects in a mouse model [106]. In another study, fusion of CD40 ligand with H5N1-hemagglutinin (HA) was also shown to improve immunogenicity and protective efficacy of HA DNA vaccine in a pekin duck model [107].

A more recently explored strategy is to target DNA encoded antigens to C-type lectin receptors, such as DEC-205. DNA vaccine encoding a fusion protein comprised of the vaccine antigen and a single-chain antibody (scFv) specific to DC-restricted DEC-205 receptor was shown to substantially increase humoral levels and cellular immune responses in the absence of DC maturation [108, 109]. Furthermore, a study demonstrated that the priming efficacy of DEC-205 targeted DNA vaccine in mice can be enhanced using adenoviral vector boost immunization regimen [110].

In a recent study, the immunogenicity of a multi-component DNA construct expressing a DEC-205 targeted antigen fused to a CD40L was evaluated. This vaccine construct was administered with DNA encoded Flt3-ligand and GM-CSF

for DC recruitment [111]. Immunization of calves with DEC-205 targeting construct mixed with the cytokine constructs induced significantly higher antibody responses, CD4 T cell proliferation, and increased number of IFN- γ producing CD4 T cells.

1.4.3 Strategies for DNA delivery

The initial method of DNA vaccination in vivo involved the injection of naked plasmid DNA. However, the efficiency of immune responses is generally low, presumably because DNA itself is not able to enter cells and is prone to degradation by extracellular nucleases. Therefore to enhance DNA delivery and transfection efficiency viral and non-viral vectors are used (reviewed in [112]). Viral vectors are by far the most efficient but they are associated with several safety concerns such as immune response to vector itself, difficulty in manufacturing, oncogenicity of transduced cells and limited DNA carrying capacity. On the other hand, non-viral vectors are gaining increased interest because of their improved safety profile, ease of preparation and adjuvant properties [112].

A myriad of non-viral carriers are currently investigated for DNA delivery including: biodegradable PLGA NPs [113], cationic liposomes [114], polycationic dendrimers [115], cationic block copolymers [116], and cationic polymers such as poly-L-lysine (PLL) [117] and polyethylenimines (PEI) [118] and chitosan [119]. In the next section, the focus will be on the applications of chitosan as a nasal DNA delivery system.

1.4.4 Chitosan as DNA carrier

Chitosan is a linear cationic polysaccharide, consisting of randomly distributed D-glucosamine and N-acetyl-D-glucosamine units, linked via β (1,4) glycosidic bonds (**Figure 1.5**) [120]. Chitosan is obtained by the alkaline deacetylation of chitin, a naturally occurring polysaccharide that is the major component of crustacean exoskeletons. The interest in chitosan as DNA delivery carrier arise

from several beneficial qualities such as availability, excellent safety-profile (low cytotoxicity and immunogenicity), biodegradability and unique biological properties due to polycationic nature [121].

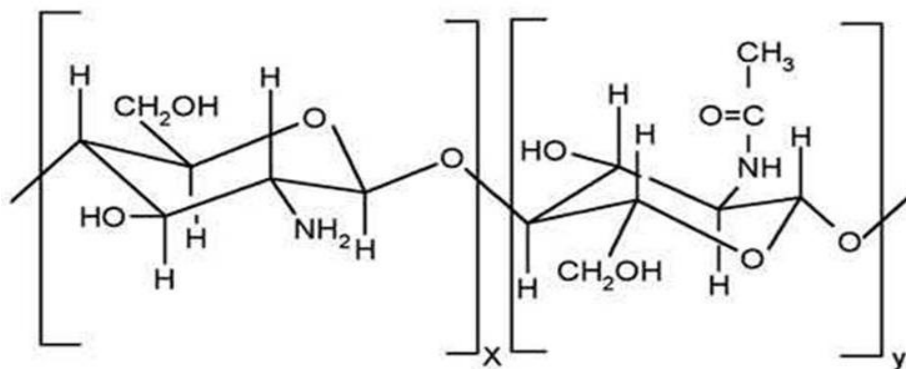


Figure 1.5 Chemical structure of chitosan. x and y represent number of D-glucosamine and N-acetyl-D-glucosamine, respectively.

The potential application of chitosan as a DNA delivery carrier is based on the presence of high cationic charge on chitosan backbone. Every D-glucosamine unit of chitosan contains a primary amine group with a pKa value of ~6.5. At acidic pH, below the pKa, the primary amine groups on glucosamine become positively charged and confer a high charge density. These protonated amine groups allow chitosan to form spontaneous complexes with anionic phosphate groups in nucleic acid backbone via electrostatic interaction [122]. Under neutral and alkaline conditions, chitosan is slightly charged and can associate with DNA molecules via hydrogen bonding and hydrophobic interactions [123].

One of chitosan's advantages is the relative simplicity in tailoring its backbone to generate delivery systems that impart target specificity and possibly improve the transfection efficiency. In one study, grafting mannose residues to chitosan was

shown to promote receptor-mediated uptake of nanoparticles into peritoneal macrophages and improved transfection efficiency [124].

Chitosan and its derivatives are extensively evaluated as DNA delivery system for in vitro and in vivo applications with particular emphasis on nasal mucosal delivery (reviewed in [125, 126]). Intranasal delivery of chitosan loaded plasmid DNA encoding for pneumococcal surface antigen A (PsaA) was shown induce antigen-specific mucosal IgA, humoral IgG, enhanced interferon-gamma (IFN- γ) secretion and protected mice against nasopharyngeal colonization by streptococcus pneumonia [127]. One study has demonstrated that intranasal delivery of chitosan nanoparticles containing a cocktail of plasmid DNA encoding for respiratory syncytial virus (RSV) antigens resulted in induction of RSV-specific IgG, nasal IgA, cytotoxic T lymphocytes, and interferon-gamma (IFN- γ) production in the lung and splenocytes. Further, in a challenge experiment these formulations were shown to protect mice from acute RSV infection [128]. Another study showed that intranasal administration of chitosan nanoparticle loaded with DNA encoding for RSV M2 protein epitope induced antigen specific cytotoxic T lymphocytes in BALB/c mice and resulted in a significant reduction of virus load in lungs of mice [129]. Intranasal delivery of hepatitis B surface antigen (HBsAg) DNA containing chitosan nanoparticles was also shown to induce antigen-specific mucosal IgA and serum IgG responses [130]. The anti-HBsAg specific IgG titers after nasal delivery of DNA in chitosan nanoparticles were in the seroprotective range. Interestingly, intranasal immunization induced significantly higher levels of Th1 (IFN- γ and IL-2) cytokines compared with alum adsorbed HBsAg. Furthermore, chitosan DNA vaccine was shown to provide protective immune responses against Coxsackievirus B3 (CVB3) virus challenge in a mouse model. In this study intranasal delivery of chitosan-DNA encoding VP1, major structural protein of CVB3, produced higher levels of systemic IgG, mucosal IgA and cytotoxic T lymphocytes and resulted in a significant reduction of viral load after acute CVB3 infection [131].

1.5 Rationale

In the previous sections, we have provided evidence from the literature on the potential role of DCs in the innate and adaptive immune responses. It is also evident from current studies at preclinical stage that DCs play a central role in shaping the immune response against vaccine antigens. Therefore, to date various strategies are explored to harness the DCs in vaccination. Broadly, *ex vivo* loading and *in vivo* DC targeted delivery of antigens has been shown to improve the quality and magnitude of immune responses. Of these two strategies *in vivo* targeted delivery of antigens is promising from clinical applicability [31].

Delivery of antigens to DCs *in vivo* using DC-receptor targeting antibody has emerged as an elegant approach to design improved vaccines. However, one of the potential limitations of current targeting strategies is genetic engineering of recombinant antibody and antigen fusion protein. Further, a new construct has to be designed for each antigen, which is a time-consuming and often a laborious process.

To achieve DC selective targeting of antigens, we have previously employed a recombinant bifunctional fusion protein (bfFp) based vector [132]. In this system, a single chain variable fragment (scFv) that recognizes mouse DC DEC-205 receptor was fused with a truncated core-streptavidin domain. The truncated core-streptavidin arm can bind with any biotinylated antigen and anti-DEC-205 scFv imparts targeting specificity to DC DEC-205 receptor. The core-streptavidin (13.5 kDa) is a recombinant version of full-length streptavidin (16.5 kDa), that lacks proteinase susceptible terminal amino acid residues [133]. Therefore, the core-streptavidin has been shown to have better stability under physiological conditions and demonstrate comparative biotin-binding ability with that of full-length streptavidin [133].

Exploring bfFp based DEC-205 targeted delivery; we have demonstrated *in vivo* targeting of four different classes of soluble biotinylated antigens, namely, proteins, peptide, gangliosides and plasmid DNA as low-dose vaccines [132]. Using this approach, a low-dose of antigen (200 nanograms) in saline together

with anti-CD40 mAb as a DC maturation stimuli, was capable of inducing a strong humoral and cellular immune response in mice. Nevertheless, bfFp based DC-targeting approach has limited antigen-carrying capacity, exposes targeted antigens to enzymatic degradation and lacks sustained antigen-release profile to boost immune responses. Therefore, to overcome these limitations of bfFp, we thought to adopt nanoparticle based vaccine delivery systems. Furthermore, it is evident from literature discussed in this chapter that particulate vaccine delivery systems can serve as an elegant alternative to soluble antigens.

For our studies we selected severe acute respiratory syndrome coronavirus (SARS CoV) nucleocapsid (N) protein and avian influenza hemagglutinin (HA) as target antigens. The choice of SARS CoV N protein was based on the fact that it is highly conserved compared to other SARS antigens; therefore it could serve as a stable vaccine candidate [134]. Furthermore, SARS CoV N protein is abundantly shed during SARS infection and N protein specific antibodies and memory T cells can be detected in SARS-recovered patients [135, 136]. On the other hand, influenza hemagglutinin (HA) is a standard antigen of choice for seasonal and pandemic influenza vaccines. Furthermore, we selected plasmid DNA based approach for SARS and influenza vaccines. Since, the DNA based vaccine antigens can be promptly engineered and manufactured on a large-scale and this approach could minimise response time in case of future SARS and influenza pandemic outbreak.

SARS CoV and influenza viruses are transmitted through mucosal routes and cause a range of respiratory complications. Therefore, in this work we were particularly interested in intranasal delivery of DNA based vaccines as intranasal delivery of DNA vaccine could potentially mimic natural virus infection as encoded antigen will get expressed in the respiratory tract. Moreover, it is evident from the number of studies that delivery of vaccines via the nasal route has been shown to induce mucosal (IgA), humoral (IgG) and cellular immune response [137]. It is also evident that mucosal IgA antibodies play a central role in evading

the entry of pathogens in the respiratory tract and act as a first-line of defence at the mucosal surfaces of the body.

1.6 Hypothesis

In the current work, we explored the feasibility of targeting nanoparticle encapsulated antigens (DNA and protein) to dendritic cells with the help of bfFp. We hypothesize that bfFp based targeting of nanoparticle formulations will benefit from targeted delivery to DCs and lead to improved immune responses (**Figure 1.6**). Furthermore, bfFp targeted delivery of nanoparticle encapsulated antigen could be a potential vaccination strategy that can combine DC-targeting ability of bfFp and antigen-carrying capacity of nanoparticles. In this work, we adopted two strategies for DC-targeted delivery of plasmid DNA vaccines. In the first strategy, biotinylated chitosan was used as a delivery vehicle for plasmid DNA encoding for nucleocapsid (N) protein of severe acute respiratory syndrome coronavirus (SARS-CoV) and hemagglutinin (HA) protein of avian (H5N1) influenza virus. The plasmid DNA loaded chitosan NPs were functionalized with bfFp for DEC-205 receptor mediated DC targeting and evaluated for immune responses following intranasal delivery.

In the second strategy, we used a fusion DNA vaccine construct for in-situ DC targeted delivery of expressed antigen. Specifically, anti- DEC-205 scFv gene was fused with SARS CoV N protein gene and cloned in pVAX vector. For the delivery of protein antigen, biotinylated PLGA polymer was employed to formulate ovalbumin (OVA) loaded nanoparticles. These formulations were decorated with bfFp to accomplish DC targeting of encapsulated antigen.

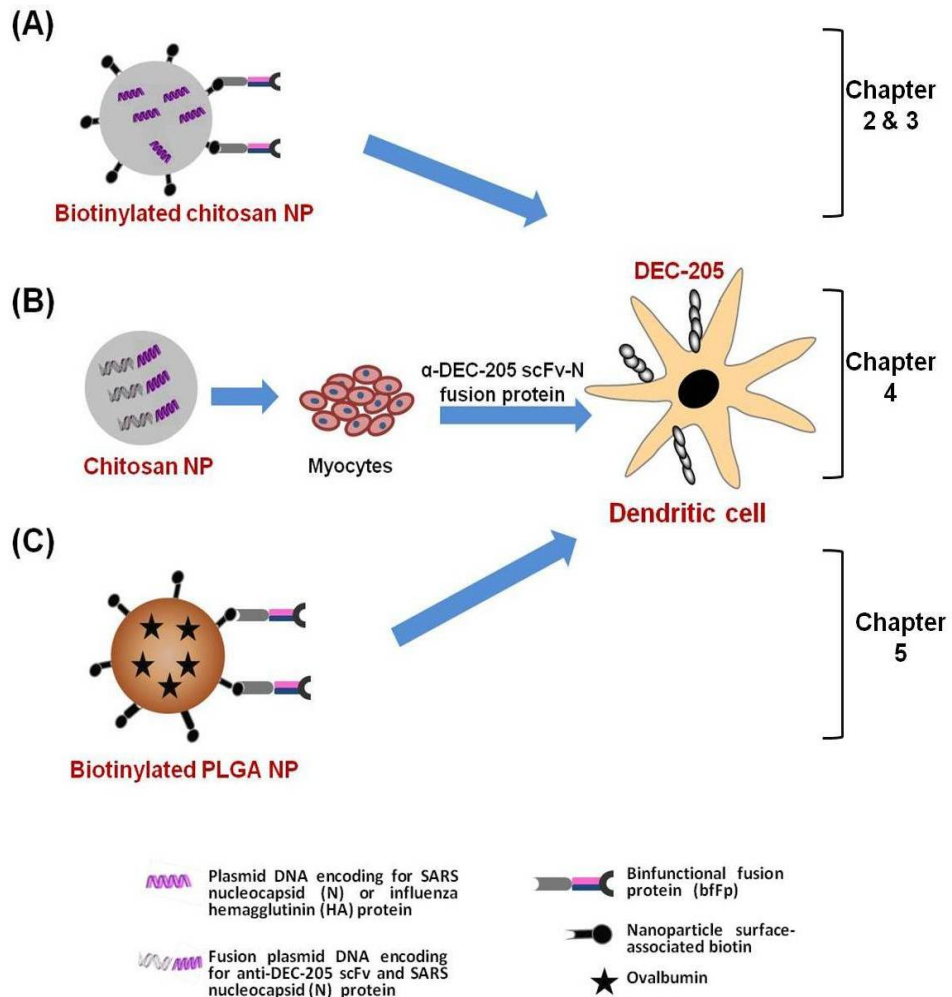


Figure 1.6 Research hypotheses. (A) Dendritic cell-targeted delivery of DNA loaded biotinylated chitosan NPs. The biotinylated chitosan NPs were formulated using biotinylated chitosan and plasmid DNA encoding for SARS CoV N protein or influenza hemagglutinin (HA). These NPs were decorated with bfFp for direct delivery of DNA vaccines to DCs. (B) Chitosan NPs for the delivery of fusion DNA vaccine. A fusion DNA construct encoding for anti-DEC scFv and SARS CoV N protein was constructed. Fusion DNA construct loaded chitosan NPs were synthesized to achieve in-situ targeted delivery of SARS CoV N protein to DCs. (C) Dendritic cell-targeted delivery of ovalbumin (OVA) loaded-biotinylated PLGA NPs. OVA-loaded biotinylated PLGA NPs were prepared using biotin-PEG-PLGA conjugate and decorated with bfFp to achieve DC targeted delivery of model antigen.

1.7 Objectives

- Formulation and evaluation of bfFp functionalized DC targeted chitosan nanoparticles for nasal DNA immunization against SARS CoV nucleocapsid (N) protein antigen (Chapter 2).
- Formulation and evaluation of bfFp functionalized DC targeted chitosan nanoparticles for nasal DNA immunization against hemagglutinin (HA) antigen of avian (H5N1) influenza A virus (Chapter 3).
- Formulation and evaluation of fusion DNA construct loaded-chitosan nanoparticles for in-situ DC targeted delivery of SARS CoV N protein (Chapter 4).
- Formulation and evaluation of bfFp functionalized DC targeted biotinylated PLGA NPs for the delivery of model antigen, ovalbumin (Chapter 5).

1.8 References

- [1] Steinman RM, Cohn ZA. Identification of a novel cell type in peripheral lymphoid organs of mice. I. Morphology, quantitation, tissue distribution. *J Exp Med* 1973;137:1142-62.
- [2] Steinman RM. Dendritic cells and the control of immunity. *Exp Hematol* 1998;26:681.
- [3] Steinman RM. The control of immunity and tolerance by dendritic cells. *Pathol Biol* 2003;51:59-60.
- [4] Shortman K, Naik SH. Steady-state and inflammatory dendritic-cell development. *Nat Rev Immunol* 2007;7:19-30.
- [5] Pulendran B, Tang H, Denning TL. Division of labor, plasticity, and crosstalk between dendritic cell subsets. *Curr Opin Immunol* 2008;20:61-7.
- [6] Pulendran B, Smith JL, Caspary G, Brasel K, Pettit D, Maraskovsky E, et al. Distinct dendritic cell subsets differentially regulate the class of immune response in vivo. *Proc Natl Acad Sci U S A* 1999;96:1036-41.
- [7] Maldonado-López R, De Smedt T, Michel P, Godfroid J, Pajak B, Heirman C, et al. CD8 α ⁺ and CD8 α ⁻ Subclasses of dendritic cells direct the development of distinct T helper cells in vivo. *J Exp Med* 1999;189:587-92.
- [8] Den Haan JMM, Lehar SM, Bevan MJ. CD8⁺ but not CD8⁻ dendritic cells cross-prime cytotoxic T cells in vivo. *J Exp Med* 2000;192:1685-95.
- [9] Pooley JL, Heath WR, Shortman K. Cutting edge: Intravenous soluble antigen is presented to CD4 T cells by CD8⁻ dendritic cells, but cross-presented to CD8 T cells by CD8⁺ dendritic cells. *J Immunol* 2001;166:5327-30.
- [10] Allan RS, Smith CM, Belz GT, Van Lint AL, Wakim LM, Heath WR, et al. Epidermal viral immunity induced by CD8 α ⁺ dendritic cells but not by langerhans cells. *Science* 2003;301:1925-8.
- [11] Iyoda T, Shimoyama S, Liu K, Omatsu Y, Akiyama Y, Maeda Y, et al. The CD8⁺ dendritic cell subset selectively endocytoses dying cells in culture and in vivo. *J Exp Med* 2002;195:1289-302.

- [12] Niess JH, Reinecker HC. Dendritic cells: The commanders-in-chief of mucosal immune defenses. *Current Opin Gastroen* 2006;22:354-60.
- [13] Alvarez D, Vollmann EH, von Andrian UH. Mechanisms and Consequences of Dendritic Cell Migration. *Immunity* 2008;29:325-42.
- [14] Hawiger D, Inaba K, Dorsett Y, Guo M, Mahnke K, Rivera M, et al. Dendritic cells induce peripheral T cell unresponsiveness under steady state conditions in vivo. *J Exp Med* 2001;194:769-79.
- [15] Granucci F, Vizzardelli C, Pavelka N, Feau S, Persico M, Virzi E, et al. Inducible IL-2 production by dendritic cells revealed by global gene expression analysis. *Nat Immunol* 2001;2:882-8.
- [16] Dalod M, Salazar-Mather TP, Malmgaard L, Lewis C, Asselin-Paturel C, Brière F, et al. Interferon α/β and interleukin 12 responses to viral infections: Pathways regulating dendritic cell cytokine expression in vivo. *J Exp Med* 2002;195:517-28.
- [17] Spörri R, Reis e Sousa C. Inflammatory mediators are insufficient for full dendritic cell activation and promote expansion of CD4⁺ T cell populations lacking helper function. *Nat Immunol* 2005;6:163-70.
- [18] Piqueras B, Connolly J, Freitas H, Palucka AK, Banchereau J. Upon viral exposure, myeloid and plasmacytoid dendritic cells produce 3 waves of distinct chemokines to recruit immune effectors. *Blood* 2006;107:2613-8.
- [19] Winzler C, Rovere P, Zimmermann VS, Davoust J, Rescigno M, Citterio S, et al. Checkpoints and functional stages in DC maturation. *Adv Exp Med Biol* 1997;417:59-64.
- [20] Trombetta ES, Mellman I. Cell biology of antigen processing in vitro and in vivo. *Annu Rev Immunol* 2005;23:975-1028.
- [21] Steinman RM, Pack M, Inaba K. Dendritic cell development and maturation. *Adv Exp Med Biol* 1997;417:1-6..
- [22] Fujii SI, Liu K, Smith C, Bonito AJ, Steinman RM. The linkage of innate to adaptive immunity via maturing dendritic cells in vivo requires CD40 ligation in

addition to antigen presentation and CD80/86 costimulation. *J Exp Med* 2004;199:1607-18.

[23] Soares H, Waechter H, Glaichenhaus N, Mougneau E, Yagita H, Mizenina O, et al. A subset of dendritic cells induces CD4 + T cells to produce IFN- γ by an IL-12-independent but CD70-dependent mechanism in vivo. *J Exp Med* 2007;204:1095-106.

[24] Kasturi SP, Skountzou I, Albrecht RA, Koutsonanos D, Hua T, Nakaya HI, et al. Programming the magnitude and persistence of antibody responses with innate immunity. *Nature* 2011;470:543-50.

[25] Cella M, Engering A, Pinet V, Pieters J, Lanzavecchia A. Inflammatory stimuli induce accumulation of MHC class II complexes on dendritic cells. *Nature* 1997;388:782-7.

[26] Figdor CG, Van Kooyk Y, Adema GJ. C-type lectin receptors on dendritic cells and langerhans cells. *Nat Rev Immunol* 2002;2:77-84.

[27] Geijtenbeek TBH, Van Vliet SJ, Engering A, T Hart BA, Van Kooyk Y. Self- and nonself-recognition by C-type lectins on dendritic cells. *Annu Rev Immunol* 2004;22:33-54.

[28] Cambi A, Koopman M, Figdor CG. How C-type lectins detect pathogens. *Cell Microbiol* 2005;7:481-8.

[29] Van Vliet SJ, García-Vallejo JJ, Van Kooyk Y. Dendritic cells and C-type lectin receptors: Coupling innate to adaptive immune responses. *Immunol Cell Biol* 2008;86:580-7.

[30] Kerrigan AM, Brown GD. C-type lectins and phagocytosis. *Immunobiology* 2009;214:562-75.

[31] Tacke PJ, De Vries IJM, Torensma R, Figdor CG. Dendritic-cell immunotherapy: From ex vivo loading to in vivo targeting. *Nat Rev Immunol* 2007;7:790-802.

[32] Jian W, Swiggard WJ, Heufler C, Peng M, Mirza A, Steinman RM, et al. The receptor DEC-205 expressed by dendritic cells and thymic epithelial cells is involved in antigen processing. *Nature* 1995;375:151-5.

- [33] Witmer-Pack MD, Swiggard WJ, Mirza A, Inaba K, Steinman RM. Tissue distribution of the DEC-205 protein that is detected by the monoclonal antibody NLDC-145 II. Expression in situ in lymphoid and nonlymphoid tissues. *Cell Immunol* 1995;163:157-62.
- [34] Mahnke K, Guo M, Lee S, Sepulveda H, Swain SL, Nussenzweig M, et al. The dendritic cell receptor for endocytosis, DEC-205, can recycle and enhance antigen presentation via major histocompatibility complex class II-positive lysosomal compartments. *J Cell Biol* 2000;151:673-83.
- [35] Bonifaz L, Bonnyay D, Mahnke K, Rivera M, Nussenzweig MC, Steinman RM. Efficient targeting of protein antigen to the dendritic cell receptor DEC-205 in the steady state leads to antigen presentation on major histocompatibility complex class I products and peripheral CD8 + T cell tolerance. *J Exp Med* 2002;196:1627-38.
- [36] Guo M, Gong S, Maric S, Misulovin Z, Pack M, Mahnke K, et al. A monoclonal antibody to the DEC-205 endocytosis receptor on human dendritic cells. *Hum Immunol* 2000;61:729-38.
- [37] Kato M, McDonald KJ, Khan S, Ross IL, Vuckovic S, Chen K, et al. Expression of human DEC-205 (CD205) multilectin receptor on leukocytes. *Int Immunol* 2006;18:857-69.
- [38] Bonifaz LC, Bonnyay DP, Charalambous A, Darguste DI, Fujii SI, Soares H, et al. In Vivo Targeting of Antigens to Maturing Dendritic Cells via the DEC-205 Receptor Improves T Cell Vaccination. *J Exp Med* 2004;199:815-24.
- [39] Butler M, Morel AS, Jordan WJ, Eren E, Hue S, Shrimpton RE, et al. Altered expression and endocytic function of CD205 in human dendritic cells, and detection of a CD205-DCL-1 fusion protein upon dendritic cell maturation. *Immunology* 2007;120:362-71.
- [40] Wang B, Kuroiwa JMY, He LZ, Charalambous A, Keler T, Steinman RM. The human cancer antigen mesothelin is more efficiently presented to the mouse immune system when targeted to the DEC-205/CD205 receptor on dendritic cells. *Ann NY Acad Sci* 2009;1174:6-17.

- [41] Small M, Kraal G. In vitro evidence for participation of DEC-205 expressed by thymic cortical epithelial cells in clearance of apoptotic thymocytes. *Int Immunol* 2003;15:197-203.
- [42] Shrimpton RE, Butler M, Morel AS, Eren E, Hue SS, Ritter MA. CD205 (DEC-205): A recognition receptor for apoptotic and necrotic self. *Mol Immunol* 2009;46:1229-39.
- [43] Van Broekhoven CL, Parish CR, Demangel C, Britton WJ, Altin JG. Targeting dendritic cells with antigen-containing liposomes: A highly effective procedure for induction of antitumor immunity and for tumor immunotherapy. *Cancer Res* 2004;64:4357-65.
- [44] Kwon YJ, James E, Shastri N, Fréchet JMJ. In vivo targeting of dendritic cells for activation of cellular immunity using vaccine carriers based on pH-responsive microparticles. *Proc Natl Acad Sci U S A* 2005;102:18264-8.
- [45] Mahnke K, Qian Y, Fondel S, Brueck J, Becker C, Enk AH. Targeting of antigens to activated dendritic cells in vivo cures metastatic melanoma in mice. *Cancer Res* 2005;65:7007-12.
- [46] Bozzacco L, Trumpfheller C, Siegal FP, Mehandru S, Markowitz M, Carrington M, et al. DEC-205 receptor on dendritic cells mediates presentation of HIV gag protein to CD8+ T cells in a spectrum of human MHC I haplotypes. *Proc Natl Acad Sci U S A* 2007;104:1289-94.
- [47] Boscardin SB, Hafalla JCR, Masilamani RF, Kamphorst AO, Zebroski HA, Rai U, et al. Antigen targeting to dendritic cells elicits long-lived T cell help for antibody responses. *J Exp Med* 2006;203:599-606.
- [48] Mukhopadhyaya A, Hanafusa T, Jarchum I, Chen YG, Iwai Y, Serreze DV, et al. Selective delivery of β cell antigen to dendritic cells in vivo leads to deletion and tolerance of autoreactive CD8+ T cells in NOD mice. *Proc Natl Acad Sci U S A* 2008;105:6374-9.
- [49] Charalambous A, Oks M, Nchinda G, Yamazaki S, Steinman RM. Dendritic cell targeting of survivin protein in a xenogeneic form elicits strong CD4+ T cell immunity to mouse survivin. *J Immunol* 2006;177:8410-21.

- [50] Do Y, Koh H, Park CG, Dudziak D, Seo P, Mehandru S, et al. Targeting of LcrV virulence protein from *Yersinia pestis* to dendritic cells protects mice against pneumonic plague. *Eur J Immunol* 2010;40:2791-6.
- [51] Keler T, Ramakrishna V, Fanger MW. Mannose receptor-targeted vaccines. *Expert Opin Biol Ther* 2004;4:1953-62.
- [52] Sallusto F, Cella M, Danieli C, Lanzavecchia A. Dendritic cells use macropinocytosis and the mannose receptor to concentrate macromolecules in the major histocompatibility complex class II compartment: Downregulation by cytokines and bacterial products. *J Exp Med* 1995;182:389-400.
- [53] Tan MCAA, Mommaas AM, Drijfhout JW, Jordens R, Onderwater JJM, Verwoerd D, et al. Mannose receptor-mediated uptake of antigens strongly enhances HLA class II-restricted antigen presentation by cultured dendritic cells. *Eur J Immunol* 1997;27:2426-35.
- [54] Apostolopoulos V, Barnes N, Pietersz GA, McKenzie IFC. Ex vivo targeting of the macrophage mannose receptor generates anti-tumor CTL responses. *Vaccine* 2000;18:3174-84.
- [55] Burgdorf S, Lukacs-Kornek V, Kurts C. The mannose receptor mediates uptake of soluble but not of cell-associated antigen for cross-presentation. *J Immunol* 2006;176:6770-6.
- [56] Tietze C, Schlesinger P, Stahl P. Mannose-specific endocytosis receptor of alveolar macrophages: Demonstration of two functionally distinct intracellular pools of receptor and their roles in receptor recycling. *J Cell Biol* 1982;92:417-24.
- [57] Stahl PD. The mannose receptor and other macrophage lectins. *Curr Opin Immunol* 1992;4:49-52.
- [58] McGreal EP, Miller JL, Gordon S. Ligand recognition by antigen-presenting cell C-type lectin receptors. *Curr Opin Immunol* 2005;17:18-24.
- [59] Pietersz GA, Li W, Popovski V, Caruana JA, Apostolopoulos V, McKenzie IFC. Parameters for using mannan-MUC1 fusion protein to induce cellular immunity. *Cancer Immunol Immunother* 1998;45:321-6.

- [60] McKenzie IFC, Apostolopoulos V, Lees C, Xing PX, Lofthouse S, Osinski C, et al. Oxidised mannan antigen conjugates preferentially stimulate T1 type immune responses. *Vet Immunol Immunopathol* 1998;63:185-90.
- [61] Ramakrishna V, Treml JF, Vitale L, Connolly JE, O'Neill T, Smith PA, et al. Mannose receptor targeting of tumor antigen pmel17 to human dendritic cells directs anti-melanoma T cell responses via multiple HLA molecules. *J Immunol* 2004;172:2845-52.
- [62] He LZ, Crocker A, Lee J, Mendoza-Ramirez J, Wang XT, Vitale LA, et al. Antigenic targeting of the human mannose receptor induces tumor immunity. *J Immunol* 2007;178:6259-67.
- [63] Geijtenbeek TBH, Krooshoop DJEB, Bleijs DA, Van Vliet SJ, Van Duijnhoven GCF, Grabovsky V, et al. DC-SIGN-1CAM-2 interaction mediates dendritic cell trafficking. *Nat Immunol* 2000;1:353-7.
- [64] Soilleux EJ, Morris LS, Leslie G, Chehimi J, Luo Q, Levroney E, et al. Constitutive and induced expression of DC-SIGN on dendritic cell and macrophage subpopulations in situ and in vitro. *J Leukoc Biol* 2002;71:445-57.
- [65] Geijtenbeek TBH, Van Duijnhoven GCF, Van Vliet SJ, Krieger E, Vriend G, Figdor CG, et al. Identification of different binding sites in the dendritic cell-specific receptor DC-SIGN for intercellular adhesion molecule 3 and HIV-1. *J Biol Chem* 2002;277:11314-20.
- [66] Caminschi I, Corbett AJ, Zahra C, Lahoud M, Lucas KM, Sofi M, et al. Functional comparison of mouse CIRE/mouse DC-SIGN and human DC-SIGN. *Int Immunol* 2006;18:741-53.
- [67] Koppel EA, Ludwig IS, Appelmelk BJ, van Kooyk Y, Geijtenbeek TBH. Carbohydrate specificities of the murine DC-SIGN homologue mSIGNR1. *Immunobiology* 2005;210:195-201.
- [68] Bashirova AA, Geijtenbeek TBH, Van Duijnhoven GCF, Van Vliet SJ, Eilering JBG, Martin MP, et al. A dendritic cell-specific intercellular adhesion molecule 3-grabbing nonintegrin (DC-SIGN)-related protein is highly expressed

on human liver sinusoidal endothelial cells and promotes HIV-1 infection. *J Exp Med* 2001;193:671-8.

[69] Schjetne KW, Thompson KM, Aarvak T, Fleckenstein B, Sollid LM, Bogen B. A mouse C κ -specific T cell clone indicates that DC-SIGN is an efficient target for antibody-mediated delivery of T cell epitopes for MHC class II presentation. *Int Immunol* 2002;14:1423-30.

[70] Tacke PJ, De Vries IJM, Gijzen K, Joosten B, Wu D, Rother RP, et al. Effective induction of naive and recall T-cell responses by targeting antigen to human dendritic cells via a humanized anti-DC-SIGN antibody. *Blood* 2005;106:1278-85.

[71] Dakappagari N, Maruyama T, Renshaw M, Tacke P, Figdor C, Torensma R, et al. Internalizing antibodies to the C-type lectins, L-SIGN and DC-SIGN, inhibit viral glycoprotein binding and deliver antigen to human dendritic cells for the induction of T cell responses. *J Immunol* 2006;176:426-40.

[72] Tacke PJ, Figdor CG. Targeted antigen delivery and activation of dendritic cells in vivo: Steps towards cost effective vaccines. *Semin Immunol* 2011;23:12-20.

[73] Caminschi I, Maraskovsky E, Heath WR. Targeting dendritic cells in vivo for cancer therapy. *Front Immunol* 2012;3.

[74] Joshi MD, Unger WJ, Storm G, van Kooyk Y, Mastrobattista E. Targeting tumor antigens to dendritic cells using particulate carriers. *J Control Release* 2012;161:25-37.

[75] Caminschi I, Shortman K. Boosting antibody responses by targeting antigens to dendritic cells. *Trends Immunol* 2012;33:71-7.

[76] Hamdy S, Molavi O, Ma Z, Haddadi A, Alshamsan A, Gobti Z, et al. Co-delivery of cancer-associated antigen and Toll-like receptor 4 ligand in PLGA nanoparticles induces potent CD8 + T cell-mediated anti-tumor immunity. *Vaccine* 2008;26:5046-57.

[77] Schlosser E, Mueller M, Fischer S, Basta S, Busch DH, Gander B, et al. TLR ligands and antigen need to be coencapsulated into the same biodegradable

microsphere for the generation of potent cytotoxic T lymphocyte responses. *Vaccine* 2008;26:1626-37.

[78] Manolova V, Flace A, Bauer M, Schwarz K, Saudan P, Bachmann MF. Nanoparticles target distinct dendritic cell populations according to their size. *Eur J Immunol* 2008;38:1404-13.

[79] Reddy ST, Rehor A, Schmoekel HG, Hubbell JA, Swartz MA. In vivo targeting of dendritic cells in lymph nodes with poly(propylene sulfide) nanoparticles. *J Control Release* 2006;112:26-34.

[80] De Temmerman ML, Rejman J, Demeester J, Irvine DJ, Gander B, De Smedt SC. Particulate vaccines: On the quest for optimal delivery and immune response. *Drug Discov Today* 2011;16:569-82.

[81] Hamdy S, Haddadi A, Hung RW, Lavasanifar A. Targeting dendritic cells with nano-particulate PLGA cancer vaccine formulations. *Adv Drug Del Rev* 2011;63:943-55.

[82] Jain S, O'Hagan DT, Singh M. The long-term potential of biodegradable poly(lactide-co-glycolide) microparticles as the next-generation vaccine adjuvant. *Expert Rev Vaccines* 2011;10:1731-42.

[83] Mundargi RC, Babu VR, Rangaswamy V, Patel P, Aminabhavi TM. Nano/micro technologies for delivering macromolecular therapeutics using poly(d,l-lactide-co-glycolide) and its derivatives. *J Control Release* 2008;125:193-209.

[84] Elamanchili P, Lutsiak CME, Hamdy S, Diwan M, Samuel J. "Pathogen-mimicking" nanoparticles for vaccine delivery to dendritic cells. *J Immunother*. 2007;30:378-95.

[85] Zhang Z, Tongchusak S, Mizukami Y, Kang YJ, Ioji T, Touma M, et al. Induction of anti-tumor cytotoxic T cell responses through PLGA-nanoparticle mediated antigen delivery. *Biomaterials* 2011;32:3666-78.

[86] Cruz LJ, Tacke PJ, Fokkink R, Joosten B, Stuart MC, Albericio F, et al. Targeted PLGA nano- but not microparticles specifically deliver antigen to human dendritic cells via DC-SIGN in vitro. *J Control Release* 2010;144:118-26.

- [87] Bandyopadhyay A, Fine RL, Demento S, Bockenstedt LK, Fahmy TM. The impact of nanoparticle ligand density on dendritic-cell targeted vaccines. *Biomaterials* 2011;32:3094-105.
- [88] Tacke PJ, Zeelenberg IS, Cruz LJ, Van Hout-Kuijter MA, Van De Glind G, Fokink RG, et al. Targeted delivery of TLR ligands to human and mouse dendritic cells strongly enhances adjuvanticity. *Blood* 2011;118:6836-44.
- [89] Wolff JA, Malone RW, Williams P, Wang C, Acsadi G, Jani A, et al. Direct gene transfer into mouse muscle in vivo. *Science* 1990;247:1465-8.
- [90] Tang D, DeVit M, Johnston SA. Genetic immunization is a simple method for eliciting an immune response. *Nature* 1992;356:152-4.
- [91] Ulmer JB, Donnelly JJ, Parker SE, Rhodes GH, Felgner PL, Dworkin RJ, et al. Heterologous protection against influenza by injection of DNA encoding a viral protein. *Science* 1993;259:1745-9.
- [92] Fynan EF, Webster RG, Fuller DH, Haynes JR, Santoro JC, Robinson HL. DNA vaccines: Protective immunizations by parenteral, mucosal, and gene-gun inoculations. *Proc Natl Acad Sci U S A* 1993;90:11478-82.
- [93] Wang B, Ugen KE, Srikantan V, Agadjanyan MG, Dang K, Refaelli Y, et al. Gene inoculation generates immune responses against human immunodeficiency virus type 1. *Proc Natl Acad Sci U S A* 1993;90:4156-60.
- [94] Liu MA. DNA vaccines: An historical perspective and view to the future. *Immunol Rev* 2011;239:62-84.
- [95] Kutzler MA, Weiner DB. DNA vaccines: Ready for prime time? *Nat Rev Genet* 2008;9:776-88.
- [96] Shedlock DJ, Weiner DB. DNA vaccination: Antigen presentation and the induction of immunity. *J Leukoc Biol* 2000;68:793-806.
- [97] Manoj S, Babiuk LA, Van Drunen Littel-van Den Hurk S. Approaches to enhance the efficacy of DNA vaccines. *Crit Rev Clin Lab Sci* 2004;41:1-39.
- [98] Tsen SWD, Paik AH, Hung CF, Wu TC. Enhancing DNA vaccine potency by modifying the properties of antigen-presenting cells. *Expert Rev Vaccines* 2007;6:227-39.

- [99] Kutzler MA, Weiner DB. Developing DNA vaccines that call to dendritic cells. *J Clin Invest* 2004;114:1241-4.
- [100] Hattori Y, Kawakami S, Nakamura K, Yamashita F, Hashida M. Efficient gene transfer into macrophages and dendritic cells by in vivo gene delivery with mannosylated lipoplex via the intraperitoneal route. *J Pharmacol Exp Ther* 2006;318:828-34.
- [101] Hattori Y, Kawakami S, Suzuki S, Yamashita F, Hashida M. Enhancement of immune responses by DNA vaccination through targeted gene delivery using mannosylated cationic liposome formulations following intravenous administration in mice. *Biochem Biophys Res Commun* 2004;317:992-9.
- [102] Un K, Kawakami S, Suzuki R, Maruyama K, Yamashita F, Hashida M. Enhanced transfection efficiency into macrophages and dendritic cells by a combination method using mannosylated lipoplexes and bubble liposomes with ultrasound exposure. *Hum Gene Ther* 2010;21:65-74.
- [103] Moulin V, Morgan ME, Eleveld-Trancikova D, Haanen JBAG, Wielders E, Looman MWG, et al. Targeting dendritic cells with antigen via dendritic cell-associated promoters. *Cancer Gene Ther* 2012;19:303-11.
- [104] Sudowe S, Ludwig-Portugall I, Montermann E, Ross R, Reske-Kunz AB. Prophylactic and therapeutic intervention in IgE responses by biolistic DNA vaccination primarily targeting dendritic cells. *J Allergy Clin Immunol* 2006;117:196-203.
- [105] Ni J, Nolte B, Arnold A, Fournier P, Schirmacher V. Targeting anti-tumor DNA vaccines to dendritic cells via a short CD11c promoter sequence. *Vaccine* 2009;27:5480-7.
- [106] Hauser H, Chen SY. Augmentation of DNA vaccine potency through secretory heat shock protein-mediated antigen targeting. *Methods* 2003;31:225-31.
- [107] Yao Q, Fischer KP, Li L, Agrawal B, Berhane Y, Tyrrell DL, et al. Immunogenicity and protective efficacy of a DNA vaccine encoding a chimeric

protein of avian influenza hemagglutinin subtype H5 fused to CD154 (CD40L) in Pekin ducks. *Vaccine* 2010;28:8147-56.

[108] Demangel C, Zhou J, Choo ABH, Shoebridge G, Halliday GM, Britton WJ. Single chain antibody fragments for the selective targeting of antigens to dendritic cells. *Mol Immunol* 2005;42:979-85.

[109] Nchinda G, Kuroiwa J, Oks M, Trumpfheller C, Chae GP, Huang Y, et al. The efficacy of DNA vaccination is enhanced in mice by targeting the encoded protein to dendritic cells. *J Clin Invest* 2008;118:1427-36.

[110] Grossmann C, Tenbusch M, Nchinda G, Temchura V, Nabi G, Stone GW, et al. Enhancement of the priming efficacy of DNA vaccines encoding dendritic cell-targeted antigens by synergistic toll-like receptor ligands. *BMC Immunol* 2009;10:43.

[111] Njongmeta LM, Bray J, Davies CJ, Davis WC, Howard CJ, Hope JC, et al. CD205 antigen targeting combined with dendritic cell recruitment factors and antigen-linked CD40L activation primes and expands significant antigen-specific antibody and CD4 + T cell responses following DNA vaccination of outbred animals. *Vaccine* 2012;30:1624-35.

[112] Nguyen DN, Green JJ, Chan JM, Langer R, Anderson DG. Polymeric materials for gene delivery and DNA vaccination. *Adv Mater* 2009;21:847-67.

[113] O'Hagan DT, Singh M, Dong C, Ugozzoli M, Berger K, Glazer E, et al. Cationic microparticles are a potent delivery system for a HCV DNA vaccine. *Vaccine* 2004;23:672-80.

[114] Henderson A, Propst K, Kedl R, Dow S. Mucosal immunization with liposome-nucleic acid adjuvants generates effective humoral and cellular immunity. *Vaccine* 2011;29:5304-12.

[115] Daftarian P, Kaifer AE, Li W, Blomberg BB, Frasca D, Roth F, et al. Peptide-conjugated PAMAM dendrimer as a universal DNA vaccine platform to target antigen-presenting cells. *Cancer Res* 2011;71:7452-62.

[116] Lai TC, Kataoka K, Kwon GS. Pluronic-based cationic block copolymer for forming pDNA polyplexes with enhanced cellular uptake and improved transfection efficiency. *Biomaterials* 2011;32:4594-603.

- [117] Incani V, Lin X, Lavasanifar A, Uludağ H. Relationship between the extent of lipid substitution on poly(l-lysine) and the DNA delivery efficiency. *ACS Appl Mater Interfaces* 2009;1:841-8.
- [118] Hsu CYM, Hendzel M, Uludağ H. Improved transfection efficiency of an aliphatic lipid substituted 2 kDa polyethylenimine is attributed to enhanced nuclear association and uptake in rat bone marrow stromal cell. *J Gene Med* 2011;13:46-59.
- [119] MacLaughlin FC, Mumper RJ, Wang J, Tagliaferri JM, Gill I, Hinchcliffe M, et al. Chitosan and depolymerized chitosan oligomers as condensing carriers for in vivo plasmid delivery. *J Control Release* 1998;56:259-72.
- [120] Rinaudo M. Chitin and chitosan: Properties and applications. *Progress in Polymer Science (Oxford)*. 2006;31:603-32.
- [121] Mao S, Sun W, Kissel T. Chitosan-based formulations for delivery of DNA and siRNA. *Adv Drug Del Rev* 2010;62:12-27.
- [122] Ishii T, Okahata Y, Sato T. Mechanism of cell transfection with plasmid/chitosan complexes. *Biochim Biophys Acta* 2001;1514:51-64.
- [123] Messai I, Lamalle D, Munier S, Verrier B, Ataman-Önal Y, Delair T. Poly(d,l-lactic acid) and chitosan complexes: interactions with plasmid DNA. *Colloid Surface A* 2005;255:65-72.
- [124] Hashimoto M, Morimoto M, Saimoto H, Shigemasa Y, Yanagie H, Eriguchi M, et al. Gene transfer by DNA/mannosylated chitosan complexes into mouse peritoneal macrophages. *Biotechnol Lett* 2006;28:815-21.
- [125] Alpar HO, Somavarapu S, Atuah KN, Bramwell VW. Biodegradable mucoadhesive particulates for nasal and pulmonary antigen and DNA delivery. *Adv Drug Deliv Rev* 2005;57:411-30.
- [126] Kang ML, Cho CS, Yoo HS. Application of chitosan microspheres for nasal delivery of vaccines. *Biotechnol Adv* 2009;27:857-65.
- [127] Xu J, Dai W, Wang Z, Chen B, Li Z, Fan X. Intranasal vaccination with chitosan-DNA nanoparticles expressing pneumococcal surface antigen A protects mice against nasopharyngeal colonization by *Streptococcus pneumoniae*. *Clin Vaccine Immunol* 2011;18:75-81.

- [128] Kumar M, Mohapatra SS, Behera AK, Lockey RF, Zhang J, Bhullar G, et al. Intranasal gene transfer by chitosan-DNA nanospheres protects BALB/c mice against acute respiratory syncytial virus infection. *Hum Gene Ther* 2002;13:1415-25.
- [129] Iqbal M, Lin W, Jabbal-Gill I, Davis SS, Steward MW, Illum L. Nasal delivery of chitosan-DNA plasmid expressing epitopes of respiratory syncytial virus (RSV) induces protective CTL responses in BALB/c mice. *Vaccine* 2003;21:1478-85.
- [130] Khatri K, Goyal AK, Gupta PN, Mishra N, Vyas SP. Plasmid DNA loaded chitosan nanoparticles for nasal mucosal immunization against hepatitis B. *Int J Pharm* 2008;354:235-41.
- [131] Xu W, Shen Y, Jiang Z, Wang Y, Chu Y, Xiong S. Intranasal delivery of chitosan-DNA vaccine generates mucosal SIgA and anti-CVB3 protection. *Vaccine* 2004;22:3603-12.
- [132] Wang WW, Das D, Suresh MR. A Versatile Bifunctional Dendritic Cell Targeting Vaccine Vector. *Mol Pharm* 2009;6:158-72.
- [133] Sano T, Pandori MW, Chen X, Smith CL, Cantor CR. Recombinant Core Streptavidins. *J Biol Chem* 1995;270:28204-9.
- [134] Surjit M, Lal SK. The SARS-CoV nucleocapsid protein: A protein with multifarious activities. *Infect Genet Evol* 2008;8:397-405.
- [135] Rota PA, Oberste MS, Monroe SS, Nix WA, Campagnoli R, Icenogle JP, et al. Characterization of a Novel Coronavirus Associated with Severe Acute Respiratory Syndrome. *Science* 2003;300:1394-9.
- [136] Peng H, Yang L-t, Wang L-y, Li J, Huang J, Lu Z-q, et al. Long-lived memory T lymphocyte responses against SARS coronavirus nucleocapsid protein in SARS-recovered patients. *Virology* 2006;351:466-75.
- [137] Neutra MR, Kozlowski PA. Mucosal vaccines: the promise and the challenge. *Nat Rev Immunol.* 2006;6:148-58.

**CHAPTER 2: Dendritic cell targeted chitosan
nanoparticles for nasal DNA immunization against SARS
CoV nucleocapsid protein**

The content of this chapter has been published in *Molecular Pharmaceutics* 2012.

Raghuwanshi D, Mishra V, Das D, Kaur K, Suresh MR. Dendritic Cell Targeted Chitosan Nanoparticles for Nasal DNA Immunization against SARS CoV Nucleocapsid Protein. *Molecular Pharmaceutics* 2012; 9:946-56.

2.1 Introduction

Dendritic cells (DCs) are specialized antigen-presenting cells (APCs) that play a key role in the immune response by antigen uptake, processing and presentation. Among all APCs, the DCs are considered as the most efficient cells for induction and regulation of immune responses [1]. Various strategies employed to harness DC selective targeting of vaccine antigens have shown enormous potential at preclinical stage for designing low-dose vaccines [2]. DCs express a large number of endocytic receptors, such as C-type lectin receptors (CLRs) through which they recognize and take up pathogens.

Different strategies employed for targeted delivery of antigen to DCs utilize the help of antibodies or natural ligands against DC restricted CLRs. The antigen targeting to CLRs has resulted in augmented immune response, dose-sparing of antigen and skewing of immune responses [2-4]. Among CLRs, DC C-type lectin receptor DEC-205 (CD 205) receptor is best characterized. The DEC-205 is a member of the type I C-type lectin receptor family, which is primarily expressed by immature DC in skin, lymph nodes and spleen [5, 6]. The intracellular routing of DEC-205 targeted antigens enhances loading and presentation of antigenic peptides on MHC class I and class II molecules, leading to priming of antigen specific CD8⁺ and CD4⁺ T cells, respectively [7,8]. The *in vivo* targeting of antigens to murine DEC-205 receptor along with maturation stimuli has been shown to augment the efficiency of antigen presentation to both CD4⁺ and CD8⁺ T-cells [9].

To achieve DC selective targeting of biotinylated protein antigen, we have previously developed a quadroma (hybrid-hybridoma) based full-length bispecific monoclonal antibody (bsmAb). The full-length hybrid-hybridoma based bsmAb can bind with biotinylated antigen through one arm and target DEC-205 through the other arm [10]. Targeting of biotinylated ovalbumin (OVA) using bsmAb reduced the dose of antigen by ~500-fold compared with nontargeted antigen. However, quadromas produce bsmAb along with parental and unwanted heavy

and light chain combinations resulting in lower yield. Additionally, the antibody-based biotin binding is several orders weaker than the streptavidin binding.

Consequently, to overcome inherent limitations associated with bsmAb, we designed a recombinant bifunctional fusion protein (bfFp) vector for DC targeting [11]. A single chain variable fragment (scFv) that recognizes mouse DC DEC-205 was fused with a truncated core-streptavidin domain and expressed in *Escherichia coli* using the T7 expression system. The truncated core-streptavidin arm can bind with any biotinylated antigen and anti-DEC-205 scFv impart targeting specificity to DC DEC-205 receptor. Using bfFp we have demonstrated *in vivo* targeting of four different classes of biotinylated antigens, namely, proteins, peptide, gangliosides and plasmid DNA, as low-dose vaccines [11]. *In vivo* studies in mice with biotinylated OVA have shown that, in the presence of bfFp and anti-CD40 mAb, both humoral and cell-mediated responses can be augmented. In this targeting formulation, low concentration of antigen (200 ng) in saline was adequate to achieve a strong immune response in mice. In the multiple antigen targeting strategy, we also achieved enhanced humoral and cell-mediated responses for biotinylated OVA, SARS-CoV spike, Ebola glycoprotein (GP1), MUC-1 peptide, and anthrax protective antigen.

Herein, we selected nucleocapsid (N) protein of severe acute respiratory syndrome coronavirus (SARS-CoV) as vaccine antigen. The SARS-CoV contains four major structure proteins; membrane (M), spike (S), envelope (E), and nucleocapsid (N) [12, 13]. Studies have shown that N protein is highly conserved compared to other proteins such as S, E and M; therefore it could serve as a stable vaccine candidate [14]. Furthermore, N protein is abundantly shed during SARS infection and N protein specific antibodies and memory T cells can be detected in SARS-recovered patients [15, 16]. A number of studies have used recombinant N protein [17, 18] or DNA encoding N protein [19-21] as vaccine antigen to elicit humoral and cellular immune responses in animal models. In this context, we selected plasmid DNA encoding N protein (pVAXN) as vaccine antigen and chitosan as DNA delivery vehicle.

Chitosan is a natural polysaccharide consisting of repeated D-glucosamine and N-acetyl-D-glucosamine units, linked via β (1,4) glycosidic bond. The chitosan and its derivatives are ideal nucleic acid delivery vehicles due to their excellent biocompatible, biodegradable and nontoxic nature [22]. The presence of high cationic charge on chitosan provides strong binding affinity with nucleic acids resulting in an excellent gene delivery vehicle [23].

The aim of this chapter was to develop and characterize dendritic cell targeted chitosan nanoparticles as vaccine delivery systems via the nasal route. Mouse respiratory DCs subsets, such as airway DCs and alveolar DCs, express the DEC-205 receptor [24]. These respiratory DCs could serve as a primary target for uptake of targeted nanoparticles. Our strategy combines the pDNA carrying capacity of chitosan and selective targeting specificity of bfFp to respiratory DCs. Ultrapure water-soluble biotinylated chitosan hydrochloride was used to formulate pVAXN loaded nanoparticles. These pVAXN loaded biotinylated chitosan nanoparticles were surface functionalized with bifunctional fusion protein to achieve nasal DC targeting. Different NP formulations were given intranasally or intramuscularly to the mice to elicit the immune response, and the results of the immune response are presented here.

2.2 Materials and methods

2.2.1 Materials

Ultrapure chitosan hydrochloride salt (Protasan UP CL 113) was purchased from FMC Biopolymers AS (Novamatrix, Norway). pVAX1 vector and Lipofectamine 2000 were from Invitrogen (USA). Biotinamidohexanoic acid 3-sulfo-N-hydroxysuccinimide ester sodium salt (sulfo-NHS-LC-biotin), isopropyl- β -D-thiogalactopyranoside (IPTG), chitosanase (from *Streptomyces griseus*) and lysozyme were purchased from Sigma-Aldrich (Oakville, ON, Canada). Ni-NTA agarose resin was from Qiagen (Mississauga, Canada). Rat anti-mouse CD40 mAb was purified from 1C10 hybridoma, a kind gift from Dr. M. Gold

(University of British Columbia, Canada). The TMB (3,3',5,5'-tetramethylbenzidine) peroxidase substrate was from Kirkegaard and Perry Laboratory Inc. (Gaithersburg, MD). HRPO based mouse antibody isotyping kit was obtained from Southern Biotech (Birmingham, AL, USA). African green monkey SV40 transformed kidney (COS-1) cells were from American Type Culture Collection (ATCC). Dulbecco's modified Eagle medium (DMEM), penicillin–streptomycin–L-glutamine (PSG) and fetal bovine serum (FBS) were procured from Gibco (Burlington, Canada).

2.2.2 Plasmid DNA (pVAXN) construction and detection of SARS-N protein

SARS-CoV nucleocapsid (N) DNA sequence was polymerase chain reaction (PCR) amplified using pFastBacNP as DNA template with gene specific primers. The 5' primer contains a *Bam*HI restriction site, Kozak translation initiation sequence and initiation codon (ATG), and the 3' primer contains the stop codon and *Eco*RI restriction site. The PCR fragment was electrophoresed in 1% low melting point agarose gel and gel-purified using a Qiagen gel extraction kit. The purified fragment was then double digested with *Bam*HI and *Eco*RI and further gel purified. The purified fragment was ligated to *Bam*HI and *Eco*RI digested pVAX1 mammalian expression vector (Invitrogen, USA). The ligation mixture was transformed into TOP10 *E. coli* cells by the heat shock method and plated onto an LB agar plate containing 50 µg/mL of kanamycin. Recombinant positive clones were screened by plasmid DNA isolation using a Qiagen plasmid DNA isolation kit and restriction digestion fragment mapping. The resultant plasmid is designated as pVAXN and used in the present study. pVAXN used for experiments was purified using the EndoFree Plasmid Mega Kit (Qiagen, Mississauga, Canada).

To confirm the expression of encoded N protein, COS-1 cells were grown in DMEM medium supplemented with 10% FBS and 1% PSG. The cells were seeded at density of 1×10^6 per well in 6-well plate and grown overnight to 85 to 95% confluence. Next day cells were transfected with pVAXN using Lipofectamine 2000 reagent as per manufacturer's instructions and allowed to

grow for 48 h in a humidified 5% CO₂ atmosphere at 37 °C. Cells were trypsinized and pelleted, and the pellet was washed twice with PBS and lysed with RIPA buffer (150 mM NaCl, 10 mM Tris, pH 7.2, 0.1% SDS, 1.0% Triton X-100, 1% sodium deoxycholate, 5 mM EDTA). Cell lysate was cleared by centrifugation (10 min at 10,000 rpm), and cleared lysate was analyzed using 10% reducing SDS–PAGE. Subsequently the proteins were electrophoretically transferred onto a nitrocellulose membrane. The membrane was blocked with 5% skim milk and probed with anti-SARS-N protein monoclonal antibody (19C7) previously developed in our lab [25]. Finally, unbound 19C7 antibody was washed and the membrane incubated with goat anti-mouse IgG HRPO (1:5000). The blot was developed with ECL plus Western blotting reagent (Amersham Pharmacia Biotech, BaiedUrfe, Canada).

2.2.3 Preparation of biotinylated chitosan and estimation of chitosan modification using fluorescamine assay

Chitosan hydrochloride was biotinylated using biotinamidohexanoic acid 3-sulfo-*N*-hydroxysuccinimide ester sodium salt (sulfo-NHS-LC-biotin). Briefly, chitosan solution (20 mg/mL) was prepared in PBS (pH 7.4) and biotinylation was initiated by adding 10 mg of sulfo-NHS-LC-biotin. The reaction was carried out for 2 h at room temperature, and biotinylated chitosan was dialyzed against PBS overnight at 4 °C and lyophilized for 48 h.

The extent of amine group modification on glucosamine monomer of chitosan was determined to verify the attachment of biotin. The percentage of biotin substitution at primary amine group on glucosamine monomer was determined by fluorescamine assay [26]. Aqueous solutions of plain and biotinylated chitosan were made at various concentrations (0.01%, 0.03%, 0.04% and 0.05% w/v). A 50 µL/well of respective chitosan solution was added in triplicate to a 96-well black fluorescent microplate, and to this was added 100 µL of fluorescamine (0.2% w/v in anhydrous DMSO). After incubation for 30 min fluorescence intensity was recorded using a Synergy fluorescence plate reader (BioTek Instruments,

Winooski, VT) with a 360 nm, 40 nm bandwidth excitation filter and a 460 nm, 40 nm bandwidth emission filters. The sensitivity was set at 40%.

2.2.4 Formulation of pVAXN loaded biotinylated chitosan NPs

Plasmid DNA (pVAXN) loaded biotinylated chitosan nanoparticles (NPs) were prepared using modified complex coacervation method as described previously [23]. The conditions for formulation of complexes between chitosan and pVAXN were optimized. Briefly, biotinylated chitosan was dissolved in sodium acetate buffer (5 mM, pH 5.5) to obtain a final concentration of 0.1% w/v and passed through 0.22 μ m syringe filter. To obtain different weight ratios of chitosan to DNA (1 to 6), pVAXN solutions were prepared at different concentrations (1, 0.5, 0.333, 0.25, 0.2, and 0.166 mg/mL) in sodium sulfate (25 mM). The chitosan and DNA solutions were separately preheated to 50–55 °C on the water bath. Biotinylated chitosan (100 μ L, 1 mg/mL in 5 mM sodium acetate buffer, pH 5.5) solution was added to pVAXN solution (100 μ L), and the mixture was immediately vortexed for 15 s. The particles were left at room temperature for 30 min for stabilization. After stabilization, NPs were centrifuged at 14,000 rpm for 20 min and supernatants were analyzed for the presence of free DNA at absorbance 260 nm/280 nm using NanoDrop ND-1000 (Nanodrop Technologies Inc. Wilmington, Delaware) for analysis of encapsulation efficiency. The DNA encapsulation efficiency was calculated using the following formula: encapsulation efficiency (EE) = $A - B/A \times 100$, where A is the total DNA amount and B is the free DNA in the supernatant.

2.2.5 Physicochemical characterization of biotinylated chitosan NPs

2.2.5.1 Electrophoretic gel mobility assay

The complex formation between chitosan and DNA was analyzed by electrophoretic gel mobility assay. Samples of NPs (prepared at 1 to 6 weight ratios of biotinylated chitosan to pVAXN DNA) were mixed with the loading dye and loaded to a 1% agarose gel containing ethidium bromide. The gel was immersed in 1 \times tris-acetate/EDTA buffer and was exposed to 100 V for 45 min.

The DNA bands were visualized using the Alpha Imager (Alpha Innotech; San Leandro, CA). Unless otherwise mentioned, the NPs prepared at a biotinylated chitosan to pVAXN weight ratio of 4 were used for all studies.

2.2.5.2 Size and zeta potential

The particle size and zeta potential of pVAXN loaded biotinylated chitosan nanoparticles was measured using Zetasizer 3000 (Malvern, U.K.). The measurement of mean size diameter of the nanoparticles was based on the dynamic light scattering technique. For zeta potential measurements, nanoparticles were suspended in deionized water and the measurements were performed in the automatic mode.

2.2.5.3 DNase I protection assay and plasmid integrity

To see whether nanoencapsulated pVAXN is protected against nuclease digestion, nanoparticle encapsulated pVAXN and naked pVAXN were subjected to DNase I digestion. Briefly, naked pVAXN or nanoencapsulated pVAXN (4 µg) in 40 µL of deionized water was incubated with 10 units of DNase I (Invitrogen) for 30 and 60 min at 37 °C. The DNase activity was stopped by adding 0.5 M EDTA solution to a final concentration of 50 mM. Alternatively, following incubation with DNase I, the integrity of plasmid DNA within particles was analyzed by lysis of particles with chitosanase and lysozyme [23, 26]. Briefly, after treatment with DNase I for 60 min, the NPs were centrifuged and washed three times to remove DNase I and were resuspended in NaAc–HOAc buffer (50 mM). For digestion, the NPs were incubated with chitosanase (50 µL, 1 U/mL) and lysozyme (20 µL, 500 U/mL) for 4 h at 37 °C. The integrity of DNA samples was analyzed by 1% agarose gel using Alpha Imager (Alpha Innotech; San Leandro, CA).

2.2.6 Expression and purification of bfFp and SARS CoV N protein

The expression and purification of bifunctional fusion protein (bfFp), specifically anti-DEC-205 scFv fused with truncated core streptavidin, was conducted according to the reported method with slight modifications [11]. Briefly, pWET7 vector was transformed into BL21-CodonPlus (DE3)-RIPL *E. coli* cells

(Stratagene, Cedar Creek, TX) using the heat shock method. The *E. coli* transformant was cultured in 2xYT medium containing 100 µg/mL of ampicillin and 50 µg/mL of chloramphenicol and induced with 0.5 mM IPTG. Following induction, the culture was grown at 26 °C for 5 h and harvested by centrifugation. Periplasmic and cytoplasmic soluble bfFp was extracted with Bugbuster master mix reagent (Novagen Inc.) according to the manufacturer's instructions, and lysate was cleared by centrifugation and loaded onto Ni-NTA agarose. Purification of periplasmic soluble protein was performed using immobilized metal affinity chromatography (IMAC). The IMAC fractions were analyzed for purity by 10% SDS-PAGE under reducing conditions and stained with Coomassie brilliant blue. Expression and purification of full-length SARS-CoV N protein was carried out according to our published method [27]. Briefly, full-length N protein gene was codon optimized for high level bacterial expression and chemically synthesized from Genart Inc. The N protein was expressed as insoluble inclusion bodies in Top 10 *E. coli* strain and purified under denaturing conditions using IMAC column and refolded. The purified and refolded fractions of N protein were analyzed on 10% SDS-PAGE under reducing conditions. The recombinant full-length N protein was used as antigen to analyze magnitude of antibody responses and as recall antigen for stimulation of splenocytes.

2.2.7 Immunization studies

Ten to twelve week old female BALB/c mice used for this study were procured from Charles River Laboratories Inc. (Canada). Animals were housed at Health Sciences Laboratory Animals Services (HSLAS) at the University of Alberta, Edmonton, Canada. Animal treatment, care and euthanasia were carried out according to the Canadian Council of Animal Care guidelines. A total of five mice per group ($n = 5$) were used for evaluating immune response against vaccine constructs. The mice were immunized through either the intranasal or intramuscular route on day 1 and day 21 in the various combinations (**Table 2.1**). A 5 µg/mouse dose of pVAXN was administered as soluble, NPs or bfFp targeted NPs in the presence or absence of DC maturation stimuli (anti-CD40 mAb). For

intranasal delivery, mice were held in the vertical position perpendicular to the bench. While the mice were held tightly in the vertical position, the vaccine formulation (40 μ L, 20 μ L in each nostril) was delivered dropwise through a pipet tip right into the nostrils. The applied volume was naturally inhaled, and adequate care was taken to ensure proper delivery of the drops in nostrils, while avoiding any incident of swallowing. Following administration of formulations the mice were held in the vertical position for some time to ensure proper delivery. Intramuscular administration was done by injecting the vaccine formulation with a 26^{1/2} gauge needle in the quadriceps muscle in a total volume of 50 μ L.

Table 2.1 Different pVAXN formulations used for intranasal and intramuscular immunization in mice (n= 5 per group).

Groups	Formulations*
<i>Intranasal (IN)</i>	
1.	pVAXN
2.	NP
3.	NP + bfFp
4.	NP + bfFp + α CD 40
<i>Intramuscular (IM)</i>	
1.	pVAXN
2.	NP + bfFp
3.	NP + bfFp + α CD 40

* 5 μ g/mouse of pVAXN was administered either naked or as nanoparticles. A mass dose of 25 μ g of nanoparticles were used per dose, while α CD 40 mAb's dose was 25 μ g/mouse. pVAXN, DNA vaccine vector; NP, nanoparticle with encapsulated pVAXN; bfFp, bifunctional fusion protein; α CD 40, monoclonal antibody against anti CD 40 protein.

2.2.7.1 Humoral immune responses

Serum IgG titers were evaluated using recombinant N protein. Tail vein bleeds were performed on days 0, 14, 28, and 46, and terminal bleed (day 56) was collected by cardiac puncture following CO₂ asphyxiation and cervical dislocation. Nasal washings were performed immediately after cardiac puncture. Briefly, the trachea of each mouse was opened and a fine micropipettor tip was inserted. The nasal fluids were collected by flushing PBS (200 μ L) containing BSA (0.1%; w/v) through the nasal cavity and washes were collected from the nostrils. The nasal washes were kept at -20 °C until the day of analysis.

SARS N protein specific IgG and IgA titers were evaluated using enzyme-linked immunosorbent assay (ELISA). The Nunc MaxiSorp flat-bottom 96-well ELISA microplates were coated with N protein solution (100 μ L/well, 10 μ g/mL) overnight at 4 °C. The following day, plates were washed three times with PBST (0.1% Tween 20 in PBS pH 7.4) and blocked with 1% BSA solution (200 μ L) for 1 h at 37 °C. The plates were again washed with PBST (3 \times), and 100 μ L of diluted serum (1:100) from each mouse was added in duplicate and incubated overnight at 4 °C. The plates were washed with PBST, 100 μ L of goat-anti-mouse IgG HRPO (1:5000) was added followed by incubation for 1 h at 37 °C, and the plates were washed with PBST. Finally TMB substrate was added, and after 15 min optical density was measured at 650 nm using an ELISA V_{\max} kinetic microplate reader (Molecular Devices Corp, CA). The nasal IgA levels and the serum isotypes (IgG1, IgG 2a and IgG 2b) against N protein were determined using respective isotypes from Southern Biotechnology (Birmingham, AL). The same procedure as described above was followed except that at the end IgG1, IgG2a or IgG2b HRPO (1:400 dilution) or IgA HRPO (1: 250 dilution) was added to the plates for analyzing N protein specific IgA content in the nasal washes. The ABTS substrate was prepared as per manufacturer's instructions and added to plates, and the optical density was recorded at 405 nm.

2.2.7.2 Cytokine assay

Spleens from each group of mice were pooled, and cell suspension of splenocytes was prepared by disrupting the spleen between frosted slides. The splenocytes were passed through a cell strainer (70 μm) to obtain a single cell suspension. The red blood cells were lysed with ACK lysis buffer, and cells were washed twice with serum free medium. Finally, the splenocytes were resuspended in complete DMEM medium and cell density was adjusted at $1 \times 10^7/\text{mL}$. The splenocytes were seeded at the density of $1 \times 10^6/\text{well}$ and stimulated with N protein, concanavalin A (Con A) as positive control and medium as sham control. The culture supernatants were harvested after 72 h incubation at 37 °C in the humidified atmosphere at a 5% CO₂ level. The cytokine contents of supernatants were analyzed by a cytokine ELISA kit using a 96-well Corning microplate as per the manufacturer's instructions.

2.2.8 Statistical analysis

Data are presented as mean \pm standard deviation (SD) throughout the manuscript. Statistical significance of difference was tested using one way ANOVA test with Tukey's multiple comparison test. The significance level (α) was set at 0.05. Statistical difference was denoted as * $p < 0.05$, ns = no significant difference ($p > 0.05$). The data analysis was performed using Graphpad Prism (Graphpad Software Inc., La Jolla, CA, USA).

2.3. Results

2.3.1 Construction and expression of pVAXN DNA

The DNA vaccine vector used here was constructed by inserting full-length SARS-CoV N protein gene sequence between *Bam*HI and *Eco*RI restriction sites in pVAX1 mammalian expression vector to obtain pVAXN. Recombinant positive clones were isolated with kanamycin selection pressure and screened by

plasmid DNA isolation using plasmid DNA isolation kit (Qiagen), restriction digestion fragment mapping and DNA sequencing. The integrity of the pVAXN construct was evaluated using 1% agarose gel analysis.

To confirm the expression of encoded antigen, pVAXN DNA encoding for N protein was transiently transfected to COS-1 cells using Lipofectamine 2000. The transient expression of N protein was detected by Western blot using anti-SARS-CoV N protein monoclonal antibody (19C7) previously developed in our lab [25]. The result of Western blot confirms expression of N protein specific band on the COS-1 cell lysates. Mock transfected cells showed no cross-reactivity with 19C7 antibody (lane 2 in **Figure 2.1**).

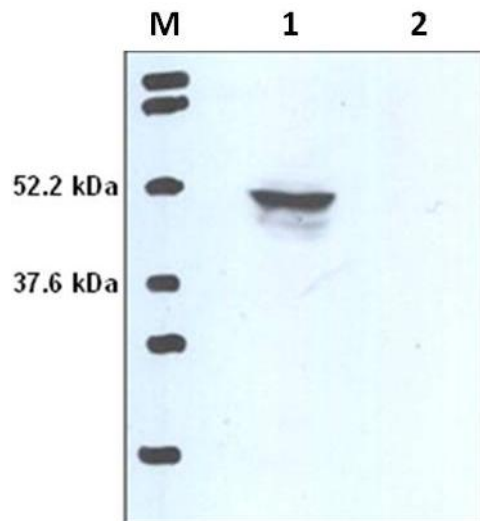


Figure 2.1 Detection of recombinant SARS CoV N protein expression by Western blot. M, Marker; Lane 1, pVAXN; Lane 2, pVAX1. The COS-1 cells were transiently transfected with pVAXN or pVAX-1 (control). N protein expression on cell lysate was analyzed by probing Western blot with mouse anti-SARS CoV N-specific monoclonal (19C7).

2.3.2 Biotinylation of chitosan and formulation of pVAXN loaded NPs

The water-soluble chitosan hydrochloride salt was biotinylated with long chain water-soluble sulfo-*N*-hydroxysuccinimide ester. This derivative of biotin incorporates an extended spacer arm provided by hexanoic acid. The spacer arm improves the interaction between avidin and biotinylated macromolecules by overcoming steric hindrance at the biotin binding sites of avidin (**Figure 2.2A**). The extent of biotinylation (i.e., substitution at the primary amine group) at the glucosamine amine group of chitosan was determined using the fluorescamine assay [26]. The fluorescamine reagent reacts rapidly with primary amines and can be used to estimate the magnitude of substitution at primary amine groups. When excited at ~365 nm wavelength, the fluorescence of the primary amine–dye complex has an emission wavelength of approximately 470 nm. The decrease in the fluorescence intensity of biotinylated chitosan can be correlated to obtain percentage substitution of biotin on amine groups of chitosan backbone. The results show the overall extent of glucosamine modification was found to be between 6 and 14% compared with plain chitosan hydrochloride (**Figure 2.2B**). Chitosan with a concentration of 0.03% (w/v) showed highest decrease in the fluorescence intensity ($13.2 \pm 1.9\%$) and therefore was most labeled with biotin.

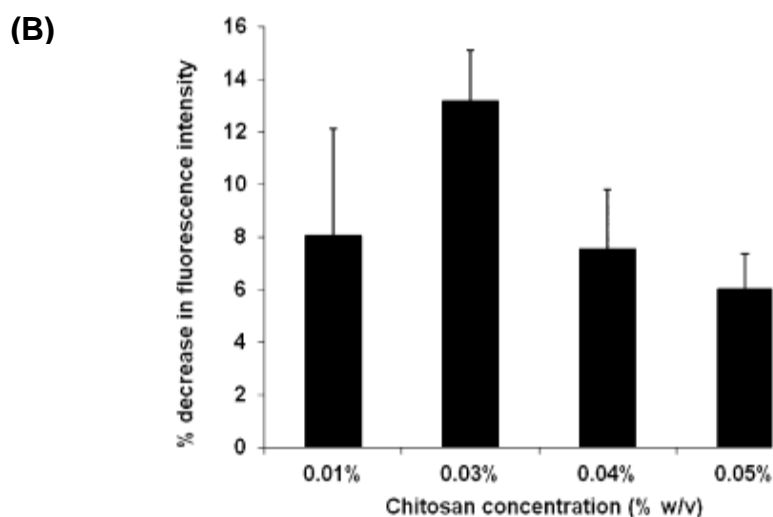
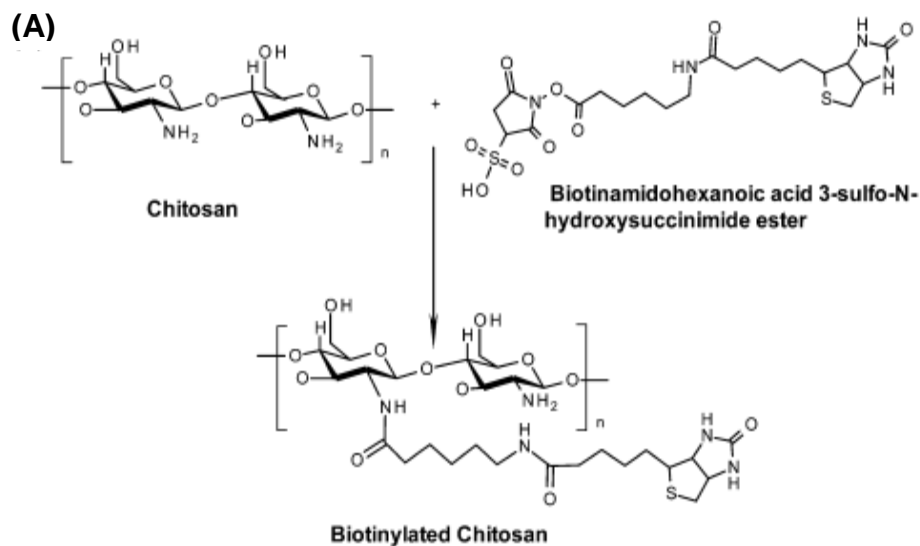


Figure 2.2 Synthesis and characterisation of biotinylated chitosan. (A) Schematic for the synthesis of biotinylated chitosan. (B) Estimation of chitosan modification using fluorescamine assay. The extent of biotinylation of the amine groups of chitosan was determined using fluorescamine, which reacts with primary amine groups. The decrease in fluorescence intensity is proportional to the percentage of biotinylated amine groups.

Nanoparticles were formulated using modified complex coacervation between negatively charged pVAXN DNA and positively charged biotinylated chitosan. Agarose gel analysis was performed to determine optimal weight ratio of biotinylated chitosan to plasmid DNA to achieve maximum encapsulation efficiency (**Figure 2.3A**). Results of agarose gel show that the weight ratio of 4:1 (biotinylated chitosan to plasmid DNA) yielded maximum efficiency of complexation with almost negligible free plasmid DNA. The loading at the 4:1 weight ratio of biotinylated chitosan to plasmid DNA was very efficient, and consistently the encapsulation efficiency of pVAXN was found to be in the range of $97.6 \pm 2.1\%$ as determined by the NanoDrop experiment.

Next, the pVAXN loaded biotinylated chitosan nanoparticles were characterized for size, surface charge and loading efficiency. The average hydrodynamic diameter of nanoparticles determined by zetasizer was found to be 210 ± 60 nm with zeta potential $+10 \pm 1.7$ mV.

Further, the results of nuclease protection assay suggest that nanoencapsulated pVAXN could be protected at high concentration of DNase I digestion (lane 2 and 4, **Figure 2.3B**), while it turned out that naked pVAXN was completely degraded under DNase I digestion (lanes 1 and 3, Figure 2.3B). DNase I treated NPs were digested with chitosanase and lysozyme. This resulted in the release of intact DNA and showed no signs of degradation (Lane 5, Figure 2.3B) suggesting that formulation process did not affect the integrity of the nanoencapsulated DNA. The nuclease protection to DNA by chitosan nanoparticles would be meaningful for the maintenance of integration and function of DNA vaccine.

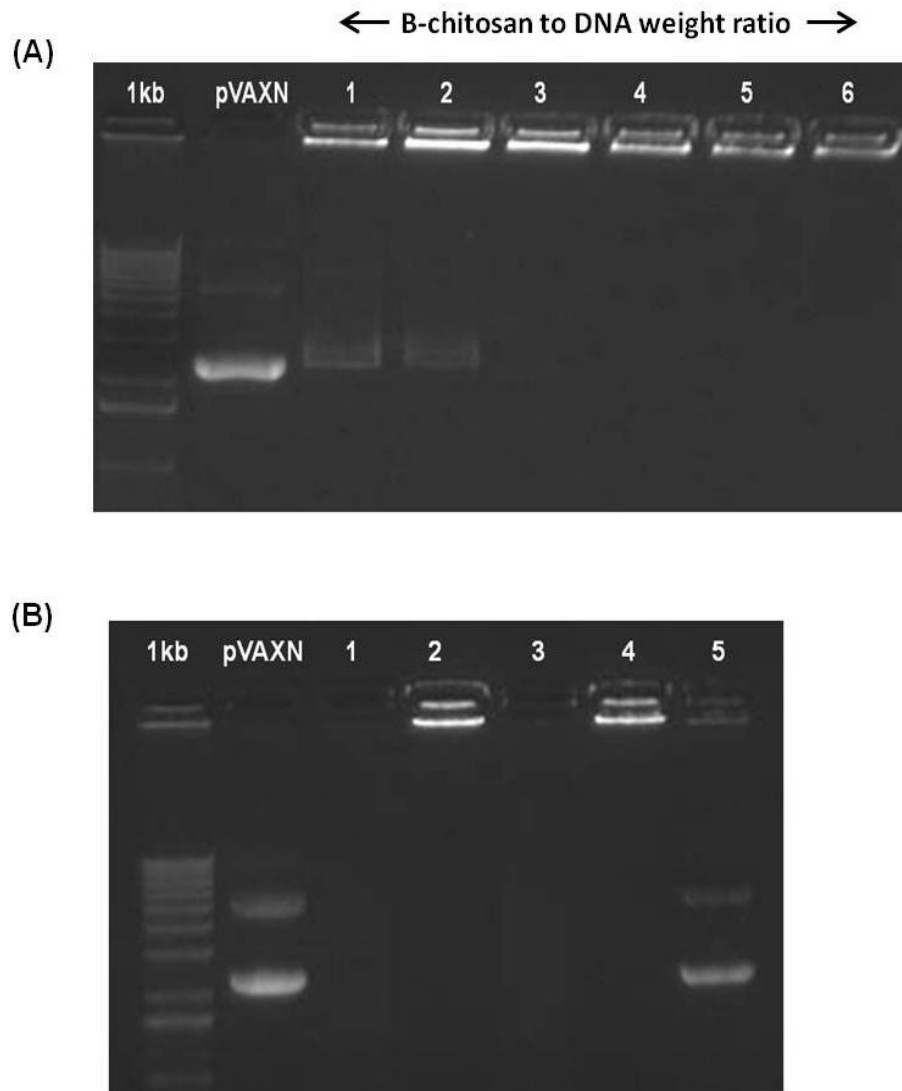


Figure 2.3 Formulation of pVAXN loaded biotinylated chitosan nanoparticles. (A) Agarose gel analysis of pVAXN DNA loaded biotinylated chitosan nanoparticles prepared at different weight ratios of B-chitosan to pVAXN DNA (1 to 6). (B) Agarose gel electrophoresis of DNase I digested naked pVAXN and nanoencapsulated pVAXN. Lane 1: pVAXN (30 min). Lane 2: nanoencapsulated pVAXN (30 min). Lane 3: pVAXN (60 min). Lane 4: nanoencapsulated pVAXN (60 min). Lane 5: Lane 4 digested with chitosanase and lysozyme.

2.3.3 Expression and medium-scale purification of bfFp and N Protein

The dendritic cell targeting vector (bfFp) was expressed and purified as periplasmic soluble protein as per our previous published methods with modifications [11, 28]. The pWET7 construct encoding for anti-DEC-205 scFv-core-streptavidin fusion protein (bfFp) was subjected to medium scale expression. The expression of bfFp was verified using anti-His₆ mAb Western blot. The bacterial cell pellet was lysed with Bug Buster Master mix reagent for efficient extraction of periplasmic and cytoplasmic soluble protein. BfFp was purified from lysate using IMAC column with a gradient of imidazole concentration in the native protein elution buffer (**Figure 2.4**). The final yield of bfFp was found to be approximately 1.0 mg/L of induced bacterial culture.

The prokaryotic full-length SARS-CoV N protein was used as antigen to analyze the antibody titers and as recall antigen for stimulating splenocytes. The N protein with C-terminal His₆ tag was expressed and purified from inclusion bodies under denaturing conditions (**Figure 2.5**) according to our previous protocols [27].

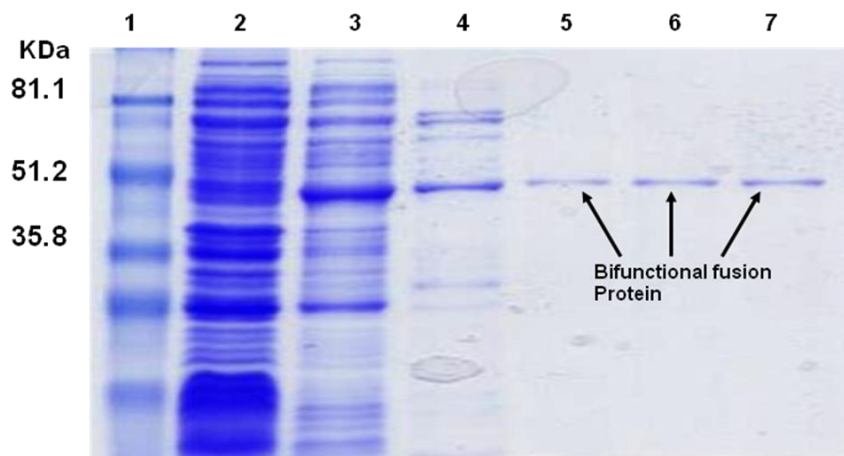


Figure 2.4 IMAC purification profile of bifunctional fusion protein (bfFp). Lane 1: Marker, 2: Unbound, 3: 20 mM Imidazole, 4: 40 mM Imidazole, 5-7: 250 mM Imidazole (Elution fractions).

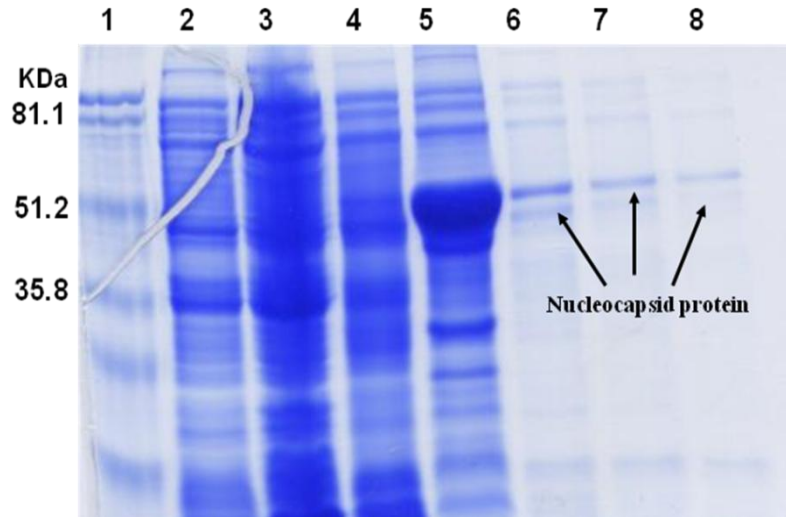


Figure 2.5 IMAC purification profile of SARS CoV N protein. Lane1:Marker, 2: Induced 3: Uninduced, 4: Total soluble protein, 5: purified inclusion bodies, 6-8: Elution fractions.

2.3.4 Systemic N protein specific IgG antibody response

The pVAXN loaded biotinylated chitosan nanoparticles were appended with bfFp for DEC-205 restricted DC targeting, and were evaluated for their *in vivo* potential to elicit immune responses following nasal administration. As the positive controls, these formulations were also administered through the intramuscular route (Table 2.1). In addition, the bfFp targeted biotinylated nanoparticles were compared for immune responses in the presence or absence of DC maturation stimuli (anti-mouse CD40 mAb). The agonistic anti-CD40 mAb binds to CD40 on DCs, resulting in activation of cells replacing the CD40-CD40L signaling via CD4⁺ T cells [29]. Anti-CD40 mAb has been used as adjuvant in combination with DEC-205 targeted protein based vaccines [30, 31]., and as an effective mucosal adjuvant upon intranasal administration in combination with influenza peptide encapsulated liposomal vaccine [32].

To examine the systemic immune responses elicited using targeted vaccines through intranasal (IN) or intramuscular (IM) routes, the presence of N protein

specific IgG antibodies was analyzed by indirect ELISA on serum samples collected during different time points (days 0, 14, 28, 46 and 56). The serum IgG profile (**Figure 2.6A**) shows that the nasal administration of bfFp targeted nanoparticles in combination with anti-CD40 mAb elicits higher levels of systemic IgG compared to naked DNA vaccine formulation administered through IN or IM route ($*p < 0.05$). Additionally, the bfFp targeted nanoparticles in the absence of any maturation stimuli (anti-CD40 mAb) elicited significantly lower levels of IgG titer compared to bfFp targeted nanoparticles administered along with anti-CD40 mAb. This trend was observed when formulations were administered by either the IN or IM route. As expected, the intramuscular group immunized with targeted nanoparticles along with maturation stimuli induced the highest level of antibody titers. Serum titers of antibodies for targeted formulations (NP + bfFp) were significantly ($*p < 0.05$) higher than naked DNA formulations following intranasal as well as intramuscular administration (Figure 2.6b). In addition, in a separate set of experiments we found that the immune response of NPs with anti-CD40 mAb was significantly lower than that observed from the targeted NPs with anti-CD40 mAb (unpublished results).

Interestingly we did not observe N protein specific IgG titers following nasal delivery of naked pVAXN or nanoparticle encapsulated pVAXN. The possible reason could be the low dose of naked or nanoencapsulated DNA, as only 5 μg /mice DNA (pVAXN) was administered. The above results show that the use of DC targeting ligand such as bfFp and the presence of maturation stimuli lead to enhanced immunogenicity of DNA vaccines. Such pDNA vaccines could provide augmented serum IgG titer at low doses.

The serum IgG isotyping profile specific for N protein following pDNA vaccine, irrespective of route of administration, indicates that targeted formulations augmented the IgG1, IgG2a and IgG2b levels. The intramuscular route, however, was found to be superior compared with the nasal route. The ratio of IgG1 to IgG2a and IgG2b indicates a Th1 biased immune response (**Figure 2.6B**).

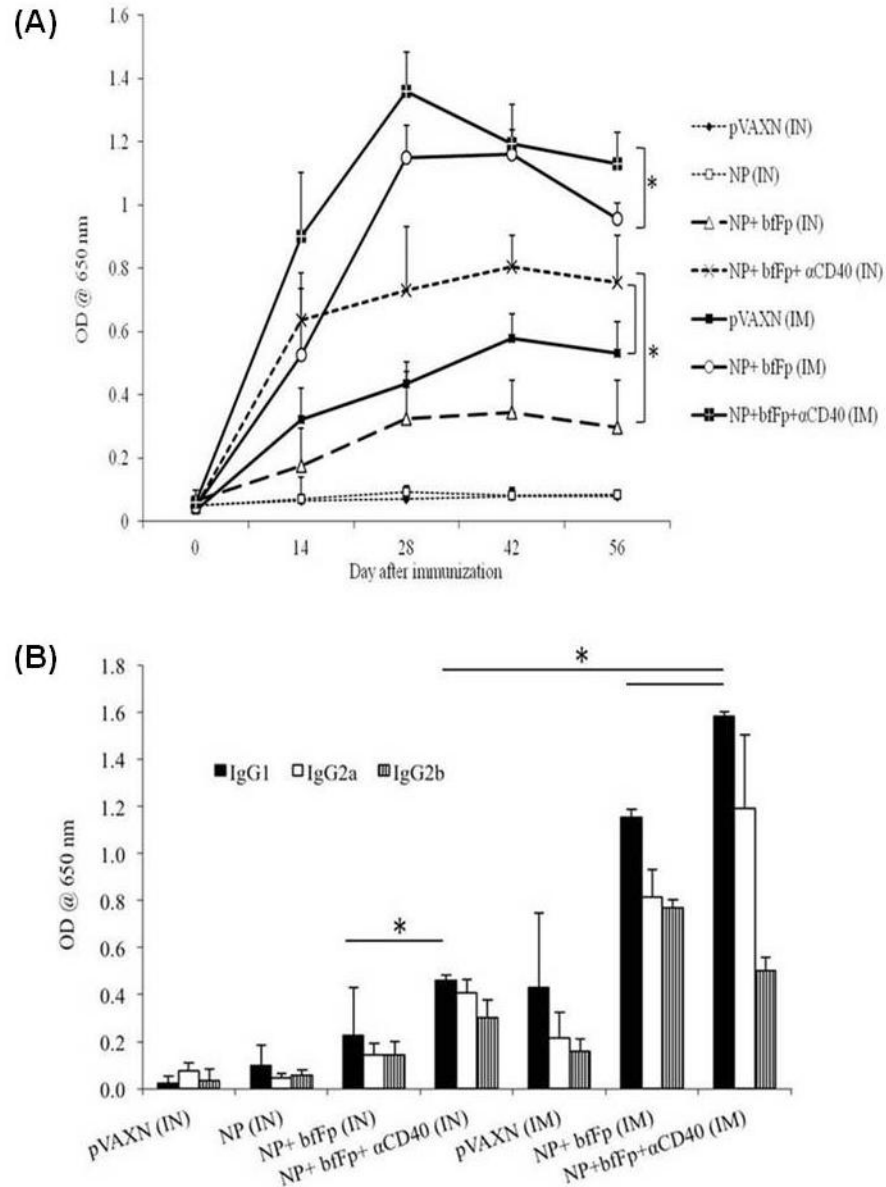


Figure 2.6 SARS CoV N protein specific IgG titers. (A) Analysis of time-dependent serum IgG against SARS-CoV N protein following IN and IM immunization with different vaccine formulations. BALB/c mice (5 per group) were immunized with 5 μ g of pVAXN on day 1 and day 21. The serum was collected at days 0, 14, 28, 42, and on day 56, and IgG response was detected using ELISA. The data are presented as group mean \pm SD at various time points. ELISA was performed at 1:100 diluted sera. (B) SARS CoV N protein specific serum IgG isotypes. IgG isotypes were determined in the serum samples obtained on day 56. Data are presented as group mean \pm SD. Statistical differences between groups are denoted as * p < 0.05. The horizontal bars compare statistical difference in IgG1 responses between different groups.

2.3.5 Mucosal N protein specific antibody response

The mucosal surfaces are rich in antigen presenting cells such as DCs. The uptake of antigen by resident DC in nasal-associated lymphoid tissue (NALT) is necessary in the induction of mucosal immune responses. Production of SARS N protein specific mucosal IgA antibodies could be vital for protection against SARS CoV infection. Previous studies have shown that the mucosal IgA plays an important role in protection against SARS-CoV virus in animal models [33]. We found significantly higher mucosal IgA levels in nasal washings following nasal administration of DC targeted nanoparticles in combination with anti-CD40 mAb compared with intranasal delivery of pVAXN, NP and bfFp targeted NPs ($*p < 0.05$) (**Figure 2.7**). Detectable mucosal IgA response was also observed following intramuscular administration of bfFp targeted nanoparticles alone or in combination with anti-CD40 mAb as maturation, and there was no significant difference between the response from either formulation (ns, $p > 0.05$). These findings can be explained on the basis of the previous observations that systemic administration of DEC-205 targeted protein vaccines could provide protection against mucosal pathogen [9]. However, merely detectable IgA response was observed following intramuscular administration of pVAXN formulations. The results clearly indicate that chitosan nanoparticles administered by the nasal route efficiently elicit mucosal immune response (IgA level). Thus, nasally administered DC targeted nanoparticles can provide the additional advantage of mucosal immunity, which could lead to neutralizing the pathogen following exposure. These observations are interesting since the SARS virus primarily infects the upper respiratory tract and induction of mucosal immunity (mucosal IgA) could limit viral attachment and pathogenesis [34].

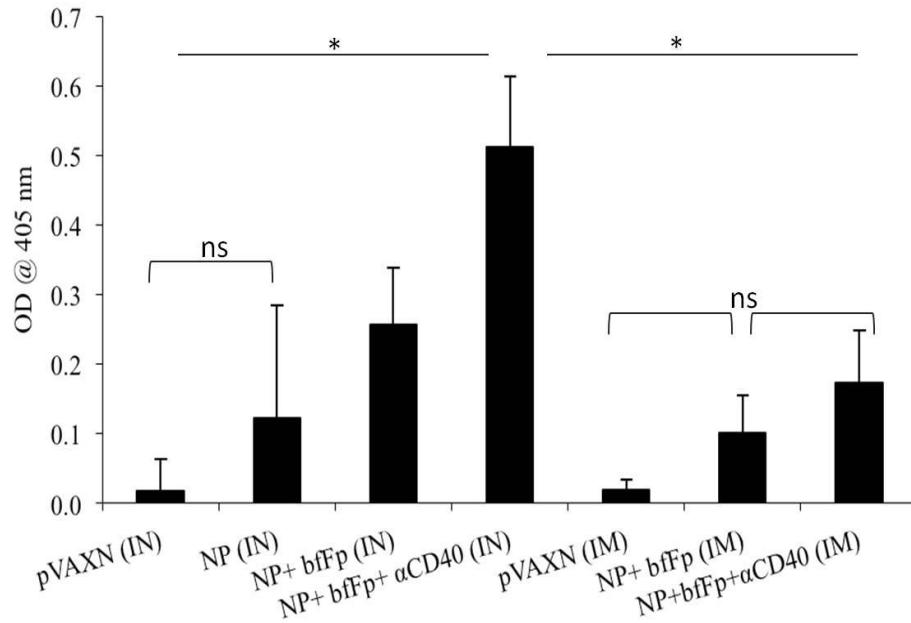


Figure 2.7 SARS-CoV N protein specific IgA levels in the nasal washes. The nasal washes were collected on day 56 following euthanasia and assayed for the presence of N protein specific IgA using ELISA. Each sample was analyzed in triplicate, and data are representative of group mean \pm SD of five mice. Statistical differences between groups are denoted as * $p < 0.05$ and ns = no significant difference ($p > 0.05$). The horizontal bars with * denote statistical difference in IgA between different groups compared with NP + bfFp + α CD40 group (IN).

2.3.6 Interferon-gamma profile

Interferon-gamma (IFN- γ) levels were measured to determine whether intranasal and intramuscular administration of targeted and nontargeted vaccines elicits cellular immunity. The recombinant N protein was used as a recall antigen, concanavalin A (Con A) served as a positive control, while medium was treated as a sham control. As shown in **Figure 2.8**, splenocytes from a group of mice treated with targeted formulations (NP + bfFp) secreted significantly higher levels of IFN- γ on stimulation with N protein by either intranasal or intramuscular route. The vaccination of mice with targeted chitosan nanoparticles and anti-CD40 mAb maturation stimuli resulted in the highest levels of IFN- γ secretion, followed by targeted chitosan nanoparticles without maturation stimuli (* $p < 0.05$). Nontargeted or naked pDNA vaccine formulations were found to be less effective in provoking significant IFN- γ levels. No detectable levels of IFN- γ were observed for splenocyte cultures treated with media alone, whereas high levels of IFN- γ (1795–2526 pg/mL) were present following stimulation with Con A.

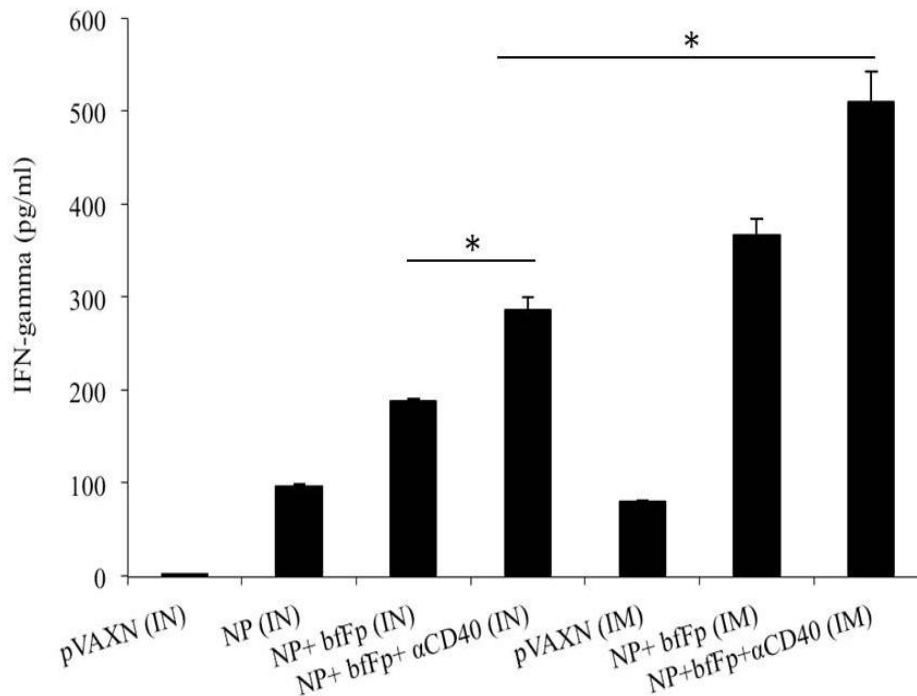


Figure 2.8 Analysis of IFN- γ levels in mice immunized with different pVAXN formulations. Splenocytes obtained from a group of immunized mice (5 mice per group) were pooled and cultured in the presence of recombinant N protein (4 μ g) in a 96-well flat bottom plate with a final volume of 200 μ L. Culture supernatants harvested after 72 h were analyzed for IFN- γ levels using an ELISA kit. Data represents mean \pm SD of triplicate cultures stimulated with N protein. Statistical differences between groups are denoted as * $p < 0.05$. * denote statistical difference in IFN- γ between different groups. IFN- γ levels obtained following stimulation with Con A were 1795–2526 pg/mL in different groups, whereas no detectable levels were observed for splenocyte culture stimulated with medium alone.

2.4 Discussion

SARS is an emerging infectious disease caused by a novel coronavirus named as SARS-CoV [12]. At the start of the twenty-first century SARS outbreak has seriously threatened healthcare agencies around the world: over 8,000 people were infected, resulting in 774 deaths. To date, there is no therapeutic treatment/vaccine available for containing future threats of SARS endemic or pandemic [34]. Since SARS is transmitted through the respiratory route, the respiratory tract serves as the most common route for virus entry and as a first line of defense. It becomes mandatory to design a vaccine delivery system which can provide antigen specific mucosal immunity. The respiratory tract harbors local DC subsets, which routinely sample and process innocuous agents. Hence, respiratory tract resident DCs could serve as the ideal target for uptake of targeted nanoparticles administered through noninvasive means.

Previous studies have shown that N protein is highly conserved and, therefore, could serve as a stable vaccine candidate [14]. However, studies performed using N protein as antigen are based on systemic immunization, and no attempt has been made to naturally mimic the route of viral infection and to target mucosal DCs. The logistics behind targeting of pDNA vaccine to DCs stems from the fact that the traditional intramuscular route of pDNA immunization results in the expression of antigens on myocytes. However, the myocytes are not professional antigen presenting cells and thus can only present antigens through MHC class I pathway. Furthermore, myocytes do not migrate to draining lymph nodes and express costimulatory molecules; both of these features are essentially required for priming and activation of T cells [35].

Therefore, the main objective of this work was to investigate mucosal DC targeting potential of the pDNA loaded chitosan nanoparticles. The mucosal delivery of DNA vaccines mimics the natural mode of virus infection and induces both humoral and cellular immune responses [36]. Naked DNA is ineffective in crossing mucosal barriers, and it is rapidly degraded by nucleases [37]. Contemporary efforts have been directed to improve the immunogenicity of DNA

vaccines. A wide range of strategies have been adopted in the literature to increase the immunogenicity profile of DNA vaccines, such as the use of heterologous prime-boost regimes, coexpression of cytokines, electroporation and the use of viral and nonviral gene delivery vehicles [36].

In the context of design of effective mucosal pDNA delivery, the nonviral vectors, such as polymeric nano/microparticle and liposome protected plasmid DNA, have shown better immunogenicity profiles. These systems can specifically deliver the pDNA to antigen presenting cells such as dendritic cells and macrophages. Additionally, these delivery systems could be surface functionalized with targeted ligands to achieve DC-selective targeted delivery of plasmid DNA through different immunization routes [22, 38]. Numerous research findings have explored the nano/microparticles formulated using chitosan and their derivatives as gene delivery vehicles [39]. Chitosan is believed to show better nasal delivery prospects through two mechanisms [40]. First, the cationic charge on chitosan confers binding to negative sialic residues in the mucus lining of the nasal epithelial cells thereby slowing clearance. Second, chitosan transiently opens the tight junctions to allow an increased paracellular transport across nasal mucosa. Additionally, the attachment of receptor specific ligands on chitosan microspheres facilitates receptor mediated endocytosis resulting in cell-specific delivery vaccine formulations [41].

We have synthesized biotinylated chitosan and used it for the formulation of pVAXN loaded nanoparticles. The biotin substitution on the chitosan backbone facilitates the attachment of bifunctional fusion protein (bfFp) through core-streptavidin arm and anti-DEC-205 scFv arm assists in guiding the nanoparticle toward DCs. The N protein gene was cloned in US FDA approved pVAX1 plasmid vector, containing a CMV promoter and BGH polyadenylation sequence for mammalian protein expression. Further, the nanoencapsulated form of pVAXN was found to resist nuclease digestion following incubation with DNase I, which is vital for *in vivo* performance of the nanoparticulate formulations. The intranasal application of bfFp targeted nanoparticulate vaccines induces systemic

and mucosal immune responses against N protein antigen. In addition, mere administration of naked pDNA or nanoencapsulated pDNA was not sufficient enough in provoking detectable serum titers against N protein. We speculate this could be due to the low dose of the pVAXN antigen (5 µg/mouse). Contemporary studies have shown induction of immune response following nasal delivery of pDNA encapsulated chitosan particles, where a high dose of encapsulated pDNA or frequent dosing was used [42, 43].

From our results, it is apparent that both systemic and mucosal N protein specific responses were induced in mice by using bfFp based targeting of nanoencapsulated pVAXN. The N protein specific serum IgG, IgG1, IgG2a and IgG2b antibodies were elicited to higher magnitude when the targeted formulations were coadministered with DC maturation/activation stimuli (anti-mouse-CD40 mAb). The splenocytes were capable of producing IFN- γ , a Th1 cytokine, upon *in vitro* stimulation with recombinant N protein. However, a significantly higher level of IFN- γ was detected for targeted formulations compared with nontargeted formulation. Codelivery of DC maturation stimuli with targeted formulations resulted in augmented IFN- γ levels, irrespective of the route of immunization.

In conclusion, we report a promising strategy for enhancing immunogenicity of low-dose DNA vaccine through targeted delivery to nasal resident dendritic cells. The vaccine strategy demonstrated here could provide a better understanding of noninvasive means of targeting vaccine antigens to the dendritic cells. This strategy has important implications for designing vaccines against SARS or infections with similar mechanisms.

2.5 References

- [1] Steinman RM. Dendritic cells in vivo: a key target for a new vaccine science. *Immunity* 2008;29:319-24.
- [2] Tacken PJ, De Vries IJM, Torensma R, Figdor CG. Dendritic-cell immunotherapy: from ex vivo loading to in vivo targeting. *Nat Rev Immunol* 2007;7:790-802.
- [3] Keler T, He L, Ramakrishna V, Champion B. Antibody-targeted vaccines. *Oncogene* 2007;26:3758-67.
- [4] Proudfoot O, Apostolopoulos V, Pietersz GA. Receptor-mediated delivery of antigens to dendritic cells: Anticancer applications. *Mol Pharm.* 2007;4:58-72.
- [5] Inaba I, Swiggard WJ, Inaba M, Meltzer J, Mirza A, Sasagawa T, et al. Tissue distribution of the DEC-205 protein that is detected by the monoclonal antibody NLDC-145 I. Expression on dendritic cells and other subsets of mouse leukocytes. *Cell Immunol* 1995;163:148-56.
- [6] Witmer-Pack MD, Swiggard WJ, Mirza A, Inaba K, Steinman RM. Tissue distribution of the DEC-205 protein that is detected by the monoclonal antibody NLDC-145 II. Expression in situ in lymphoid and nonlymphoid tissues. *Cell Immunol* 1995;163:157-62.
- [7] Jian W, Swiggard WJ, Heufler C, Peng M, Mirza A, Steinman RM, et al. The receptor DEC-205 expressed by dendritic cells and thymic epithelial cells is involved in antigen processing. *Nature* 1995;375:151-5.
- [8] Mahnke K, Guo M, Lee S, Sepulveda H, Swain SL, Nussenzweig M, et al. The dendritic cell receptor for endocytosis, DEC-205, can recycle and enhance antigen presentation via major histocompatibility complex class II-positive lysosomal compartments. *J Cell Biol* 2000;151:673-83.
- [9] Bonifaz LC, Bonnyay DP, Charalambous A, Darguste DI, Fujii S-I, Soares H, et al. In Vivo Targeting of Antigens to Maturing Dendritic Cells via the DEC-205 Receptor Improves T Cell Vaccination. *J Exp Med* 2004;199:815-24.
- [10] Wang WW, Das D, Tang XL, Budzynski W, Suresh MR. Antigen targeting to dendritic cells with bispecific antibodies. *J Immunol Methods* 2005;306:80-92.

- [11] Wang WW, Das D, Suresh MR. A versatile bifunctional dendritic cell targeting vaccine vector. *Mol Pharm* 2009;6:158-72.
- [12] Drosten C, Günther S, Preiser W, Van der Werf S, Brodt HR, Becker S, et al. Identification of a novel coronavirus in patients with severe acute respiratory syndrome. *N Engl J Med* 2003;348:1967-76.
- [13] Peiris JSM, Lai ST, Poon LLM, Guan Y, Yam LYC, Lim W, et al. Coronavirus as a possible cause of severe acute respiratory syndrome. *Lancet* 2003;361:1319-25.
- [14] Surjit M, Lal SK. The SARS-CoV nucleocapsid protein: a protein with multifarious activities. *Infect Genet Evol* 2008;8:397-405.
- [15] Peng H, Yang Lt, Wang Ly, Li J, Huang J, Lu Zq, et al. Long-lived memory T lymphocyte responses against SARS coronavirus nucleocapsid protein in SARS-recovered patients. *Virology* 2006;351:466-75.
- [16] Rota PA, Oberste MS, Monroe SS, Nix WA, Campagnoli R, Icenogle JP, et al. Characterization of a novel coronavirus associated with severe acute respiratory syndrome. *Science* 2003;300:1394-9.
- [17] Gupta V, Tabiin TM, Sun K, Chandrasekaran A, Anwar A, Yang K, et al. SARS coronavirus nucleocapsid immunodominant T-cell epitope cluster is common to both exogenous recombinant and endogenous DNA-encoded immunogens. *Virology* 2006;347:127-39.
- [18] Schulze K, Staib C, Schätzl HM, Ebensen T, Erfle V, Guzman CA. A prime-boost vaccination protocol optimizes immune responses against the nucleocapsid protein of the SARS coronavirus. *Vaccine* 2008;26:6678-84.
- [19] Kim TW, Lee JH, Hung CF, Peng S, Roden R, Wang MC, et al. Generation and characterization of DNA vaccines targeting the nucleocapsid protein of severe acute respiratory syndrome coronavirus. *J Virol* 2004;78:4638-45.
- [20] Zhao P, Cao J, Zhao L-J, Qin Z-L, Ke J-S, Pan W, et al. Immune responses against SARS-coronavirus nucleocapsid protein induced by DNA vaccine. *Virology* 2005;331:128-35.

- [21] Zhu MS, Pan Y, Chen HQ, Shen Y, Wang XC, Sun YJ, et al. Induction of SARS-nucleoprotein-specific immune response by use of DNA vaccine. *Immunol Lett* 2004;92:237-43.
- [22] Kang ML, Cho CS, Yoo HS. Application of chitosan microspheres for nasal delivery of vaccines. *Biotechnol Adv* 2009;27:857-65.
- [23] Mao HQ, Roy K, Troung-Le VL, Janes KA, Lin KY, Wang Y, et al. Chitosan-DNA nanoparticles as gene carriers: Synthesis, characterization and transfection efficiency. *J Control Release* 2001;70:399-421.
- [24] Wikstrom ME, Stumbles PA. Mouse respiratory tract dendritic cell subsets and the immunological fate of inhaled antigens. *Immunol Cell Biol* 2007;85:182-8.
- [25] Kammila S, Das D, Bhatnagar PK, Sunwoo HH, Zayas-Zamora G, King M, et al. A rapid point of care immunoswab assay for SARS-CoV detection. *J Virol Methods* 2008;152:77-84.
- [26] Corsi K, Chellat F, Yahia LH, Fernandes JC. Mesenchymal stem cells, MG63 and HEK293 transfection using chitosan-DNA nanoparticles. *Biomaterials* 2003;24:1255-64.
- [27] Das D, Suresh MR. Copious production of SARS-CoV nucleocapsid protein employing codon optimized synthetic gene. *J Virol Methods* 2006;137:343-6.
- [28] Wang WWS, Das D, McQuarrie SA, Suresh MR. Design of a bifunctional fusion protein for ovarian cancer drug delivery: Single-chain anti-CA125 core-streptavidin fusion protein. *Eur J Pharm Biopharm* 2007;65:398-405.
- [29] Elgueta R, Benson MJ, De Vries VC, Wasiuk A, Guo Y, Noelle RJ. Molecular mechanism and function of CD40/CD40L engagement in the immune system. *Immunol Rev* 2009;229:152-72.
- [30] Bonifaz L, Bonnyay D, Mahnke K, Rivera M, Nussenzweig MC, Steinman RM. Efficient targeting of protein antigen to the dendritic cell receptor DEC-205 in the steady state leads to antigen presentation on major histocompatibility complex class I products and peripheral CD8+ T cell tolerance. *J Exp Med* 2002;196:1627-38.

- [31] Trumpfheller C, Finke JS, López CB, Moran TM, Moltedo B, Soares H, et al. Intensified and protective CD4+ T cell immunity in mice with anti-dendritic cell HIV gag fusion antibody vaccine. *J Exp Med* 2006;203:607-17.
- [32] Ninomiya A, Ogasawara K, Kajino K, Takada A, Kida H. Intranasal administration of a synthetic peptide vaccine encapsulated in liposome together with an anti-CD40 antibody induces protective immunity against influenza A virus in mice. *Vaccine* 2002;20:3123-9.
- [33] See RH, Zakhartchouk AN, Petric M, Lawrence DJ, Mok CPY, Hogan RJ, et al. Comparative evaluation of two severe acute respiratory syndrome (SARS) vaccine candidates in mice challenged with SARS coronavirus. *J Gen Virol* 2006;87:641-50.
- [34] Roper RL, Rehm KE. SARS vaccines: Where are we? *Expert Review of Vaccines* 2009;8:887-98.
- [35] Kutzler MA, Weiner DB. Developing DNA vaccines that call to dendritic cells. *J Clin Invest* 2004;114:1241-4.
- [36] Kutzler MA, Weiner DB. DNA vaccines: Ready for prime time? *Nat Rev Genet* 2008;9:776-88.
- [37] Wang D, Christopher ME, Nagata LP, Zabielski MA, Li H, Wong JP, et al. Intranasal immunization with liposome-encapsulated plasmid DNA encoding influenza virus hemagglutinin elicits mucosal, cellular and humoral immune responses. *J Clin Virol* 2004;31:S99-S106.
- [38] Garg NK, Mangal S, Khambete H, Sharma PK, Tyagi RK. Mucosal delivery of vaccines: Role of mucoadhesive/biodegradable polymers. *Recent Pat Drug Deliv Formul* 2010;4:114-28.
- [39] Csaba N, Garcia-Fuentes M, Alonso MJ. Nanoparticles for nasal vaccination. *Adv Drug Deliv Rev* 2009;61:140-57.
- [40] Yeh T-H, Hsu L-W, Tseng MT, Lee P-L, Sonjae K, Ho Y-C, et al. Mechanism and consequence of chitosan-mediated reversible epithelial tight junction opening. *Biomaterials* 2011;32:6164-73.

- [41] Jiang HL, Kang ML, Quan JS, Kang SG, Akaike T, Yoo HS, et al. The potential of mannosylated chitosan microspheres to target macrophage mannose receptors in an adjuvant-delivery system for intranasal immunization. *Biomaterials* 2008;29:1931-9.
- [42] Khatri K, Goyal AK, Gupta PN, Mishra N, Vyas SP. Plasmid DNA loaded chitosan nanoparticles for nasal mucosal immunization against hepatitis B. *Int J Pharm* 2008;354:235-41.
- [43] Xu J, Dai W, Wang Z, Chen B, Li Z, Fan X. Intranasal Vaccination with Chitosan-DNA Nanoparticles Expressing Pneumococcal Surface Antigen A Protects Mice against Nasopharyngeal Colonization by *Streptococcus pneumoniae*. *Clin Vaccine Immunol* 2011;18:75-81.

CHAPTER 3: Dendritic cell targeted chitosan nanoparticles for mucosal and systemic genetic immunization against avian influenza

A version of this chapter will be submitted to *Journal of Drug Targeting*.
Raghuwanshi D, Das D, Mishra V, Kaur K and Suresh MR: Dendritic cell targeted nanoparticles for mucosal and systemic genetic immunization against avian influenza.

3.1 Introduction

Recent outbreaks of the highly pathogenic avian H5N1 influenza A viruses and transmission of infection from birds to humans has raised the serious concerns that next influenza pandemic may evolve from this subtype [1]. It is speculated that highly virulent 1918 influenza A virus strain was derived from an avian virus [2]. This virus was responsible for 1918 “Spanish Flu” that resulted in 40-50 million deaths world-wide. Therefore, development of effective prophylactic vaccine is necessary to prevent the mortality associated with a future human influenza pandemic. Several vaccination strategies have been explored to date, vaccination with formaldehyde inactivated virus remains the most widely used preventive measure [3]. These vaccines are grown in embryonated eggs and to provide reasonable protection against circulating influenza strains, the components of these vaccines are adjusted annually, which is a time-consuming process. Furthermore, in the case of emerging pandemic strains, current production methods are not optimal to meet the global supply demand [4].

Influenza A viruses are transmitted through mucosal routes and cause a range of severe respiratory and gastrointestinal complications. Conversely, currently available vaccines are mostly administered parenterally and protective immunity is generally based on the induction of strain-specific systemic IgG antibodies against hemagglutinin (HA) antigen. Parenteral immunization can effectively induce humoral and cellular immune responses, however, it is often nonefficacious and sub-optimal for induction of mucosal immunity. In contrast, administration of vaccines through mucosal routes can provide both systemic and mucosal immunity [5]. Since influenza virus primarily infects and multiplies in upper respiratory tract, induction of potent mucosal and cell-mediated immune responses could potentially play an important role in the formulation of effective influenza vaccine [6].

Mucosal immunization induces secretion of immunoglobulin A (IgA), which can form first line of defence against invading pathogens, preventing virus attachment to epithelial cells, promoting capture in the mucus and induction of antigen-

specific IgA antibodies at distant mucosal sites [7]. However, the mucosal immunization by inactivated and subunit influenza vaccines results in poor immunogenicity and requires adjuvants, such as *Escherichia coli* heat-labile toxin (LT) or toll-like receptor ligands [8, 9]. Mucosal vaccination with nanoparticulate antigen delivery systems such as liposomes [10], immune stimulating complexes [11], virosomes [12] and chitosan based formulations [13, 14] have shown to provide protective immunity.

Influenza DNA vaccines have emerged as powerful alternatives to traditional egg based vaccines. DNA vaccines can be constructed based on genetic information of circulating strain, manufactured on large scale for mass distribution and thus could minimize the damage in the event of pandemic threat [15, 16]. Furthermore, the ability of parenterally administered HA-based DNA vaccines has been shown to confer protective immunity against lethal homologous and heterologous influenza virus challenge in various animal models [17-19]. Nasal administration of HA DNA vaccines can provoke protective local immune responses (IgA) [10, 20]. Furthermore, immune response to nasal DNA vaccines appears to mimic that of natural virus infections as encoded antigen is expressed in the respiratory tract.

In this study, we investigated the comparative immunogenicity of chitosan nanoparticle encapsulated H5N1 HA plasmid DNA vaccines following intranasal (IN) and intramuscular (IM) administration. As mentioned in Chapter 2, chitosan is a promising DNA delivery vehicle and its strong mucoadhesive properties facilitate paracellular transport by opening tight junctions [21]. Chitosan nanoparticles can be chemically cross-linked with ligands to achieve targeted delivery to mucosal antigen-presenting cells such as dendritic cells (DCs) [22]. To facilitate DC targeted delivery of biotinylated soluble and particulate vaccines, bifunctional fusion protein vector (bfFp) can be used [23].

In this chapter, plasmid DNA encoding for H5N1 hemagglutinin (HA) was selected as a vaccine antigen and biotinylated chitosan as a DNA carrier. The DNA loaded biotinylated chitosan nanoparticles were functionalized with bfFp for DC targeted delivery. A comparative evaluation of systemic, mucosal and cellular

immune responses is demonstrated, following intranasal and intramuscular delivery of soluble DNA and nanoencapsulated DNA with or without DC targeting.

3.2 Materials and Methods

3.2.1 Materials

Plasmid DNA pCAG α -HA, encoding for mammalian codon optimized hemagglutinin (HA) gene of influenza A virus strain A/Hanoi/30408/2005 (Hanoi05, H5N1) was generously provided by Drs. Darwyn Kobasa and Gary Kobinger, National Microbiology Laboratory, Public Health Agency of Canada, Winnipeg, Canada. Construction and expression of pCAG α -HA has been described elsewhere [17]. Oligonucleotides were purchased from Integrated DNA Technologies (Coralville, Iowa, USA). Restriction enzymes: NdeI, EcoRI and T4 DNA Ligase were purchased from New England Biolabs (Freezer Program, Canada). Ultrapure chitosan hydrochloride salt (Protasan UP CL 113) was purchased from FMC Biopolymers (Novamatrix, Norway). Ni-NTA agarose resin and endofree plasmid DNA isolation kit was purchased from Qiagen (Mississauga, Canada). Rat anti-mouse CD40 mAb was purified from 1C10 hybridoma, a kind gift from Dr. M. Gold (University of British Columbia, Canada).

3.2.2 Expression and purification of HA1

The nucleotide sequences of Hanoi05 H5N1 hemagglutinin (HA) gene were codon optimized for *E. coli* expression and chemically synthesized by GENEART Inc. Germany. The codon optimized HA gene and HA1 fragment were PCR amplified and digested with *NdeI* and *EcoRI*, gel purified and ligated in correct reading frame in pBM802 expression vector with His₆ tag at C-terminal for purification [24]. The ligation mixtures were transformed in *E. coli* top 10 cells

and bacterial colonies were analyzed by plasmid DNA isolation and restriction digestion fragment mapping.

For medium scale expression a single bacterial colony containing HA1 plasmid (pDS25HA1) was inoculated in 10 ml TB (Terrific Broth) medium (1.2% Tryptone, 2.4% Yeast extract, 0.4% (v/v) glycerol and 25 mM HEPES pH 7.2) containing 5 µg/ml of tetracycline and allowed to grow overnight at 37 °C orbital shaker. The overnight culture was diluted (1:100) in fresh TB medium containing tetracycline (5µg/ml) and allowed to grow at 37 °C until an OD_{600nm} of 0.5–0.6 was reached. The bacterial culture was then induced with 0.2% w/v arabinose, grown for ~16 h at 37 °C and harvested by centrifugation at 5,000xg for 10 min at 4 °C. Total cell protein (TCP) from induced and uninduced culture was analyzed by SDS–PAGE and Western blot probed with anti-His₆ MAb. Bacterial pellets were lysed by French Press (20,000 psi) and inclusion bodies were purified according to previously published methods [25]. For purification of HA1, inclusion bodies were solubilised in a denaturing buffer (8 M urea, 100 mM NaH₂PO₄, 10 mM Tris.HCl pH 8.0) and separated from insoluble material by centrifugation at 27,000xg for 30 min at 4°C. Denatured soluble protein was loaded on pre-equilibrated Ni-NTA column (5 ml) and washed with 5 bed volumes of buffer containing 8 M urea, 100 mM NaH₂PO₄, 10 mM Tris.HCl, pH 6.3. Bound protein was eluted with a buffer containing 8 M urea, 100 mM NaH₂PO₄, 10 mM Tris.HCl, pH 4.5. All fractions were analyzed by reducing SDS-PAGE using 10% gel. Eluted protein fractions were pooled and diluted to ~75 µg/ml with Tris-arginine (TA) buffer (50 mM Tris pH 8.0, 0.4 M L-arginine) and refolding was done by dialysis in TA buffer in the presence of 1.0 mM GSH (glutathione, reduced), 0.1 mM GSSG (glutathione, oxidized) for 3 days with two changes at 4 °C. Refolded protein was dialyzed in PBS pH 7.4 at 4 °C and any aggregates were removed by centrifugation.

3.2.3 Plasmid DNA, biotinylated chitosan and bfFp

pCAG α -HA plasmid encoding for H5N1 HA gene was transformed into Subcloning EfficiencyTM *E.coli* DH5 α TM chemically competent cells (Invitrogen,

USA) and transformants were selected over LB agar plates with ampicillin (100 µg/ml). Plasmid DNA (pDNA) was scaled up and purified using Endofree plasmid mega kit (Qiagen). Chitosan hydrochloride was biotinylated using biotinamido hexanoic acid 3-sulfo-*N*-hydroxysuccinimide ester sodium salt (sulfo-NHS-LC-biotin) as per previous protocol (Chapter 2, section 2.2.3) and used for formulating nanoparticles [26]. Expression and purification of recombinant bifunctional fusion protein (bfFp) was carried out using our published protocols (also described in Chapter 2, section 2.2.6) [23, 26].

3.2.4 Formulation and characterization of pCAG α -HA loaded biotinylated chitosan nanoparticles

Plasmid DNA (pCAG α -HA) loaded biotinylated chitosan nanoparticles (NPs) were formulated using according to reported procedure (also described in Chapter 2, section 2.2.4) [26]. Briefly, 1 mg/ml solution of biotinylated chitosan was prepared in 5 mM sodium acetate buffer (pH 5.5). pCAG α -HA solutions in sodium sulfate (25mM) were prepared at different concentrations (1 to 0.2 mg/mL). Both solutions were preheated to 50-55 °C on the water bath and then 100 µL of chitosan solution was mixed with 100 µL of DNA solution and vortexed for 15 seconds. The mixture was kept for 30 min at room temperature for stabilization. A gel retardation assay was applied for monitoring NP formation by loading mixture onto 1% agarose gel containing ethidium bromide. The gel was run at 100 V for 45 min and bands visualized using Alpha Imager (Alpha Innotech, CA). For estimating encapsulation of DNA, NPs were spun down at 14,000 rpm for 20 min and supernatants were assayed for the presence of free DNA at absorbance 260 nm/280 nm using NanoDrop ND-1000 (Nanodrop Technologies Inc. Wilmington, Delaware). Encapsulation efficiency was calculated as follows: encapsulation efficiency (EE) = $A - B/A \times 100$, where *A* is the total DNA amount and *B* is the free DNA in the supernatant. Measurements of particle size and zeta potential of DNA loaded biotinylated chitosan NPs were performed using Zetasizer 3000 (Malvern Instruments, Malvern, UK).

3.2.5 Mice and immunizations

Female BALB/c mice were procured from Charles River Laboratories Inc. (Canada) and were eight-to-ten weeks old when the experiments were initiated. Animals were housed at Health Sciences Laboratory Animals Services (HSLAS) at the University of Alberta, Edmonton, Canada. Animal treatment, care and euthanasia were carried out according to the Canadian Council of Animal Care guidelines. The mice were divided in different groups of five mice (5 mice/group) and immunized through intranasal (IN) or intramuscular (IM) route on day 1 and day 21 with various vaccine formulations containing DNA (10 µg) as detailed in **Table 3.1**. A 10 µg/mouse dose of DNA (pCAGα-HA) was selected based on the results of previous studies from Dr. Kobasa's group, showing complete protection of mice [17]. DC targeted biotinylated chitosan nanoparticles were synthesized by incubating nanoparticles and bfFp (20 µg/dose) for 30 min. Anti-CD40 mAb (25 µg/dose) was added to nanoparticle formulations, immediately before performing immunizations. For IM immunizations, a 50 µL volume of the vaccine formulations was injected into the quadriceps muscle with a 26¹/₂ gauge needle. For IN immunization, mice were held in the vertical position, and 40 µL of vaccine formulations (20 µL in each nostril) were inoculated dropwise with a micropipettor right into the nostrils. The applied formulations were naturally inhaled and adequate care was taken to ensure proper delivery, any mice observed swallowing the vaccine formulation were excluded from the experiment.

Table 3.1 Immunization schedule and HA DNA vaccine formulations

Groups	Formulations*	Route	Dose (μg)
1	pHA (pCAG α -HA)	IN/IM	10
2	NP	IN/IM	10
3	NP +bfFp	IN/IM	10
4	NP+ bfFp+ α CD40	IN/IM	10

* Five mice per group were immunized with 10 μg of DNA and administered as naked or in nanoparticles (NPs), while α CD40 mAb's dose was 25 μg /mouse. pHA: pCAG α HA DNA vector; NP: nanoparticle with encapsulated pCAG α HA; bfFp, bifunctional fusion protein; α CD40, monoclonal antibody against CD40 ligand. Mice were immunized by intramuscular (IM) and intranasal (IN) route on day 1 and 21.

3.2.5.1 Sample collection

Mice were bled for serum collection on day 0, 14, 28, 46, and euthanized on day 56 by CO₂ asphyxiation and cervical dislocation. Following euthanasia serum, spleen, nasal and vaginal washings were collected for immunological studies. For nasal washings, the trachea of each mouse was opened and nasal fluids were collected by flushing PBS (200 μL) containing 0.1% w/v BSA through the nasal cavity using a fine micropipettor. Vaginal washes were performed according to the published method [27]. Briefly, 50 μL of PBS containing 0.1% w/v BSA was introduced into the vaginal tract of mice with a micropipettor. These 50 μL aliquots were withdrawn and reintroduced five times. The nasal and vaginal washes were kept at -20 °C until the day of analysis.

3.2.5.2 Detection of IgG, IgA and HI titers

HA protein-specific IgG and IgA titers were determined using ELISA. The flat-bottom 96-well ELISA microplates (Nunc MaxiSorp) were coated with 100 μL of HA1 protein (1 μg /well) overnight at 4 °C and washed with PBST (0.1% Tween

20 in PBS pH 7.4). After blocking with 1% BSA solution for 1 h, a 100 µl of diluted serum (1:100) from each mouse was added in duplicate and incubated overnight at 4 °C. After washing HRPO conjugated goat anti-mouse IgG was added and incubated for 1 hr. Plates were washed thrice and developed with TMB substrate for 15 min and optical density was recorded at 650 nm using a microplate reader (Molecular Devices Corp, CA). Similarly, HA1-specific IgG1 and IgG2a isotypes were determined using HRPO conjugated secondary IgG1 and IgG2a antibodies. The HA1-specific IgA antibodies in nasal and vaginal washings were analyzed at 1/10 dilution of samples. Hemagglutination inhibition (HI) assays were determined in Dr. Kobasa's lab, National Microbiology Laboratory, Winnipeg, using turkey red blood cells and a published protocol [17].

3.2.5.3 Cytokine release assay

Splenocytes were isolated by compressing the spleen between two frosted glass slides and erythrocytes were lysed with ACK lysis buffer. A single cell suspension was prepared by passing through a cell strainer. Splenocytes were suspended in RPMI 1640 containing 10 % fetal bovine serum and 1% penicillin-streptomycin-L-glutamine (PSG). The splenocytes were seeded at the density of 1×10^6 /well in a 96-well flat bottom plate and stimulated with HA1 protein at a final concentration of 20 µg/ml, while untreated cells served as control. The cultures were incubated for 72 h at 37 °C in a humidified CO₂ incubator. The released cytokine in culture supernatants were analyzed by a cytokine ELISA kit as per the manufacturer's instructions.

3.3 Results

3.3.1 Formulation and characterization of chitosan NPs

Chitosan nanoparticles were obtained by complex coacervation between positively charged chitosan and negatively charged DNA. Formation of nanoparticles at different weight ratio of biotinylated chitosan to DNA was monitored using agarose gel electrophoresis (**Figure 3.1**). On increasing the weight ratio of chitosan to DNA from 1 to 5, the amount of free plasmid DNA decreased. At a weight ratio of 1 and 2, the migration of free plasmid DNA was observed (**Figure 3.1**), however when weight ratio was 3 or more, free plasmid DNA could hardly be observed. Free DNA migrated from cathode to anode under the influence of electric field, but chitosan-DNA nanoparticles with positive charge did not migrate and were retained in loading well. Therefore, nanoparticle formulations used for in vitro and in vivo applications were formulated at weight ratio of 4.

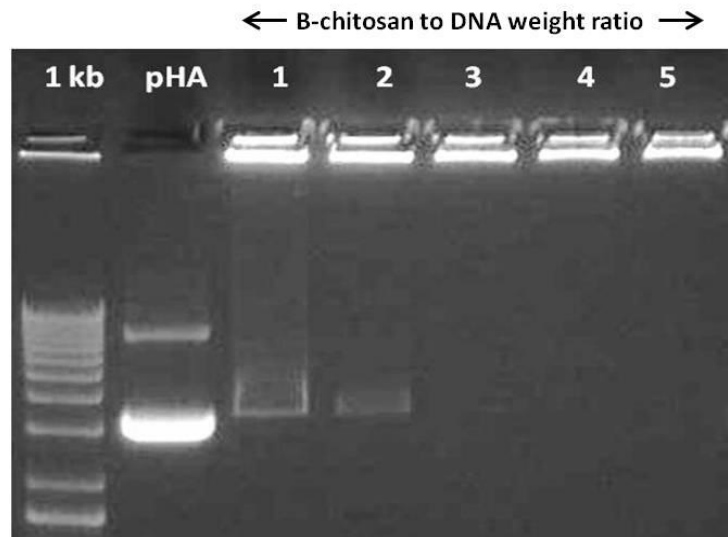


Figure 3.1 Optimization of pHA (pCAG α -HA) loaded biotinylated chitosan nanoparticles. Gel retardation assay of pHA DNA loaded biotinylated chitosan nanoparticles formulated at different weight ratios of biotinylated chitosan to pHA DNA 1 to 5 using complex-coacervation method.

The size of chitosan-DNA nanoparticles formulated at weight ratio 4 averaged 225 ± 15.5 nm. The zeta potential of nanoparticles prepared at this ratio was 12.5 ± 2.6 mV. The encapsulation of plasmid DNA at weight ratio of 4 was very efficient and was found to be in the range of $98.1 \pm 1.5\%$ (n=5). Cationic charge on chitosan backbone is crucial to form complexes with DNA. The pKa of glucosamine amino groups is ~ 6.5 which renders majority of amino groups (>90%) protonated at pH ~ 5.5 , while the positive charge is neutralized at physiological pH. This unique property of chitosan ensures that nanoparticles formulated at pH 5.5 could remain stable at the physiological pH without chemical cross-linking.

3.3.2 Expression and purification of HA1 in *E. coli*

To evaluate the antibody and cell-mediated immune responses elicited by vaccine formulations we expressed and purified HA1 as an antigen. The plasmid DNA (pDS25HA1) encoding HA1 (globular head region) was transformed in Top 10 *E. coli* and scaled up for expression. The bacterial HA1 protein was expressed as insoluble protein. Total cell protein was analyzed for HA1 expression using SDS-PAGE and Western blot probed with anti-His6 mAb (**Figure 3.2 A and B**). It is evident from the size of protein (~ 37 kDa) and results of Western blot confirmed that protein is indeed HA1. The HA1 was affinity purified under denaturing conditions using urea as a solubilising agent. A pH gradient was used for elution of Ni-NTA resin bound HA1. The purification profile was analyzed by loading different fractions on SDS-PAGE using 10 % gel (**Figure 3.2 C**). It is evident from the gel profile that purified protein does not contain non-specific bacterial proteins. The denatured protein was refolded using L-arginine buffer and a glutathione redox pair. The final yield of refolded protein was more than 70%. Bacterial HA1 was used to immunize rabbits and generate polyclonal antibodies against HA1. Polyclonal anti-HA1 antibodies raised in rabbit were found to cross-react with cell-lysate of pCAG α -HA transfected HEK 293T cells.

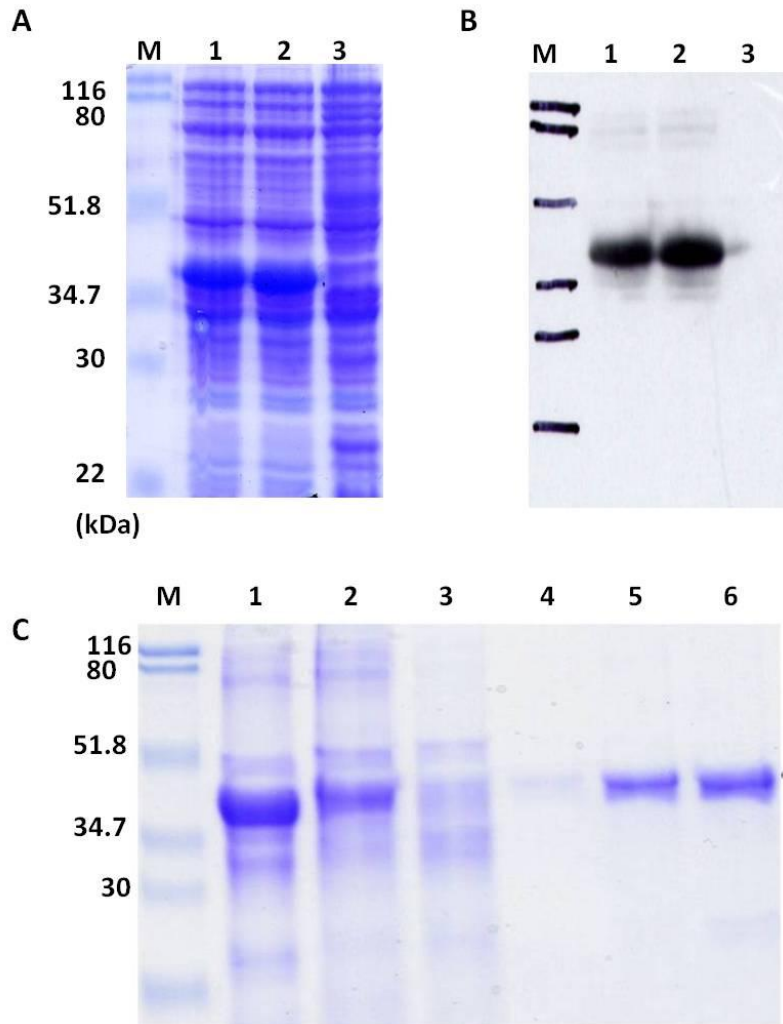


Figure 3.2 Expression and purification of recombinant HA1 in *E. coli*. (A) SDS-PAGE analysis of HA1 expression. Lane 1-2, induced culture; Lane 3, uninduced culture. (B) Western blot analysis using anti-His₆ mAb to confirm expression of HA1. Lane 1-2, induced culture; Lane 3, uninduced culture. (C) SDS-PAGE analysis of HA1 IMAC purification profile. Lane 1, Solubilised inclusion bodies; Lane 2, Unbound; Lane 3, wash I; Lane 4, wash II; Lane 5-6, Elution fractions.

3.3.3 HA-specific systemic IgG response

The efficacy of different formulations, namely, soluble DNA, DC targeted and non-targeted nanoparticle encapsulated DNA vaccines was evaluated for induction of systemic IgG responses. A head-to-head comparison of these formulations was carried out using intranasal (IN) and intramuscular (IM) route of administration (Table 3.1). It is evident from the HA1-specific IgG titers that IN immunization with naked DNA and non-targeted nanoparticle (NPs) formulations elicited basal IgG levels (**Figure 3.3 A**). This can be argued based on the low-dose (10 µg DNA/mouse on day 1 and 21) used for immunization studies. However, nanoparticle formulations functionalized with bfFp induced higher levels of HA1-specific IgG titers indicating that bfFp based dendritic cell targeting contributes to enhance immunogenicity of low-dose chitosan encapsulated DNA. We next tested whether the IgG titer of bfFp functionalized nanoparticle formulations can be improved with a DC maturation stimulus (anti-CD40 mAb). Our data suggests that coadministration of anti-CD40 antibody resulted in significant increase in the HA1-specific IgG titers irrespective of route of immunization (**Figure 3.3**). Our results demonstrate that IM vaccination with plasmid DNA was superior to IN route for induction of systemic IgG responses, irrespective of vaccine formulation used for immunization. The anti-CD40 mAb has been used as DC maturation stimuli with DEC-205 targeted protein antigens and shown to augment the antibody and cell-mediated immune responses [28]. Anti-CD40 mAb can also act as effective mucosal adjuvant along with liposomal vaccines [29]. Intranasal administrations of liposome encapsulated peptide vaccine along with anti-CD40 mAb induced significantly higher levels of cytotoxic T cell responses against influenza A virus.

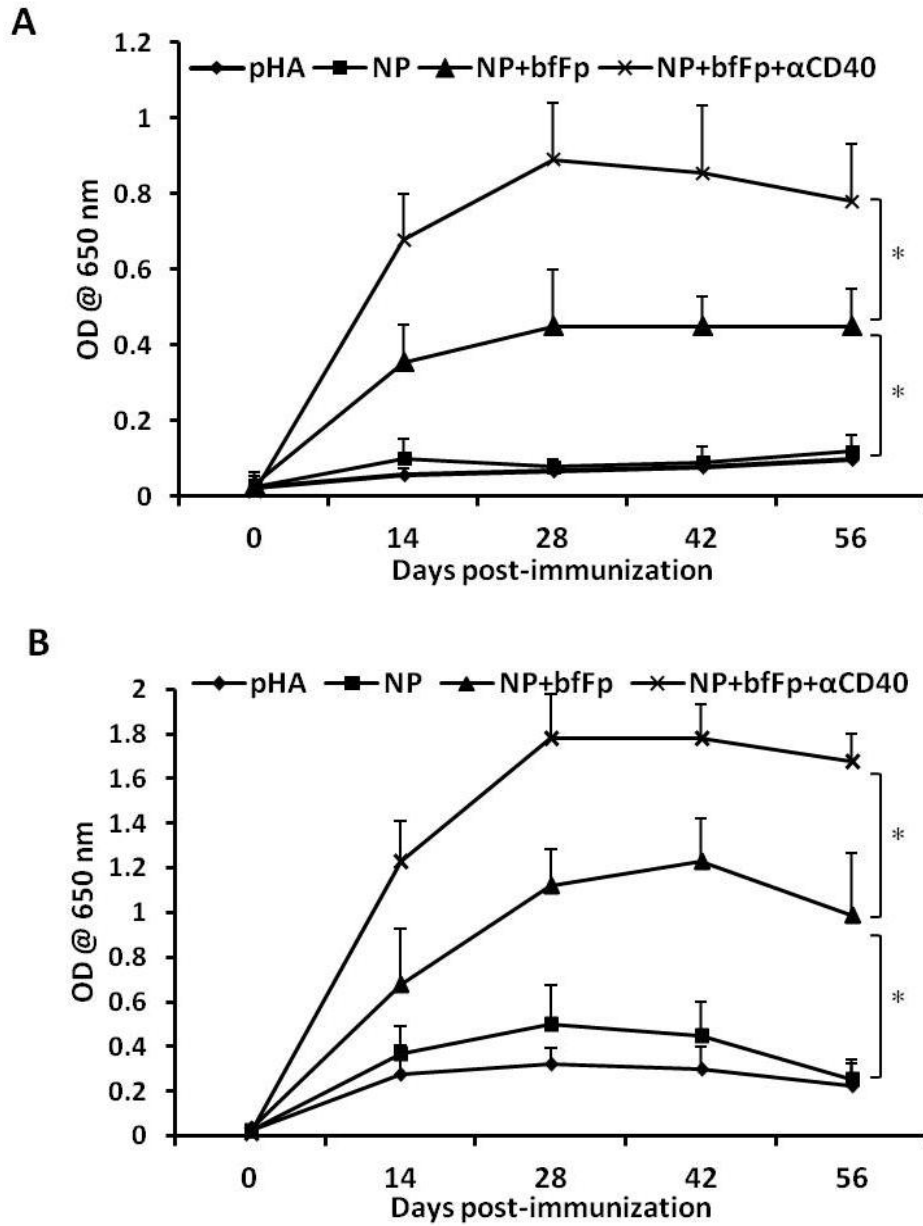


Figure 3.3 HA-specific systemic IgG response in mice vaccinated with various DNA vaccine formulations using intranasal (A) and intramuscular (B) route of administration. BALB/c mice (5 per group) were immunized with indicated vaccine formulations and serum was collected at day 0, 14, 28, 42 and 56. Serum was analyzed for the presence of HA1-specific IgG using ELISA. Data are presented as group mean±SD at various time-points. The * indicates statistically significant difference between different vaccine formulations (*P < 0.05).

3.3.4 HA-specific mucosal IgA response

Mucosal IgA plays a key role in evading the entry of pathogens through respiratory route, and therefore serves as a first-line of defence. Therefore, induction of IgA responses at nasal and distant mucosal surfaces is vital for designing an optimum influenza vaccine formulation. In our experiments, we compared IN and IM routes for induction of HA1-specific IgA titers in nasal and vaginal fluids (**Figure 3.4**). In agreement with the results of SARS CoV N experiments described in chapter 2, no IgA was detected following IN administration with naked DNA formulations and even a low-dose nanoparticle encapsulated DNA failed to induce IgA secretions. However, the titers of IgA were shown to improve after bfFp functionalized nanoparticles were used. In good alignment with IgG data, co-administration of bfFp targeted formulations with anti-CD40 mAb resulted in significantly higher IgA responses compared with only targeted formulations. The increase in mucosal IgA levels is in accordance with the fact that non-adjuvanted vaccine formulations perform poorly when administered through mucosal route [10, 20]. In contrast to nasal delivery, IM route failed to induce any detectable levels of nasal and vaginal IgA. Therefore, strong mucosal responses are induced only after administration of bfFp functionalized formulations together with a DC activation stimulus.

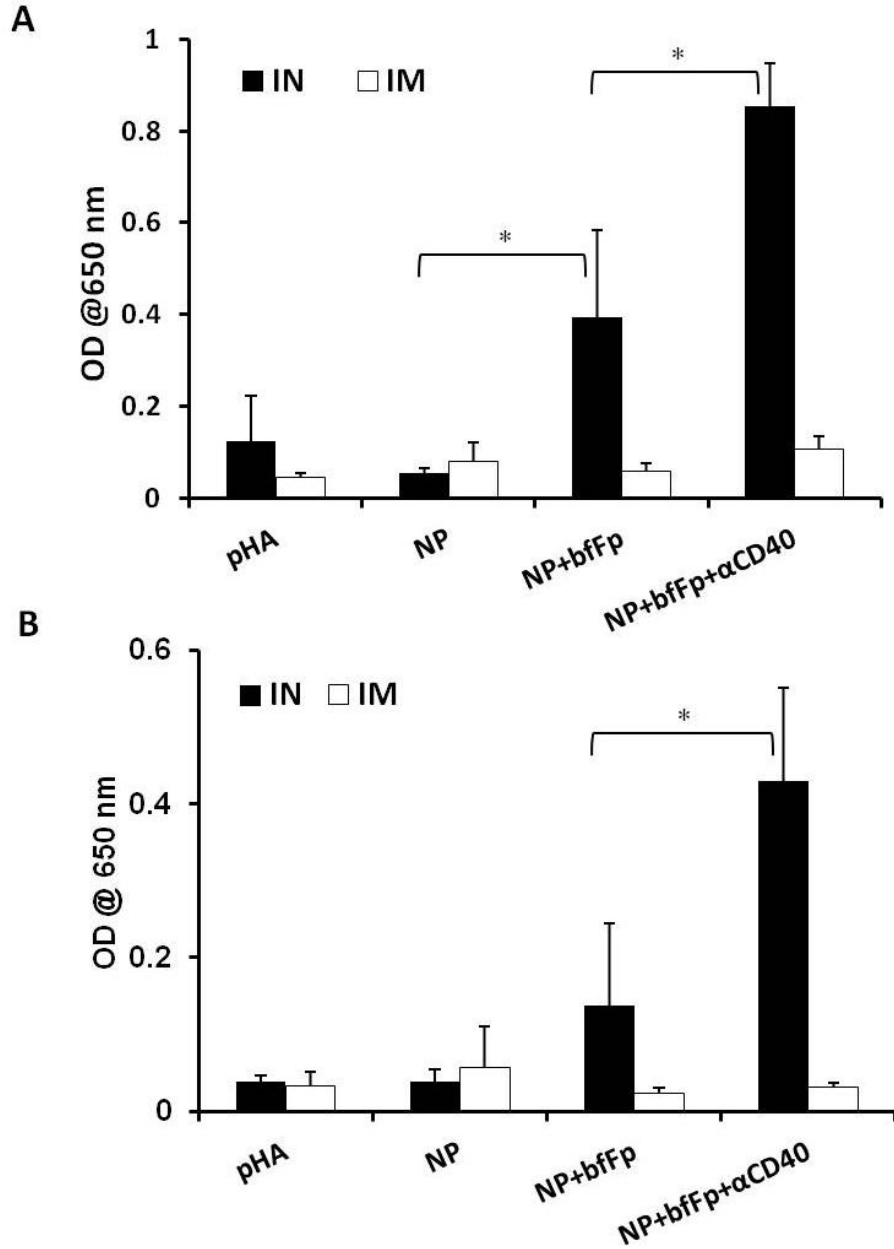


Figure 3.4 HA-specific mucosal IgA responses in the nasal washes (A) and vaginal washes (B). BALB/c mice (5 per group) were vaccinated with various DNA vaccines using intranasal (IN) and intramuscular (IM) route of administration. At day 56, mice were euthanized and nasal and vaginal washes were collected for analysis of HA1-specific IgA titers using ELISA. Data are presented as group mean \pm SD. The * denotes statistically significant difference between groups of mice immunized with different vaccine formulations (* $P < 0.05$).

3.3.5 Ex vivo cytokine production

To determine cellular immune response to plasmid DNA vaccine formulation, ex vivo cytokine profile were examined using ELISA assay. Splenocytes were harvested from spleen at day 56 and restimulated with HA1 protein. The splenocytes of mice immunized with bfFp targeted formulations together with anti-CD40 mAb produced significantly higher amounts of IFN- γ and IL-4 compared with only bfFp targeted formulations (**Figure 3.5**). Only low amounts of IFN- γ and IL-4 were detected when non-formulated and nanoparticle encapsulated DNA vaccine formulations were used for immunization. As expected, the IM route of immunization was shown to induce higher levels of IFN- γ and IL-4 cytokines irrespective of the vaccine formulation. Overall the results suggest that splenocytes are capable of secreting higher levels of antigen-specific Th1 cytokine IFN- γ and a moderate level of the Th2 cytokine IL-4 upon in vitro stimulation with HA1 protein. The IFN- γ is an effector cytokine and plays a key role in activation of macrophages, dendritic cells and inhibition of viral infections [30]. These findings indicate that intranasal delivery of bfFp based DC targeted HA DNA vaccination is effective in the activation of cellular immune responses.

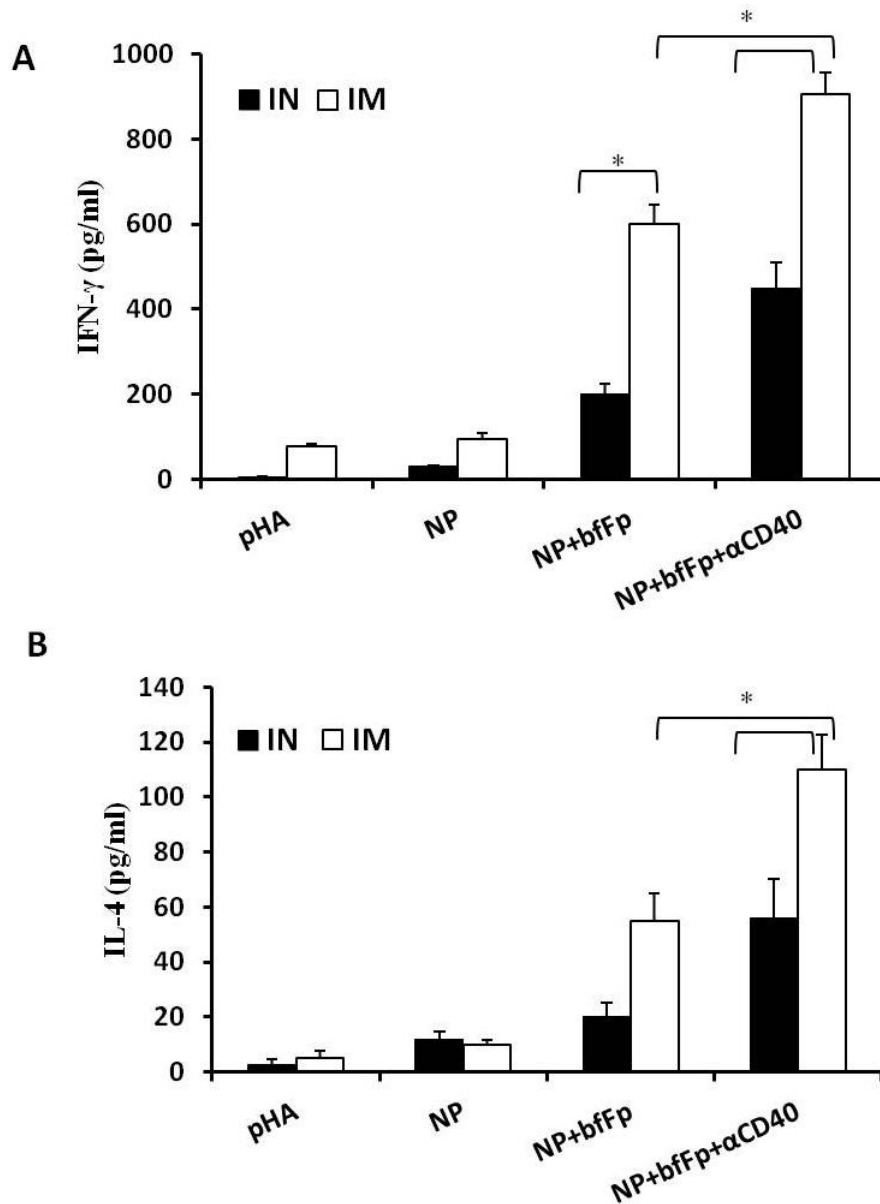


Figure 3.5 HA-specific IFN- γ and IL-4 responses. BALB/c mice (five per group) were immunized on day 1 and 21 either by IM or IN route of administration and euthanized on day 56. Splenocytes were isolated and stimulated with HA1 as recall antigen for 72 h. Cell culture supernatants were analyzed in triplicates for the presence of IFN- γ (A) and IL-4 (B) using ELISA kit. Data are represented as mean \pm SD of triplicates cultures. The * denotes statistically significant difference in IFN- γ and IL-4 cytokine levels between different groups of mice immunized with indicated vaccine formulations (* $P < 0.05$).

3.4 Discussion

Avian influenza (H5N1) viruses are highly pathogenic and recent outbreaks have suggested that some subtypes of avian influenza viruses can replicate in human respiratory tract and result in severe respiratory complications and morbidity [1]. Therefore, development of an effective mucosal vaccine is the best strategy to prevent a potential pandemic of this virus. However, the traditional egg based vaccine approach against H5N1 viruses is not a suitable strategy since these viruses are lethal in chicken embryos and therefore manufacturing of H5N1 vaccines on large scale is not a viable option [31].

Since these viruses infect respiratory tract, development of an effective vaccine that can provide mucosal immunity at the nasal mucosal epithelium, can be administered by non-invasive means and produced on a large-scale in short duration without the use of traditional egg based approach is an important goal for development of H5N1 vaccines [6]. In this reference, DNA vaccine can serve as an ideal alternative vaccine platform against H5N1 viruses. As they can be readily constructed based on merely pathogens genetic information and can be produced in bacteria bypassing the need of time-consuming egg based manufacture. DNA vaccine are non-infectious and nonreplicating, thereby diminish safety concerns associated with live attenuated vaccines. However, despite excellent qualities and approval for veterinary purposes, these vaccines show poor immunogenicity profile in humans. Therefore, many strategies have been devised to improve the immunogenicity of DNA vaccines [32]. In recent studies, the two approaches have been mainly explored: direct targeting of DNA vaccine to dendritic cells and optimal formulation or mode of delivery.

Utilizing both of the approaches, here, we explored feasibility of dendritic cell targeted delivery of nanoparticle encapsulated H5N1 DNA vaccine by intranasal and intramuscular immunization. The chitosan was used a carrier for DNA vaccine, as it has several favorable properties for this purpose. In this study the plasmid DNA loaded biotinylated chitosan nanoparticles were functionalized with bfFp to achieve non-invasive targeting of DNA vaccines to respiratory DCs.

Respiratory DCs continuously sample and process environmental agents and could serve as ideal target for targeted delivery of vaccine antigens [33]. Moreover, mouse respiratory tract DC subsets; such as airway, alveolar and interstitial DCs express DEC-205 receptor [33, 34]. Thus, targeted delivery of DNA loaded chitosan nanoparticles with the help of bfFp can be achieved. Our results suggest that bfFp targeted delivery of nanoparticulate DNA vaccine can significantly improve the immunogenicity of encoded antigen. We demonstrate that the immunogenicity of these DC targeted formulation can be further improved by the coadministration of a DC maturation stimuli (anti-CD40 mAb).

Although DC targeted DNA vaccine formulations together with DC maturation stimuli were found to be the best for the induction of humoral and systemic immune responses irrespective of the route of immunization, only intranasal route of administration induced secretion of mucosal IgA responses. In contrast, intranasal delivery of naked DNA or non-targeted nanoencapsulated DNA did not provoke IgA secretions. Both IgA and IgG antibodies play significant role in protection against influenza infection, however, many studies have shown that secretory IgA is primarily involved in protection against infection in upper respiratory tract, whereas the serum IgG plays a key role in lower respiratory tract [7]. Furthermore, it is evident based on findings that secretory IgA induced by natural infection or vaccines is cross-protective against heterologous virus infection than serum IgG induced following parenteral route [6, 20]. Intranasal DNA immunization also induced antigen-specific IgA in vaginal secretions; it is expected because of overlapping tissue sites in the common mucosal immune system and these observations are in accordance with previous studies [20, 27]. Despite strong IgG titers, no detectable hemagglutination inhibition (HI) titers were observed. However, despite absence of detectable HI titers before virus challenge complete protection of mice was frequently observed [17].

Overall our results show that the DC targeting, delivery vehicle and route of immunization are critical determinants that govern immunogenicity of plasmid DNA based H5N1 vaccines. We speculate that the intranasal administration of

DC targeted DNA vaccines together with an adjuvant could provide protection to influenza virus infections by provoking mucosal, humoral and cellular immune responses. Moreover, using bfFp based approach DC targeting can be achieved through noninvasive route of administration. We expect that the DNA vaccine strategy described herein should be further evaluated as potentially affordable and viable alternate for designing low-dose prophylactic DNA vaccines against influenza and other respiratory infections.

3.5 References

- [1] Beigel JH, Farrar J, Han AM, Hayden FG, Hyer R, De Jong MD, et al. Avian influenza A (H5N1) infection in humans. *N Engl J Med* 2005;353:1374-85.
- [2] Taubenberger JK, Reid AH, Lourens RM, Wang R, Jin G, Fanning TG. Characterization of the 1918 influenza virus polymerase genes. *Nature* 2005;437:889-93.
- [3] Palese P. Making better influenza virus vaccines? *Emerg Infect Dis* 2006;12:61-5.
- [4] Treanor JJ, Campbell JD, Zangwill KM, Rowe T, Wolff M. Safety and immunogenicity of an inactivated subvirion influenza A (H5N1) vaccine. *N Engl J Med* 2006;354:1343-51.
- [5] Neutra MR, Kozlowski PA. Mucosal vaccines: the promise and the challenge. *Nat Rev Immunol* 2006;6:148-58.
- [6] Hasegawa H, Ichinohe T, Tamura SI, Kurata T. Development of a mucosal vaccine for influenza viruses: preparation for a potential influenza pandemic. *Expert Rev Vaccines* 2007;6:193-201.
- [7] Renegar KB, Small Jr PA, Boykins LG, Wright PF. Role of IgA versus IgG in the control of influenza viral infection in the murine respiratory tract. *J Immunol* 2004;173:1978-86.
- [8] Mutsch M, Zhou W, Rhodes P, Bopp M, Chen RT, Linder T, et al. Use of the inactivated intranasal influenza vaccine and the risk of Bell's palsy in Switzerland. *N Engl J Med* 2004;350:896-903.
- [9] Ichinohe T, Aina A, Tashiro M, Sata T, Hasegawa H. PolyI:polyC 12U adjuvant-combined intranasal vaccine protects mice against highly pathogenic H5N1 influenza virus variants. *Vaccine* 2009;27:6276-9.
- [10] Wang D, Christopher ME, Nagata LP, Zabielski MA, Li H, Wong JP, et al. Intranasal immunization with liposome-encapsulated plasmid DNA encoding influenza virus hemagglutinin elicits mucosal, cellular and humoral immune responses. *J Clin Virol* 2004;31:S99-S106.

- [11] Coulter A, Harris R, Davis R, Drane D, Cox J, Ryan D, et al. Intranasal vaccination with ISCOMATRIX® adjuvanted influenza vaccine. *Vaccine* 2003;21:946-9.
- [12] Durrer P, Glück U, Spyr C, Lang AB, Zurbriggen R, Herzog C, et al. Mucosal antibody response induced with a nasal virosome-based influenza vaccine. *Vaccine* 2003;21:4328-34.
- [13] Read RC, Naylor SC, Potter CW, Bond J, Jabbal-Gill I, Fisher A, et al. Effective nasal influenza vaccine delivery using chitosan. *Vaccine* 2005;23:4367-74.
- [14] Sui Z, Chen Q, Fang F, Zheng M, Chen Z. Cross-protection against influenza virus infection by intranasal administration of M1-based vaccine with chitosan as an adjuvant. *Vaccine* 2010;28:7690-8.
- [15] Laddy D, Weiner D. From plasmids to protection: A review of DNA vaccines against infectious diseases. *Int Rev Immunol* 2006;25:99-123.
- [16] Kim JH, Jacob J. DNA vaccines against influenza viruses: Vaccines for Pandemic Influenza. In: Compans RW, Orenstein WA, editors.: Springer Berlin Heidelberg; 2009: 197-210.
- [17] Patel A, Tran K, Gray M, Li Y, Ao Z, Yao X, et al. Evaluation of conserved and variable influenza antigens for immunization against different isolates of H5N1 viruses. *Vaccine* 2009;27:3083-9.
- [18] Chen Q, Kuang H, Wang H, Fang F, Yang Z, Zhang Z, et al. Comparing the ability of a series of viral protein-expressing plasmid DNAs to protect against H5N1 influenza virus. *Virus Genes* 2009;38:30-8.
- [19] Rao S, Kong WP, Wei CJ, Yang ZY, Nason M, Styles D, et al. Multivalent HA DNA vaccination protects against highly pathogenic H5N1 avian influenza infection in chickens and mice. 2008;3(6):e2432.
- [20] Torrieri-Dramard L, Lambrecht B, Ferreira HL, Van Den Berg T, Klatzmann D, Bellier B. Intranasal DNA vaccination induces potent mucosal and systemic immune responses and cross-protective immunity against influenza viruses. *Mol Ther* 2011;19:602-11.

- [21] Kang ML, Cho CS, Yoo HS. Application of chitosan microspheres for nasal delivery of vaccines. *Biotechnol Adv* 2009;27:857-65.
- [22] Jiang HL, Kang ML, Quan JS, Kang SG, Akaike T, Yoo HS, et al. The potential of mannosylated chitosan microspheres to target macrophage mannose receptors in an adjuvant-delivery system for intranasal immunization. *Biomaterials* 2008;29:1931-9.
- [23] Wang WW, Das D, Suresh MR. A versatile bifunctional dendritic cell targeting vaccine vector. *Mol Pharm* 2009;6:158-72.
- [24] Das D, Suresh MR. Copious production of SARS-CoV nucleocapsid protein employing codon optimized synthetic gene. *J Virol Methods* 2006;137:343-6.
- [25] Das D, Mongkolaungkoon S, Suresh MR. Super induction of dengue virus NS1 protein in *E. coli*. *Protein Expr Purif* 2009;66:66-72.
- [26] Raghuwanshi D, Mishra V, Das D, Kaur K, Suresh MR. Dendritic cell targeted chitosan nanoparticles for nasal DNA immunization against SARS CoV nucleocapsid protein. *Mol Pharm* 2012;9:946-56.
- [27] Khatri K, Goyal AK, Gupta PN, Mishra N, Vyas SP. Plasmid DNA loaded chitosan nanoparticles for nasal mucosal immunization against hepatitis B. *Int J Pharm* 2008;354:235-41.
- [28] Bonifaz L, Bonnyay D, Mahnke K, Rivera M, Nussenzweig MC, Steinman RM. Efficient targeting of protein antigen to the dendritic cell receptor DEC-205 in the steady state leads to antigen presentation on major histocompatibility complex class I products and peripheral CD8 + T cell tolerance. *J Exp Med* 2002;196:1627-38.
- [29] Ninomiya A, Ogasawara K, Kajino K, Takada A, Kida H. Intranasal administration of a synthetic peptide vaccine encapsulated in liposome together with an anti-CD40 antibody induces protective immunity against influenza A virus in mice. *Vaccine* 2002;20:3123-9.
- [30] Wu C-y, Kirman JR, Rotte MJ, Davey DF, Perfetto SP, Rhee EG, et al. Distinct lineages of TH1 cells have differential capacities for memory cell generation in vivo. *Nat Immunol* 2002;3:852-8.

- [31] Takada A, Kuboki N, Okazaki K, Ninomiya A, Tanaka H, Ozaki H, et al. Avirulent Avian influenza virus as a vaccine strain against a potential human pandemic. *J Virol* 1999;73:8303-7.
- [32] Kutzler MA, Weiner DB. DNA vaccines: ready for prime time? *Nat Rev Genet* 2008;9:776-88.
- [33] Blank F, Stumbles P, von Garnier C. Opportunities and challenges of the pulmonary route for vaccination. *Expert Opin Drug Deliv* 2011;8:547-63.
- [34] Langlois RA, Legge KL. Respiratory dendritic cells: mediators of tolerance and immunity. *Immunol Res* 2007;39:128-45.

**CHAPTER 4: Chitosan nanoparticle encapsulated fusion
DNA vaccine for dendritic cell targeted delivery of SARS-
coronavirus nucleocapsid protein**

A version of this chapter will be submitted to *Molecular Pharmaceutics* journal:
Raghuwanshi D., Sharma SS., Das D, Arivazhagan P, Kaur K.* and Suresh M.R.
Chitosan nanoparticle encapsulated fusion DNA vaccine for dendritic cell targeted
delivery of SARS coronavirus nucleocapsid protein.

4.1 Introduction

DNA vaccination represents a novel strategy for generating antigen-specific immune responses against a range of pathogens [1]. DNA vaccines can be easily manufactured on a large scale, repeatedly administered and have better stability profile compared with recombinant protein based vaccines. Furthermore, in case of pandemic or bioterrorism threats, DNA vaccines can be promptly engineered based on pathogens genetic code and formulated in short time frame [2]. However, the major obstacle to the successful application of DNA vaccines is their poor immunogenicity profile. Thus, numerous strategies are under intensive investigation to improve the immunogenicity profile of DNA vaccines.

Recent studies suggest that immunogenicity of DNA vaccines can be enhanced by several means such as plasmid optimization, application of electroporation or gene-gun, use of cationic polymer based gene delivery systems, use of immune modulators as adjuvants, and targeting of plasmid DNA or encoded antigen to professional antigen presenting cells (APCs), such as dendritic cells (DCs) (reviewed in [2, 3]).

Among different strategies, targeting of DNA vaccines to DCs has caught particular attention as DCs play a key role in initiating the primary immune responses after DNA vaccination [4-6]. On the contrary, following intramuscular (IM) or intradermal (ID) administration of a plasmid DNA in mice, the encoded antigen is primarily expressed in myocytes and keratinocytes, respectively and only a small number of DCs present at the site of injection get directly transfected. Therefore, poor transfection of DCs is often considered as one of the reason behind sub-optimal performance of DNA vaccines.

In this context, accumulating evidence suggests that potency of DNA vaccine can be improved by direct transfection followed by expression of antigen by DCs. The direct targeting of DNA vaccines to DCs can be achieved using two approaches: (i) by using DC-specific promoters such as CD11c, DC-SIGN [7, 8] or (ii) by direct targeting of nanoparticle encapsulated DNA vaccines with the help of DC-receptor specific ligands. Although direct transfection provides better

immunogenicity but the number of DCs transfected in vivo is usually low [5]. In Chapters 2 and 3, we have adopted similar approach.

As an alternative strategy, DC targeting of DNA encoded antigen can be realized by linkage of antigen to the molecule capable of binding to DC surface receptors (e.g scFv for DEC-205). For instance, a fusion plasmid DNA construct that encodes for antigen of interest and DC-receptor ligand, can be constructed [9, 10]. Upon transfection of fusion DNA construct, the secreted antigen is taken up by the DCs via receptor mediated endocytosis and gets processed for presentation to T cells. To accomplish in situ targeted delivery of SARS CoV nucleocapsid (N) protein to DCs, we constructed a fusion DNA construct that encodes for mouse anti-DEC-205 scFv and SARS CoV nucleocapsid protein. We speculate that in vivo expression of fusion protein, anti-DEC-205 scFv-SARS CoV N protein (referred as DECN fusion protein) would result in DEC-205 receptor mediated targeting of DCs.

In this chapter, two DNA constructs, pVAXN and pDECN are compared for the immune responses (**Figure 4.1**). pVAXN encodes for SARS CoV N protein, whereas pDECN encodes for fusion protein consisting of mouse anti-DEC-205 scFv and SARS CoV N protein. A water soluble, ultrapure chitosan was used to formulate DNA encapsulated nanoparticles. For in vivo immunization studies pVAXN or pDECN loaded chitosan nanoparticles were administered intramuscularly either alone or with a DC maturation stimulus (anti-CD40 mAb).

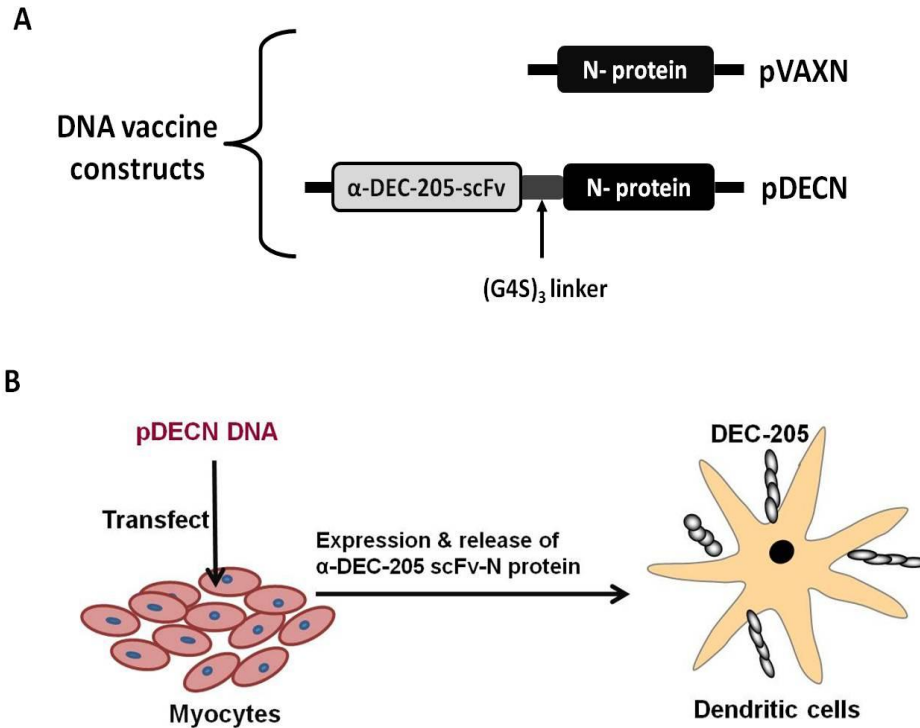


Figure 4.1 DNA vaccine constructs and dendritic cell targeting strategy. (A) Schematic representation of plasmid constructs. pDECN was constructed by inserting anti-DEC-205 scFv gene upstream of SARS CoV N protein gene, whereas pVAXN consists of SARS CoV N protein gene only. (B) A schematic representation of in situ DC targeting using pDECN vaccine constructs.

4.2 Materials and Methods

4.2.1 Materials

pVAX1 plasmid was purchased from Invitrogen (USA). pVAXN and pWET7 plasmids reported previously in chapter 2 [11, 12], containing ORFs (Open Reading Frame) for SARS-CoV N protein and bfFp respectively, were used to construct pDECN. Oligonucleotides were purchased from Integrated DNA Technologies (Coralville, Iowa, USA). Restriction Enzymes: *NotI*, *XbaI*, *BamHI* and *EcoRI*, T4 DNA Ligase were purchased from New England Biolabs (Freezer Program, Canada). Ultrapure chitosan hydrochloride salt (Protasan UP CL 113)

was purchased from FMC Biopolymers AS (Novamatrix, Norway). HRPO based mouse antibody isotyping kit was obtained from Southern Biotech (Birmingham, AL USA). HEK 293 T cell were a kind gift from Dr. Hasan Uludag's Laboratory (University of Alberta, Canada). DC 2.4, a DEC-205 expressing mouse bone marrow DC cell-line transduced with GM-CSF, *myc* and *raf* oncogenes was obtained from Dr. Kenneth Rock (University of Massachusetts, Worcester, MA). A green fluorescent protein reporter plasmid (pEGFP-C1) was obtained from Dr. Deborah Burshtyn (University of Alberta). Anti-SARS CoV N protein mAb (19C7) was FITC labeled with FITC antibody labeling kit (Thermo Fisher Scientific Inc. USA).

4.2.2 Plasmid DNA constructs and DNA preparation

Plasmid DNA construct, pDECN, encoding for anti-DEC-205 scFv fused with SARS CoV N protein was constructed by performing a Splice Overlap Extension (SOE) Polymerase Chain Reaction (PCR) between bfFp (anti-DEC-205 scFv) and SARS CoV N protein ORFs. Overlap primers were synthesized containing sequences coding for 3' end of anti-DEC205 scFv, a (G₄S)₃ linker and 5' end of SARS N protein gene. Briefly, individual PCRs were performed to amplify nucleotide sequences coding for anti-DEC205 scFv and SARS CoV N protein using pWET7 and pVAXN plasmids respectively. PCR amplicons were electrophoresed on low melting agarose (0.8%) and purified using QIAquick gel extraction kit. 100 ng of each amplicon was employed as template for the SOE PCR using a *NotI* restriction site incorporated terminal primer coding for the 5' end of anti-DEC205 scFv and an *XbaI* restriction site incorporated primer coding for the 3' end of SARS N protein gene. SOE PCR product was electrophoresed on low melting agarose and purified using QIAquick gel extraction kit. pVAX1 vector and SOE PCR product were digested with *NotI* and *XbaI*, electrophoresed on low melting agarose and purified using QIAquick gel extraction kit. T4 DNA Ligase was used to ligate DECN gene into pVAX1 vector, which was transformed into Subcloning EfficiencyTM *E.coli* DH5 α TM chemically competent cells (Invitrogen, USA). Transformants were selected over LB agar plates with

kanamycin (50 µg/ml) and screened using colony PCR. Plasmid DNA (pDECN) was prepared from positive clones using QIAprep Spin Miniprep kit and further analyzed by restriction digestion and sequencing using ABI 3730 DNA Analyzer (Applied Biosystems, USA). pVAXN and pDECN plasmids were scaled up and purified using Endotoxin free giga plasmid isolation kit (Qiagen) and used for all applications.

4.2.3 Transfection and expression of antigens

HEK 293T cells were grown in DMEM medium supplemented with 10% FBS and 1% PSG. The recombinant plasmid pVAXN and pDECN were transfected into HEK 293T cells using Fugene HD transfecting reagent according to manufacturer's instructions. Native pVAX1 was similarly transfected and used as a control vector. Briefly, HEK 293T cells were seeded at the density of 1 million/well in a 6-well cell culture plate and grown overnight. Following day, cells were transfected with indicated plasmid constructs and allowed to grow for 48 h. After 48 h, cells were dislodged with pipetting. Cell suspension was centrifuged at 1,500 rpm for 10 min. Subsequently, cell culture supernatants and cell pellet were analyzed for the expression of SARS CoV N protein or fusion anti-DEC-205 scFv-SARS CoV N protein, DECN protein, using mouse anti-SARS CoV N protein monoclonal antibody (19C7) as a probe in Western blot [13]. The cell culture supernatants were also used for analysis of in vitro DC binding studies as described below.

4.2.4 In-vitro DC binding studies

Immortal murine dendritic cell line DC2.4, that stably express DEC-205 receptor [14] was propagated in DMEM supplemented with 10% FBS. For analysis of binding, cells were detached with pipetting, centrifuged at 12,00 rpm for 5 min and adjusted to 1×10^6 /ml with PBS supplemented with 2% FBS. Fc receptors were blocked with anti-mouse CD16/CD32 antibody (eBioscience, San Diego, CA) at 4 °C for 30 min and washed. A 100 µl of cell suspension containing 1×10^5 cells was separately incubated with supernatant (1 mL) from pVAX1, pVAXN or

pDECN transfected 293T cells at 4 °C for 30 min. Cells were then washed with ice cold PBS and incubated with FITC-labeled anti-SARS CoV N protein mAb (19C7). The samples were run on FACS Canto II flow cytometer and data was analyzed using Flowjo software (Tree Star Inc.)

4.2.5 Formulation of DNA loaded chitosan nanoparticles (NPs)

Plasmid DNA loaded chitosan nanoparticles were prepared using a modified coacervation method as described in chapter 2 (section 2.2.4). Briefly, ultrapure chitosan hydrochloride salt (Protasan UP CL 113) was dissolved in 5 mM sodium acetate buffer (pH 5.5) at a final concentration of 1 mg/ml and passed through 0.22 µm syringe filter. The solutions of pVAXN (250 µg/mL) and pDECN (500 µg/mL) were prepared in 25 mM sodium sulphate. The chitosan and DNA solutions were separately pre-heated to 50–55 °C on the water bath and 100 µl of chitosan solution was added to equal volume of DNA solution and vortexed for 15 seconds. Mixture was kept at room temperature for 30 min to stabilize the nanoparticles. For estimating encapsulation efficiency of DNA, NPs were spun at 14,000 rpm for 20 min and supernatants assayed for the presence of free DNA at absorbance 260 nm/280 nm using NanoDrop ND-1000 (Nanodrop Technologies Inc. Wilmington, Delaware). To analyze the in vitro transfection efficiency pEGFP-C1 loaded chitosan nanoparticle were formulate as described above.

The complex formation between chitosan and DNA was monitored by electrophoretic gel mobility assay. Mixture of NPs prepared at different weight ratios was mixed with the loading dye and run on an ethidium bromide containing 1% agarose gel. The gel was immersed in tris-acetate/EDTA buffer and allowed to run for 45 min at 100 V. DNA bands were visualized using the Alpha Imager (Alpha Innotech; San Leandro, CA). Unless otherwise mentioned, the NPs formulated at 4:1 weight ratio chitosan to DNA were used for all studies. The nanoparticle suspension was prepared in MilliQ water, and the size and zeta-potential of pVAXN and pDECN loaded nanoparticles was determined using Zetasizer 3000 (Malvern Instruments, UK).

To check the stability against nuclease digestion, DNA loaded nanoparticles formulations or the naked DNA was subjected to DNase I digestion. Briefly, 4 µg of naked or nanoencapsulated DNA in deionised water (40 µl) was incubated with 10 U DNase I (Invitrogen) for 30 and 60 min at 37 °C. The DNase activity was stopped by adding EDTA solution to final concentration of 50 mM. The nanoparticles were centrifuged, washed to remove DNase I, and the integrity of the DNA in the samples was analyzed on agarose gel and photographed using Alpha Imager (Alpha Innotech; San Leandro, CA).

4.2.6 In vitro transfection

In vitro transfection efficiency of the chitosan nanoparticles was measured as GFP expression in HEK 293T cells using flow cytometry. To analyze transfection efficiency, pEGFP-C1 plasmid loaded chitosan NPs were synthesized at 4:1 weight ratio of chitosan to DNA, as described in section 4.2.5. HEK 293T cells were propagated in DMEM supplemented with 10% FBS and 1% PSG. A day before transfection, cells were seeded in a 24-well plate at a density of 50,000 cells/well. Next day, media was aspirated and cells were treated with pEGFP-C1 loaded chitosan NP, containing 2.5 µg DNA with OptimMEM medium for 5 h. Thereafter, the supernatants were discarded and fresh culture medium (DMEM containing 10% FBS) was added, and cells were incubated for 48 h. As control, cells were treated with Lipofectmine™ 2000 (Invitrogen) and soluble pEGFP-C1 DNA or left untreated. After incubation, cells were trypsinized and fixed using 300 µl of 3.5% formaldehyde. Cells were analysed on a FACS Canto II flow cytometer (Becton Dickinson). The transfection efficiency was determined as the percentage of GFP-positive cells.

4.2.7 Animals and immunization

Female BALB/c mice were procured from Charles River Laboratories Inc. (Canada) and used at eight to twelve weeks of age. Animals were housed at Health Sciences Laboratory Animals Services (HSLAS) at the University of Alberta, Edmonton, Canada. Animal treatment, care and euthanasia were carried

out according to the Canadian Council of Animal Care guidelines. A total of five mice per group (n=5) were used for evaluating immune response against different vaccine constructs. The mice were immunized via intramuscular route on day 0 and day 21. A 5 µg/mouse dose of plasmid DNA (pVAXN or pDECN) was administered as soluble, nanoparticles and nanoparticles in the presence of DC maturation stimuli (anti-CD40 mAb). Intramuscular administration was done by injecting the vaccine formulations with 26 1/2 gauge needle in the quadriceps muscle in a total volume of 50 µl. Two weeks after administering booster dose, mice were sacrificed by CO₂ asphyxiation and cervical dislocation and blood was collected by cardiac puncture. Blood samples were allowed to clot for 1 h at 4 °C and serum was separated by centrifugation at 5,000 rpm for 10 min and stored at -20 °C until analyzed. Spleen were removed and used for ex vivo cytokine assays.

4.2.7.1 Humoral immune responses

To determine the systemic IgG titers using ELISA, the SARS CoV N protein and N protein fragments (NP1.1, amino acid, aa 1-140; NP1.2, aa 141-280; NP1.3, aa 281-422) were expressed and purified according to our published protocols [15]. Briefly, flat-bottom 96-well ELISA microtiter plates (Nunc MaxiSorp) were coated with 100 µl/well of N protein or fragments (10 µg/ml) overnight at 4 °C, then washed with PBST (PBS with 0.1 % Tween 20) and blocked with 1% BSA solution for 1 hr at 37 °C. The plates were washed and diluted serum (100 µl, 1:100) from each mouse was added in duplicates, and incubated overnight at 4 °C. The plates were washed followed by addition of goat-anti-mouse IgG HRPO incubation for 1 hr at 37 °C. Finally, plates were developed with TMB substrate and after 15 min optical density was recorded at 650 nm using ELISA microplate reader (Molecular Devices Corp, CA).

4.2.7.2 Cytokine assay

Single cell suspension of splenocytes was prepared by disrupting the spleen between frosted slides. The splenocytes were passed through cell strainer (70 μm) to obtain single cell suspension. The red blood cells were lysed with ACK lysis buffer and cells were washed twice with serum free media. Finally, the splenocytes were resuspended in complete DMEM medium seeded at the density of 1×10^6 /well and stimulated with SARS CoV N protein. The culture supernatants were harvested after 72 h incubation at 37 °C in the humidified atmosphere at 5% CO₂ level. The cytokine contents of supernatants were analyzed by cytokine ELISA kit using 96-well Corning microplate as per manufacturer's instructions.

4.2.8 Statistical analysis

The data are presented as mean \pm standard deviation. Statistical differences between means were investigated using one way ANOVA test in conjunction with Tukey's multiple comparison test. The differences between the means were considered significant at * $p < 0.05$. The data analysis was performed using Graphpad Prism (Graphpad Software Inc., La Jolla, CA, USA).

4.3 Results

4.3.1 Construction and expression of pDECN DNA vaccine

To facilitate the DEC-205 receptor mediated targeting of SARS CoV N protein; we constructed a fusion DNA construct, pDECN. In this construct, a mouse anti-DEC-205 scFv gene was cloned upstream to SARS CoV N protein and inserted in eukaryotic expression vector, pVAX1 (Figure 4.1A). It is expected that upon transfection, the pDECN construct will express the fusion protein consisting of anti-DEC-205 scFv and SARS CoV N protein, and subsequent secretion will lead to DEC-205 receptor mediated targeting of DCs (Figure 4.1B). The pVAX1 is highly safe US FDA approved nonfusion vector and contains a human cytomegalovirus immediate-early (CMV) promoter for high-level expression in mammalian cells and bovine growth hormone (BGH) polyadenylation signal for efficient transcription termination and polyadenylation of mRNA. The pDECN construct was verified for gene insertion by restriction fragment digestion with *NotI* and *XbaI*, and sequence analysis (**Figure 4.2A**). In order to characterize the expression of encoded antigens, HEK 293 T cells were transfected with different vaccine constructs and Western blot analysis was performed. Blots were probed with an anti-SARS CoV N protein specific monoclonal antibody (19C7) previously developed in our lab [13]. **Figure 4.2B** shows that the expressed antigens are of expected molecular size, and expected shift in molecular weight of fusion protein was noticed in case of pDECN construct.

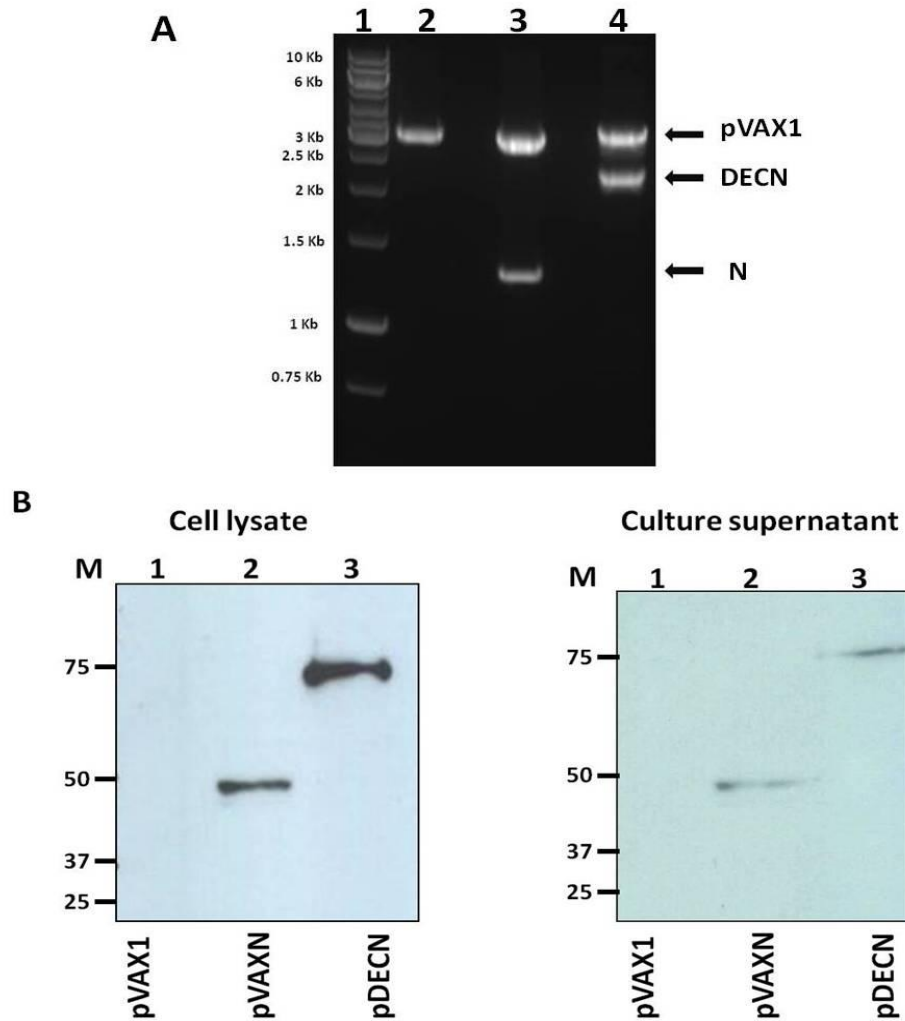


Figure 4.2 Cloning and expression of vaccine vectors. Panel A shows restriction digestion profile of pVAX1, pVAXN and pDECN. Lane 1: GeneRuler 1Kb DNA Ladder; Lane 2: Linearized pVAX1 vector, Lane 3: pVAXN digested with *Bam*HI and *Eco*RI; Lane 4: pDECN digested with *Not*I and *Xba*I. Panel B, Analysis of protein expression. HEK 293T cells were transfected with pVAX1 (control), pVAXN and pDECN. Cell lysate and culture supernatants were Western blotted using anti-SARS CoV N protein mAb (19C7). The position of protein markers (M) in kDa are shown on the left.

Next, to verify that expressed fusion protein binds with mouse dendritic cell line, DC2.4, which stably expresses DEC-205 receptor, was used. To assess binding cell culture supernatants from HEK 293T cells transfected with pVAX1, pVAXN or pDECN were incubated with DC2.4 cells, probed with FITC-conjugated SARS-CoV N protein specific antibody (19C7) and analyzed using flow cytometry. It is evident from the binding experiment that only supernatants of cells transfected with pDECN demonstrate binding to DC2.4 cells (**Figure 4.3**). Thus, results of in vitro DC binding study indicate that expressed fusion protein (anti-DEC 205 scFv-SARS CoV N protein) is functionally active and capable of binding to murine DEC-205 receptor.

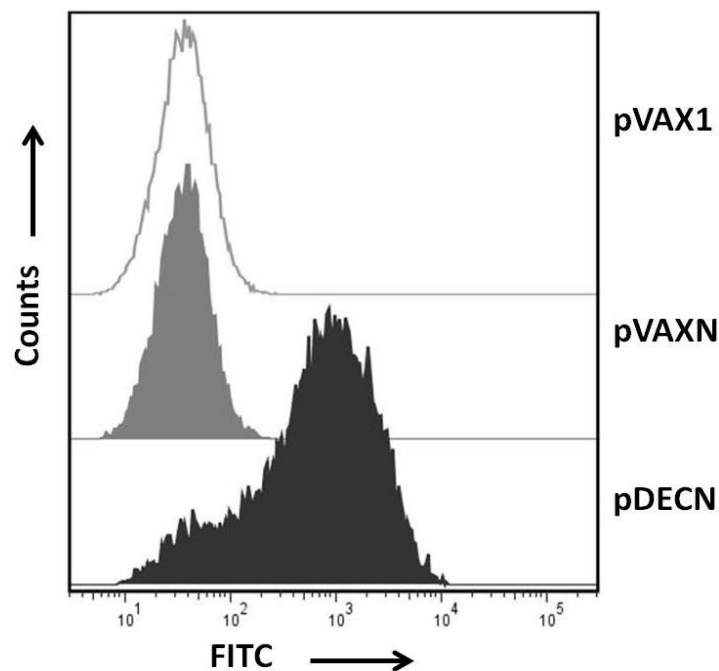


Figure 4.3 Dendritic cell binding study of expressed antigens. Cell culture supernatants from pVAX1 (control), pVAXN (N protein), pDECN (α DECN fusion protein) transfected HEK 293T cells were incubated with DC2.4 cells, expressing murine DEC-205 receptor. After washing, DC2.4 cells were stained with FITC-labeled SARS CoV N protein specific (19C7) monoclonal antibody and binding to DEC-205 receptor was analyzed by flow cytometry.

4.3.2 Formulations and characterization of DNA loaded chitosan NPs

Chitosan NPs loaded with pVAXN and pDECN were formulated using complex coacervation method. The electrophoretic mobility assay of NPs, with chitosan:DNA weight ratios of 2:1 and 4:1 was performed to analyze complex formation (**Figure 4.4A**). At 2:1 weight ratio, complexation of DNA to chitosan was not complete as some of DNA migrated into the gel. However, nanoparticles formulated at 4:1 weight ratio, showed almost complete DNA binding with chitosan and were therefore used for subsequent studies. At 4:1 ratio, encapsulation efficiency for both pVAXN and pDECN was found to be more than 98%. The hydrodynamic diameter of pVAXN and pDECN loaded chitosan nanoparticles was 291.9 ± 11.6 nm and 295.2 ± 9.3 nm, respectively (**Table 4.1**). No significant difference in the size of nanoparticles was recorded with varied size of plasmid DNA constructs.

Protection of DNA from nuclease digestion is vital for proper transfection and expression of encoded antigen. Therefore, we challenged the DNA loaded nanoparticles to DNase I digestion. Our results indicate that the nanoencapsulation of pVAXN and pDECN DNA provided protection against nuclease digestion (Lanes 2 and 4 in **Figure 4.4B**), whereas, the naked plasmid DNA was completely digested with DNase I (Lanes 1 and 3, **Figure 4.4B**). Further, nuclease concentration employed in the current experiments is markedly higher than that present under physiological conditions [16]. Thus, we speculate that chitosan nanoparticle formulations can protect plasmid DNA against nuclease digestion following in vivo applications.

It is worth mentioning that an optimum ratio of chitosan to DNA at its least was used for the formulation of DNA encapsulated chitosan NPs. A higher ratio of chitosan to DNA might result in slow release of plasmid DNA and thus can reduce the magnitude of transfection. It is evident from previous studies that an optimum ratio of chitosan allows for higher transfection efficiency due to easy dissociation of complexes [17].

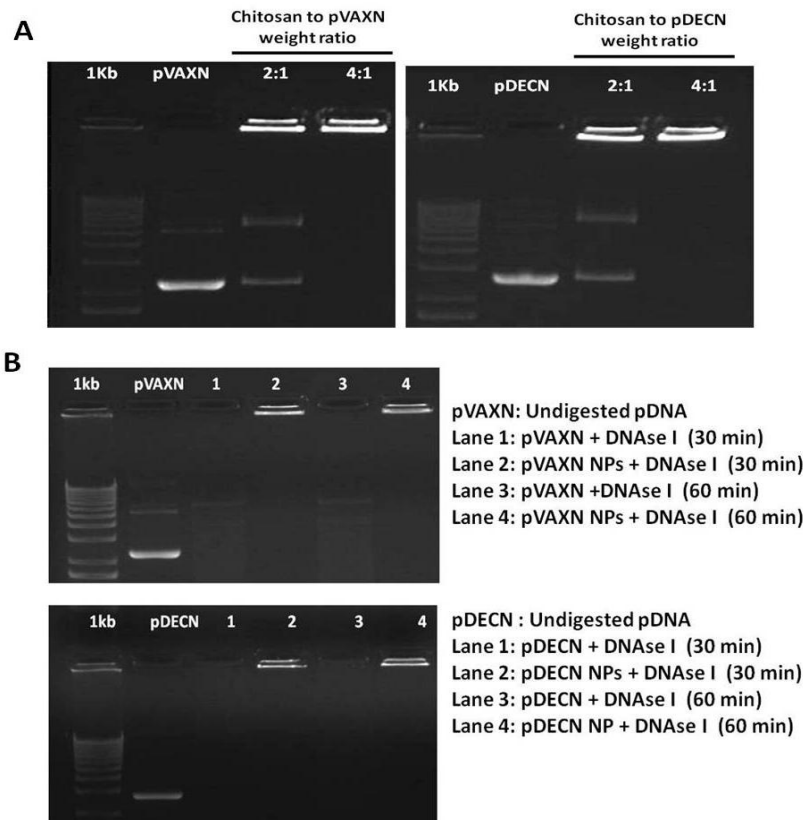


Figure 4.4 Formulation and nuclease digestion profile of chitosan nanoparticles. (A) Electrophoretic mobility assay of pVAXN and pDECN loaded chitosan nanoparticles prepared at different weight ratio of chitosan to pVAXN and pDECN. (B) Nuclease digestion profile of pVAXN and pDECN loaded chitosan nanoparticles. Naked DNA and chitosan NPs formulated at 4:1 weight ratio of chitosan to DNA were digested with DNase I for 30 and 60 min at 37 °C. The reaction was stopped with EDTA and samples were run on ethidium bromide containing 1% agarose gel.

Table 4.1 Characterization of pVAXN and pDECN loaded chitosan NPs.

Formulation*	Size (nm)	PI	Zeta potential (mV)
pVAXN chitosan NP	291.9 ± 11.6	0.256 ± 0.13	26.4 ± 2.6
pDECN chitosan NP	295.2 ± 9.3	0.261 ± 0.01	26.2 ± 3.4

* The nanoparticles were formulated at 4:1 weight ratio of chitosan to DNA. PI: polydispersity index.

In vitro transfection efficiency of chitosan nanoparticles was verified using HEK 293T cells, and was compared with that of positive control lipofectamine. For this purpose we used a GFP-reporter plasmid and percent of GFP positive cells were analyzed after 48 h using flow cytometry. Transfection of HEK 293T cells with pEGFP-C1 loaded chitosan nanoparticles resulted in $\sim 12 \pm 4$ % GFP positive cells; whereas transfection with lipofectamine resulted in $\sim 72 \pm 6$ % GFP positive cells (**Figure 4.5**). Transfection with lipofectamine resulted in approximately five-fold higher transfection compared with chitosan nanoparticles. The low-transfection efficiency of chitosan might be explained based on the high molecular weight of chitosan employed in our studies, preventing easy dissociation of DNA [18]. Beside this, physiological pH range of transfection medium could have resulted in reduced charge density on chitosan NPs ultimately leading to lower transfection. Naked plasmid pEGFP-C1 was least effective in transfecting cells and approximately 1% of GFP positive cells were transfected, which is equal to background.

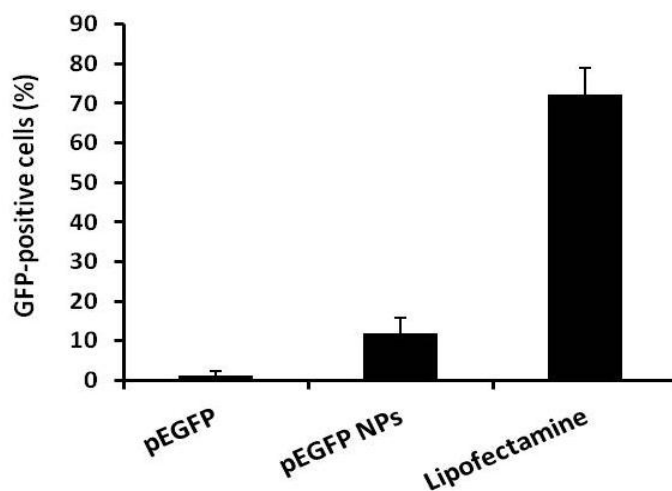


Figure 4.5 In vitro transfection efficiency of pEGFP-C1 loaded chitosan nanoparticles. HEK 293T cells were treated with either (i) soluble, (ii) nanoparticle encapsulated or (iii) lipofectamine complexed pEGFP-C1 DNA and allowed to grow for 48 h, afterwards, the percentage of GFP positive cells was analyzed using flow cytometer. Results are summarized as per cent GFP-positive cells (means \pm SD of triplicate wells).

4.3.3 Antibody responses to SARS CoV N protein and fragments

To evaluate whether the presence of DEC-205 targeting scFv will improve the humoral immune responses, BALB/c mice were primed on day 0 and boosted on day 21 with pVAXN or pDECN constructs. Two weeks after boosting, serum was harvested and SARS CoV N protein and fragments specific IgG titers were determined using ELISA. It is evident from the results that IgG titers obtained with pDECN DNA immunized mice are significantly higher compared with pVAXN construct (* $p < 0.05$) (**Figure 4.6A**). Immunization of mice with pDECN construct induced higher IgG titer compared to pVAXN, irrespective of administration in soluble or nanoparticulate form. Furthermore, the nanoparticle encapsulated vaccine formulations benefited from the coadministration of soluble anti-CD40 mAb as DC maturation stimuli.

Next, we evaluated whether the IgG antibody responses against fragments (N-terminal, central and C-terminal region) of SARS nucleocapsid protein. Our data shows that C-terminal is dominant region for the N protein specific IgG responses (**Figure 4.6B**). This is in good agreement with previous findings showing the presence of three immunodominant epitopes of SARS CoV N protein in BALB/c mice, of which the C-terminal region (NP1.3, amino acid 281-422) was shown to be most antigenic [19, 20].

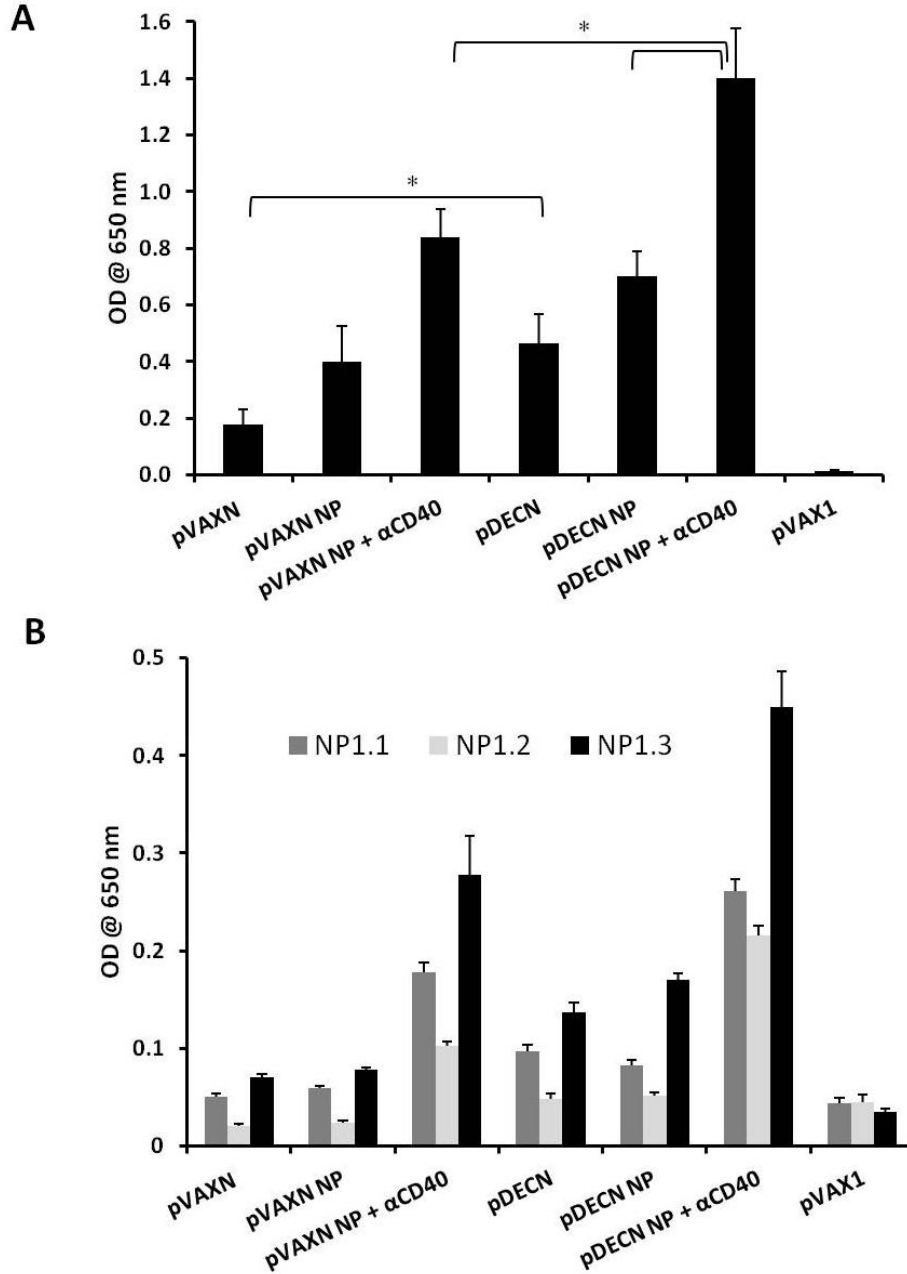


Figure 4.6 Detection of SARS CoV N protein and N protein fragment-specific humoral immune response in the mice immunized with various DNA vaccine formulations. Sera was collected from mice two weeks after final immunization and analyzed for IgG response against SAR CoV N protein (panel A) and N protein fragments (N-terminal region, NP1.1 aa 1-140; Middle-region, NP1.2 aa 141-280; C-terminal region NP1.3, aa 281-422) (panel B) using ELISA. Data are presented as group means±SD of five mice. The differences between the means were considered significant at * $p < 0.05$

4.3.4 SARS N protein specific cytokine responses

To evaluate the efficacy of pDECN and pVAXN in provoking cell-mediated immune responses, we evaluated the IFN- γ and IL-2 secretion profile of splenocytes using N protein as recall antigen (**Figure 4.7**). Splenocytes of mice immunized with pDECN constructs secreted significantly higher levels of IFN- γ and IL-2 compared with pVAXN immunized mice. Further, inclusion of anti-CD40 antibody along with nanoparticulate vaccine formulations improved the levels of IFN- γ and IL-2. Thus, it is evident that both pVAXN and pDECN constructs seem to benefit from adjuvant effects of anti-CD40 antibody. These results are in agreement with previous findings showing that, DEC-205 targeted delivery of protein antigen to DCs has been shown to improve T cell mediated immune responses; on contrary the absence of maturation stimuli was shown to induce peripheral CD8 T cell response was noticed [21, 22].

Furthermore, the vaccine formulation containing pDECN encapsulated chitosan NPs in combination of anti-CD40 mAb was shown to induce highest levels of Th1 cytokines (IFN- γ and IL-2) compared to all other formulations evaluated in our studies. The induction of multiple cytokine producing Th1 cells has been shown to strongly correlate with ability of vaccine formulations to provide protection against virus challenge and in the induction of long-lasting memory responses [23, 24].

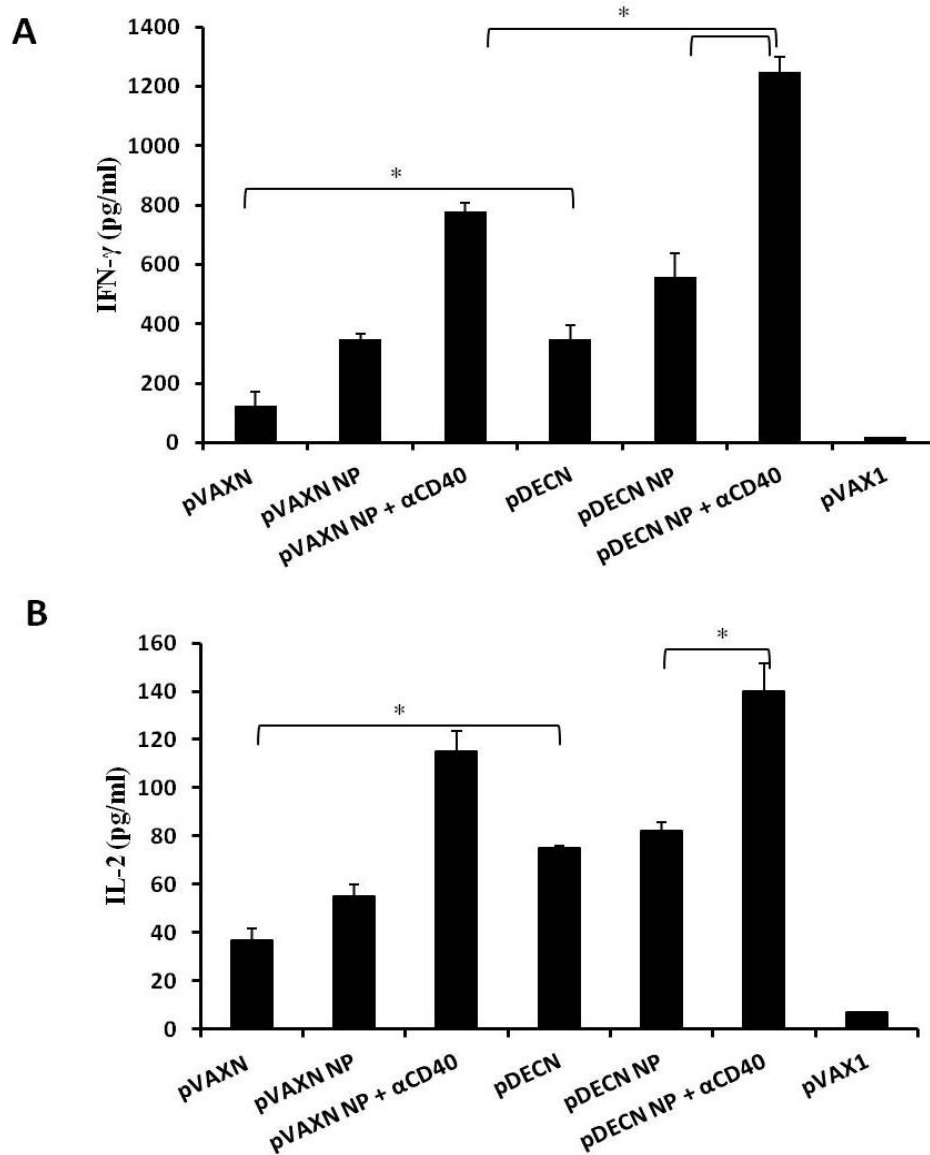


Figure 4.7 SARS CoV N protein specific ex-vivo cytokines secretion profile. Splenocytes from different groups of mice were stimulated with SARS CoV N protein for 72 hr and culture supernatants were analyzed for presence of IFN- γ (panel A) and IL-2 (panel B) using cytokine specific ELISA. Data represent mean \pm SD of triplicate cultures. The differences between the means were considered significant at * $p < 0.05$.

4.4 Discussion

SARS emerged as a first infectious disease of the twenty first century, and causative agent of SARS was identified as a novel coronavirus named SARS CoV [25, 26]. SARS CoV contains four major structural proteins: nucleocapsid (N), membrane (M), spike (S) and envelop (E) protein. The N protein is abundantly expressed during infection and helps in the replication and transcription of viral mRNA and therefore critical for SARS CoV pathogenesis. Furthermore, N protein is highly conserved within different isolates and abundantly shed during infection. Moreover, the presence of longer lasting N protein-specific antibodies and memory T cells are found in SARS CoV recovered patients [27, 28]. Thus, N protein represents a key antigen for development of vaccines.

Numerous studies have used N protein based DNA vaccine approach [20, 29, 30]. In an elegant study, a fusion DNA vaccine consisting of calreticulin fused with SARS N protein was shown to elicit potent N protein specific antibody and CD8⁺ T cell responses in mice [29]. Intramuscular DNA vaccination of mice with calreticulin fused N protein significantly reduced the titer of recombinant vaccinia virus expressing SARS CoV N protein after the challenge. A previous study demonstrated that magnitude of N protein specific antibody and T cell responses can be enhanced by controlling the trafficking of DNA-encoded antigens to lysosomal/endosomal vesicular compartment for MHC class II presentation [30]. Immunization of mice with fusion DNA vaccine consisting of N protein linked to lysosome-associated membrane protein (LAMP) induced stronger and long-lasting memory T cell response. These studies demonstrate that immunogenicity of N protein encoding DNA vaccines can be improved by routing them to specific antigen-processing and presentation compartments. Although an improved immune response can be obtained, the intracellular targeting strategies do not provide targeted delivery of DNA encoded antigens to DCs.

DCs targeting of DNA vaccines can be achieved using two approaches: direct transfection of DCs or use of fusion plasmid DNA that encodes for antigen and DC-surface specific receptor ligand (scFv to DEC-205). Direct transfection can be

achieved by means of targeted delivery of DNA to DC surface receptors. Using this approach DNA encapsulated nanoparticulate delivery systems can be targeted with the help of DC receptor ligands. We have demonstrated in chapter 2, that DC targeted delivery of pVAXN loaded biotinylated chitosan resulted in improved immune response following intramuscular and intranasal delivery [11]. In this strategy pVAXN loaded nanoparticles were formulated using biotinylated chitosan polymer and these nanoparticles were functionalized with bfFp for DC targeting.

Although, bfFp based targeting resulted in enhanced immune responses, the immunogenicity of core-streptavidin arm can prevent repeated administration of bfFp targeted nanoparticles. Beside, this number of DCs transfected can also be limiting factor in this case. Therefore, in the current strategy we adopted an indirect approach to accomplish the DC targeted delivery of encoded antigen. For realization of DEC-205 mediated DC targeting, SARS N protein antigen was linked to a single chain antibody that target DEC-205 receptor on DCs. We demonstrated using *in vitro* experiments that expressed antigen is indeed taken up by DC via DEC-205 receptor mediated endocytosis. To study whether the outcome of immune responses can be influenced by this strategy, we carried out a head-to-head comparison of pDECN and pVAX construct in soluble and nanoparticulate form.

Our results suggest that efficacy of SARS N protein DNA vaccines can be enhanced by fusing antigen with anti-DEC-205 scFv. Immunization of mice with pDECN DNA construct resulted in significantly higher N protein specific IgG titers and cytokine secretion (IFN- γ and IL-2). We show that irrespective of delivery in soluble or particulate form, pDECN DNA construct that is capable of binding with DCs elicited improved immune responses compared to pVAXN. Furthermore, the magnitude of immune responses obtained with the nanoparticulate delivery of pDECN and pVAXN was improved upon co-administration of anti-CD40 antibody as DC maturation stimuli.

The chitosan nanoparticle based formulations stabilized the encapsulated DNA and thus prevented premature degradation, a step which is of paramount importance in case of designing low-dose vaccines. These nanoparticles can also be used for co-delivery of multiple DNA antigens and other immunomodulators such as CpG or poly I:C. The results of this study raises the possibility that DNA strategy employing scFv linked to SARS E, M, S protein may elicit neutralization antibodies. Alternatively, a plasmid DNA encoding for cytokines, which can recruit DCs to the inoculation site can also be incorporated for enhancing the efficacy of fusion DNA vaccine constructs.

The fusion DNA based DC targeting approach can particularly beneficial for the recombinant protein antigens such as SARS N protein, which are highly unstable, autocatalytic in nature and often require cold-chain storage. The strategy proposed in general can be applied as an alternate to protein based DC targeted vaccines, which require time-consuming optimization and protein production. The fusion DNA based vaccines can be promptly engineered and produced on large-scale and thus can serve as valuable tools in case of possible SARS CoV or other pandemic or bioterrorism threats to minimize the extent of damage.

4.5 References

- [1] Gurunathan S, Wu C-Y, Freidag BL, Seder RA. DNA vaccines: a key for inducing long-term cellular immunity. *Curr Opin Immunol* 2000;12:442-7.
- [2] Kutzler MA, Weiner DB. DNA vaccines: ready for prime time? *Nat Rev Genet* 2008;9:776-88.
- [3] Tsen S-WD, Paik AH, Hung C-F, Wu TC. Enhancing DNA vaccine potency by modifying the properties of antigen-presenting cells. *Expert Rev Vaccines* 2007;6:227-39.
- [4] Kutzler MA, Weiner DB. Developing DNA vaccines that call to dendritic cells. *J Clin Invest* 2004;114:1241-4.
- [5] Bot A, Stan AC, Inaba K, Steinman R, Bona C. Dendritic cells at a DNA vaccination site express the encoded influenza nucleoprotein and prime MHC class I-restricted cytolytic lymphocytes upon adoptive transfer. *Int Immunol* 2000;12:825-32.
- [6] Condon C, Watkins SC, Celluzzi CM, Thompson K, Falo Jr LD. DNA-based immunization by in vivo transfection of dendritic cells. *Nat Med* 1996;2:1122-8.
- [7] Ni J, Nolte B, Arnold A, Fournier P, Schirmacher V. Targeting anti-tumor DNA vaccines to dendritic cells via a short CD11c promoter sequence. *Vaccine* 2009;27:5480-7.
- [8] Moulin V, Morgan ME, Eleveld-Trancikova D, Haanen JBAG, Wielders E, Looman MWG, et al. Targeting dendritic cells with antigen via dendritic cell-associated promoters. *Cancer Gene Ther* 2012;19:303-11.
- [9] Demangel C, Zhou J, Choo ABH, Shoebridge G, Halliday GM, Britton WJ. Single chain antibody fragments for the selective targeting of antigens to dendritic cells. *Mol Immunol* 2005;42:979-85.
- [10] Nchinda G, Kuroiwa J, Oks M, Trumpfheller C, Chae GP, Huang Y, et al. The efficacy of DNA vaccination is enhanced in mice by targeting the encoded protein to dendritic cells. *J Clin Invest* 2008;118:1427-36.

- [11] Raghuwanshi D, Mishra V, Das D, Kaur K, Suresh MR. Dendritic cell targeted chitosan nanoparticles for nasal DNA immunization against SARS CoV nucleocapsid protein. *Mol Pharm* 2012;9:946-56.
- [12] Wang WW, Das D, Suresh MR. A versatile bifunctional dendritic cell targeting vaccine vector. *Mol Pharm* 2009;6:158-72.
- [13] Kammila S, Das D, Bhatnagar PK, Sunwoo HH, Zayas-Zamora G, King M, et al. A rapid point of care immunoswab assay for SARS-CoV detection. *J Virol Methods* 2008;152:77-84.
- [14] Shen Z, Reznikoff G, Dranoff G, Rock KL. Cloned dendritic cells can present exogenous antigens on both MHC class I and class II molecules. *J Immunol* 1997;158:2723-30.
- [15] Das D, Suresh MR. Copious production of SARS-CoV nucleocapsid protein employing codon optimized synthetic gene. *J Virol Methods* 2006;137:343-6.
- [16] Guliyeva Ü, Öner F, Özsoy Ş, Haziroğlu R. Chitosan microparticles containing plasmid DNA as potential oral gene delivery system. *Eur J Pharm Biopharm* 2006;62:17-25.
- [17] Mao S, Sun W, Kissel T. Chitosan-based formulations for delivery of DNA and siRNA. *Adv Drug Deliv Rev* 2010;62:12-27.
- [18] Strand SP, Lelu S, Reitan NK, de Lange Davies C, Artursson P, Vårum KM. Molecular design of chitosan gene delivery systems with an optimized balance between polyplex stability and polyplex unpacking. *Biomaterials* 2010;31:975-87.
- [19] He Y, Zhou Y, Wu H, Kou Z, Liu S, Jiang S. Mapping of antigenic sites on the nucleocapsid protein of the severe acute respiratory syndrome coronavirus. *J Clin Microbiol* 2004;42:5309-14.
- [20] Dutta NK, Mazumdar K, Lee BH, Baek MW, Kim DJ, Na YR, et al. Search for potential target site of nucleocapsid gene for the design of an epitope-based SARS DNA vaccine. *Immunol Lett* 2008;118:65-71.
- [21] Bonifaz LC, Bonnyay DP, Charalambous A, Darguste DI, Fujii SI, Soares H, et al. In vivo targeting of antigens to maturing dendritic cells via the DEC-205 receptor improves T cell vaccination. *J Exp Med* 2004;199:815-24.

- [22] Bonifaz L, Bonnyay D, Mahnke K, Rivera M, Nussenzweig MC, Steinman RM. Efficient targeting of protein antigen to the dendritic cell receptor DEC-205 in the steady state leads to antigen presentation on major histocompatibility complex class I products and peripheral CD8⁺ T cell tolerance. *J Exp Med* 2002;196:1627-38.
- [23] Kannanganat S, Ibegbu C, Chennareddi L, Robinson HL, Amara RR. Multiple-cytokine-producing antiviral CD4 T cells are functionally superior to single-cytokine-producing cells. *J Virol* 2007;81:8468-76.
- [24] Wu C-y, Kirman JR, Rotte MJ, Davey DF, Perfetto SP, Rhee EG, et al. Distinct lineages of TH1 cells have differential capacities for memory cell generation in vivo. *Nat Immunol* 2002;3:852-8.
- [25] Drosten C, Günther S, Preiser W, Van der Werf S, Brodt HR, Becker S, et al. Identification of a novel coronavirus in patients with severe acute respiratory syndrome. *N Engl J Med* 2003;348:1967-76.
- [26] Peiris JSM, Lai ST, Poon LLM, Guan Y, Yam LYC, Lim W, et al. Coronavirus as a possible cause of severe acute respiratory syndrome. *Lancet* 2003;361:1319-25.
- [27] Leung DTM, Chi Hang TF, Chun Hung M, Sheung Chan PK, Cheung JLK, Niu H, et al. Antibody response of patients with severe acute respiratory syndrome (SARS) targets the viral nucleocapsid. *J Infect Dis* 2004;190:379-86.
- [28] Peng H, Yang Lt, Wang Ly, Li J, Huang J, Lu Zq, et al. Long-lived memory T lymphocyte responses against SARS coronavirus nucleocapsid protein in SARS-recovered patients. *Virology* 2006;351:466-75.
- [29] Kim TW, Lee JH, Hung CF, Peng S, Roden R, Wang MC, et al. Generation and characterization of DNA vaccines targeting the nucleocapsid protein of severe acute respiratory syndrome coronavirus. *J Virol* 2004;78:4638-45.
- [30] Yang K, Sun K, Srinivasan KN, Salmon J, Marques ET, Xu J, et al. Immune responses to T-cell epitopes of SARS CoV-N protein are enhanced by N immunization with a chimera of lysosome-associated membrane protein. *Gene Ther* 2009;16:1353-62.

CHAPTER 5: Ovalbumin encapsulated dendritic cell-targeted PLGA nanoparticles for enhanced immune responses

A version of this chapter is under revision with *Vaccine* journal: Raghuwanshi D., Mishra V., Kaur K.* and Suresh M.R. A simple approach for enhanced immune response using engineered dendritic cell targeted PLGA nanoparticles.

5.1 Introduction

Polymeric micro- and nanoparticle based vaccine delivery systems are emerging as viable platform for improving immune response against a number of vaccine antigens [1-4]. Several studies have demonstrated that nanoparticulate vaccines composed of poly(D,L-lactic-*co*-glycolic acid) (PLGA) polymer can induce both humoral and cell-mediated immune responses in animals [5-9]. These nano-sized antigen delivery systems offer several benefits over soluble antigens, such as sustained-antigen release, co-encapsulation of multiple vaccine components and protection from degradation by enzymes [10, 11]. Additionally, nanoparticles can be functionalized with DC receptor-specific ligands to achieve active targeting and ensure delivery of large amounts of Ag to DCs.

Despite extensive research on PLGA nanoparticle based vaccines, only some studies have reported active targeting of these nanovaccine formulations to DCs. Recently, active targeting of Ag-loaded PLGA nanoparticles with the help of DC receptor-specific antibodies has shown to strongly enhance vaccine efficacy [12-14]. Although promising, current strategies to formulate antibody-targeted particulate vaccines are limited and often require sophisticated chemistry. Therefore, a more stable and feasible approach to formulate DC targeted nanoparticle based vaccines is required.

To achieve DC selective targeting of soluble biotinylated antigens, in this chapter we explored a recombinant bifunctional fusion protein (bfFp) based approach [15]. The bfFp is a fusion protein, where a single chain variable fragment (scFv) that recognizes mouse DC DEC-205 is fused with a core-streptavidin. The core-streptavidin arm can form a complex with any biotinylated antigen and anti-DEC-205 scFv facilitates DC targeting. Using this strategy, a low-dose of biotinylated antigen (protein, peptide, ganglioside and plasmid DNA) in the presence of DC maturation stimuli (anti-CD40 mAb) was adequate to provide a strong immune response in mice [15]. Herein, we extend the feasibility of bfFp based approach for DC targeting by designing biotinylated PLGA nanoparticles for the delivery of protein antigen(s) where the antigen is encapsulated inside the NPs. Biotinylated

PLGA nanoparticles loaded with a model antigen, ovalbumin (OVA), were formulated using biotin-PEG-PLGA polymer and were decorated with bfFp for DC targeting. The DC targeted and non-targeted nanoparticle formulations were investigated for in vitro uptake and modulation of DC functions. Subsequently, these formulations were evaluated for the induction of humoral and cell-mediated immune responses.

5.2 Material and Methods

5.2.1 Materials

Acid end group-terminated poly(D,L-lactide-co-glycolic) acid PLGA copolymer with monomer ratio 50:50 and molecular weight 18,000 Da, was purchased from Lakeshore Biomaterials (Birmingham, AL, USA). Heterobifunctional PEG derivative (biotin-PEG2,000-amine) was from Laysan Bio, Inc. (Arab, AL, USA). Chicken ovalbumin (Grade-V), poly(vinyl alcohol) (PVA, 87-89 % hydrolysed, mol wt 31-50 kD), Horseradish peroxidase (HRPO) conjugated goat anti-mouse IgG secondary antibody and Complete Freund's Adjuvant (CFA) were purchased from Sigma-Aldrich (Oakville, ON, Canada). Micro bicinchoninic acidTM (microBCA) protein assay kit was from Pierce (Rockford, IL). Fluorescent probe tetramethylrhodamine (TMRD) labeled dextran (mol wt 70,000 g/mol) and Fluoreporter biotin quantitation kits were obtained from Molecular Probes (Eugene, OR). All cytokine-specific ELISA kits were from eBioscience (San Diego, CA). TMB (3,3',5,5'-tetramethylbenzidine) peroxidase substrate was from Kirkegaard and Perry Laboratory Inc. (Gaithersburg, MD). HRPO-conjugated goat anti-mouse IgG1, IgG2b, IgG2c secondary antibodies were from Southern Biotech (Birmingham, AL). Rat anti-mouse CD40 monoclonal antibody was purified from hybridoma (clone 1C10), procured from Dr. M. Gold (University of British Columbia, Canada).

5.2.2 Synthesis of biotin-PEG-PLGA conjugate

Biotinylation of PLGA polymer associated carboxylic acid group was done using bifunctional PEG derivative (biotin-PEG2,000-amine) [16]. Briefly, PLGA (540 mg, 0.03 mM) was dissolved in DMF (10 ml) and carboxyl groups were activated by addition of HCTU [2-(6-Chloro-1H-benzotriazole-1-yl)-1,1,3,3-tetramethylaminium hexafluorophosphate] (25 mg, 0.06 mM) in the presence of *N,N* diisopropylethylamine (DIPEA, 50 μ l) under continuous stirring for 8-10 min. The solution turned dark brown indicating activation of PLGA carboxylic acid groups. To this end, biotin-PEG2,000-amine (103 mg, 0.045 mM) solution in dry DMF was added and reaction mixture was stirred at 25 °C for 24 hr. Product was precipitated by slowly adding to ice cold diethyl ether (100 mL) and collected by centrifugation at 3,500 rpm for 10 min. Supernatant was decanted and precipitate was washed with diethyl ether (3x 25 ml). Finally; biotin-PEG-PLGA conjugate was dried for 48 hr under vacuum at room temperature. The yield of final product was approximately 475 mg (~75%). Similarly, methoxy PEG2,000-amine was used for the synthesis of pegylated PLGA. The incorporation of biotin-PEG-amine in PLGA polymer was characterized using ¹H NMR spectroscopy and spectra were obtained on Bruker 600 MHz spectrometer using deuterated-DMSO as solvent.

5.2.3 Formulation of nanoparticles

PLGA nanoparticles containing OVA protein were prepared using modified water/oil/water (W/O/W) double emulsion solvent evaporation method. Briefly, OVA protein (3 mg in 200 μ L PBS pH 7.4) was added to the polymer solution (4 mL, 25 mg/ml) in dichloromethane and sonicated for 30s at 25 % amplitude using a microtip sonicator, Vibra-Cell (Sonics and Materials, Newtown, CT). The resulting primary emulsion (W/O) was further emulsified in PVA (16 mL, 1% w/v) and sonicated for 120 s at 40 % amplitude. The double emulsion was then added drop wise into distilled water (20 mL) and stirred overnight for removal of dichloromethane and nanoparticles were harvested by centrifugation at 19,000 rpm for 20 min. The pellet was resuspended and washed with cold PBS (pH 7.4)

to remove residual PVA, washing step was repeated three times. Finally, NPs were suspended in water and freeze dried for 48 hr using benchtop freeze dryer (Labconco, USA). Fluorescent NPs were formulated by using TMR-dextran conjugate (1% w/w ratio to polymer), while blank PLGA NPs were synthesized using PBS in place of ovalbumin.

5.2.4 Characterization of formulations

5.2.4.1 Particle size and surface charge (ζ potential)

The particle size and zeta-potential (ζ) of PLGA and biotinylated PLGA nanoparticles were measured by dynamic light scattering (DLS) technique using ZetaSizer 3000 HS (Malvern, UK). For size analysis, a suspension of NPs (1 mg/ml) was prepared in distilled water and sonicated on water bath for a minute and size was measured at 25 °C.

5.2.4.2 Morphology

The nanoparticle shape and surface morphology was assessed by scanning electron microscopy (Philips/FEI LaB6 Environmental Scanning Electron Microscope, ESEM). Briefly, lyophilized NPs were coated on the adhesive carbon tapes by sprinkling the nanoparticles with a fine brush. The NPs were coated with gold in sputter under vacuum before mounting the samples in SEM.

5.2.4.3 Qualitative and quantitative estimation of NP surface associated biotin

Binding of Oregon green 488 conjugated neutravidin (NAv) (Invitrogen, Eugene, OR) with NPs formulated using biotinylated PLGA (biotin-PEG-PLGA) or pegylated PLGA (methoxy-PEG-PLGA) was used to qualitatively analyze presence of surface associated biotin. Briefly, 100 μ L samples of NP suspension (~1 mg/mL) formulated using biotinylated or pegylated PLGA were incubated with graded amounts of NAv conjugate for 15-20 minutes in dark while shaking. After incubation, 1 ml PBS was added and suspension was centrifuged (13,000 rpm) for 10 min and supernatant was discarded. NP pellet was resuspended and washed with PBS (1 ml) and centrifuged again. Steps were repeated three times

to ensure removal of unbound NAv conjugate. Finally, NPs were uniformly suspended in PBS and fluorescence intensity of samples was measured using FACS Canto II flow cytometer.

Quantitative estimation of NP surface associated biotin was done using Fluoreporter® biotin quantitation assay [17]. This assay uses Biotective Green reagent, which consists of fluorescent dye labeled avidin and with a quencher dye ligand occupying biotin binding sites. Through fluorescence resonance energy transfer (FRET), the ligand quenches fluorescence and addition of biotin displaces the quencher dye from Biotective Green reagent, yielding fluorescence proportional to the amount of added biotin. NP suspension was prepared at different concentrations (1.0, 0.5 and 0.25 mg/ml) and the assay was performed in triplicate with two batches as per vendor's protocol. The background obtained with NP formulated using non-biotinylated PLGA nanoparticles was subtracted from biotinylated PLGA nanoparticles. A standard curve of biotin-PEG2,000-amine was used to calculate unknown quantity of biotin present on the NPs. The fluorescence intensity was measured in Synergy microplate reader (Biotek Instruments, Winooski, VT) using typical fluorescein wavelengths (excitation/emission maxima ~485/530 nm).

5.2.4.4 Estimation of antigen content

The quantity of entrapped OVA in NPs was determined using microBCA protein assay kit. Briefly, NPs (10 mg) were dissolved in NaOH solution (2 mL, 0.5 N) containing 0.1% w/v of sodium dodecyl sulfate (SDS) and incubated overnight at 37°C on incubator shaker at 100 rpm for complete lysis. The solution was centrifuged at 13,000 rpm for 5 minutes, neutralized and diluted before protein analysis. Absorbance of plain NPs was subtracted from absorbance of protein loaded NPs and amount of OVA per mg of nanoparticle weight was calculated from standard curve generated with OVA.

5.2.5 Bone-marrow derived dendritic cell (BMDCs) culture

BMDCs were generated from bone marrow precursors isolated from femurs and tibias of wild type C57BL/6 mice according to established protocols [18]. Briefly, bone marrow precursors were cultured at the density of 2×10^6 per 100-mm culture dish in 10 ml complete RPMI (RPMI-1640 supplemented with gentamycin (80 $\mu\text{g/ml}$), L-glutamine (2 mM), and 10% heat inactivated FBS) containing 20 ng/ml of murine GM-CSF. At day 3, 10 ml of 20 ng/ml of GM-CSF containing complete RPMI media was added. At day 6, half of the culture supernatants were replaced with fresh media containing 10 ng/ml of GM-CSF. Non-adherent or semi-adherent BMDCs were harvested and purity of cells was determined based on expression of CD11c and found to be more than 70%.

5.2.6 BfFp decoration to nanoparticles

The dendritic cell targeting vector (bfFp) was expressed and purified as periplasmic and cytoplasmic soluble protein according to our previous protocols with minor modifications [15, 19]. Prior to all studies, bfFp was passed through Detoxi-GelTM Endotoxin Removing Gel (Thermo Fisher Scientific Inc. IL, USA) for removal of endotoxins. Targeted NPs were formulated by incubation of bfFp with suspension of biotinylated PLGA NPs in PBS with continuous shaking for 30 min at room temperature. Specifically, 100 μl of bfFp (250 $\mu\text{g/ml}$) was added to 1 mg of NPs suspended in 100 μl of PBS. Following incubation, NPs were centrifuged at 13,000 rpm for 10 min and supernatants were analyzed for unbound bfFp using microBCA protein assay. Apparently all bfFp was bound to nanoparticles as no protein could be detected in the supernatants.

5.2.7 Uptake of nanoparticles by BMDCs

Uptake studies of DC-targeted and non-targeted biotinylated PLGA by BMDCs were performed using flow cytometry. For uptake studies, TMRD-dextran loaded biotinylated PLGA were treated as non-targeted NPs, while targeted NPs were synthesized by conjugation of bfFp (25 $\mu\text{g/mg}$ of NPs) as described in previous section.

Briefly, BMDCs were seeded at the density of 1×10^6 /mL in complete RPMI media in a 6-well plate and allowed to adhere for 2 hr. Additionally to verify specificity of receptor-mediated uptake of targeted NPs, BMDCs were incubated with 25 μ g/well of anti-DEC-205 mAb (clone NLDC 145) for 30 min before adding targeted NPs. A 100 μ g/well of nanoparticle (targeted and non-targeted) suspension was added and cells were incubated for 1 hr at 37°C. After incubation, media was aspirated and wells were flushed with ice cold FACS buffer (PBS with 5% fetal calf serum, and 0.09% sodium azide). Cells were harvested and washed to remove non-internalized particles. Fc receptors were blocked with anti-mouse CD16/CD32 antibody for 30 min, and thereafter cells were washed and stained with FITC conjugated anti-mouse CD11c antibody for 30 min. Finally, the cells were washed twice and resuspended in FACS buffer (500 μ l). Cells were analyzed for TMRD positivity and cell-associated fluorescence using a FACS Canto II system (Becton Dickinson, USA) and data was processed using Flowjo software v7.6.5 (TreeStar Inc.).

5.2.8 Cytokine secretion and maturation of BMDCs

Semi-adherent and non-adherent BMDCs at Day 6 of culture were harvested and seeded at the density of 1×10^6 /mL in a 6-well plate for 24 hr. Next, cells were treated with 100 μ g of biotinylated NPs (blank NPs), OVA loaded biotinylated NPs (NP), bfFp functionalized OVA loaded NP (targeted NP), and bfFp functionalized OVA loaded NP (targeted NP) along with the soluble anti-CD40 mAb. Lipopolysaccharide (LPS) at a concentration of 1 μ g/ml was used as positive control, while untreated cells served as media control. Where applicable, each milligram of nanoparticles contains 23.5 μ g of encapsulated OVA and 25 μ g of surface associated bfFp. A total quantity of 2.5 μ g/well of anti-CD40 mAb, either alone or with targeted particle was used as DC maturation stimuli. Cells treated with equivalent amounts of soluble OVA, bfFp and anti-CD40 mAb were treated as relevant controls. After incubation for 24 hr with indicated formulations, culture supernatants were harvested and stored at -80°C for analysis of interleukin-6 (IL-6), interleukin-12 (IL-12) and interleukin-10 (IL-10) using

cytokine-specific ELISA kits. For the measurement of DC activation markers, cells were washed to remove uningested formulations and harvested with the help of a scraper. Cells were then treated with Fc receptor block for 30 min and washed. Finally, cells were stained with anti-mouse CD 11C (FITC), CD 86 (PE-Cy5) and CD 40 (APC) antibodies for 30 min. After washing free antibodies, samples were analyzed on FACS Canto II system and data was processed using Flowjo software. CD11c⁺ subset of cells was analyzed for expression of CD86 and CD40.

5.2.9 Immunization experiments

Wild-type C57BL/6 mice were procured from Charles River Laboratories Inc. (Canada) and housed at Health Sciences Laboratory Animals Services (HSLAS) at the University of Alberta, Edmonton, Canada. All experiments were performed using 8-12 week old female mice. Animal studies were conducted in accordance with the Canadian Council on Animal Care Guidelines and Policies and approved by the Animal Care and Use Committee (Health Sciences) at the University of Alberta. A total of 5 mice per group were immunized subcutaneously (s.c.) near inguinal lymph node with 0.1 mL of various formulation as detailed in **Table 5.1**. A 20 µg/mouse dose of OVA was administered in soluble or particulate form. The targeted formulations were prepared by mixing bfFp with appropriate amounts of biotinylated nanoparticles for 30 minute, as described earlier. Where applicable, the dose of anti-CD40 mAb as DC maturation stimuli was 25µg per dose. The anti-CD40 mAb was added to formulations immediately before administration to avoid any non-specific attachment on nanoparticles. Group of mice primed with Complete Freund's adjuvants (CFA) were boosted with OVA emulsified in Incomplete Freund's adjuvant (IFA). On day 21, a booster dose of respective formulations containing 20 µg of OVA was injected. Ten days after boosting, mice were sacrificed by CO₂ asphyxiation and cervical dislocation. Blood was collected by cardiac-puncture for evaluation of humoral immune response, while spleens were aseptically removed for ex vivo cytokine responses.

Table 5.1 OVA and PLGA nanoparticle vaccine formulations.

Formulations	Description*
OVA	OVA as soluble form
NP	OVA encapsulated within biotinylated NPs
Targeted NP	OVA encapsulated biotinylated NPs decorated with bfFp
Targeted NP+ α CD40	OVA encapsulated biotinylated NPs decorated with bfFp + soluble anti-CD40 mAb (25 μ g/dose)
CFA	OVA emulsified in Freund's adjuvant

* Mice were subcutaneously (S.C.) immunized twice on day 0 and 21. A 20 μ g/mouse dose of OVA was administered in each formulation. For the targeted NPs, 25 μ g of bfFp was conjugated to the NPs. In Complete Freund's adjuvant group, mice were boosted with Incomplete Freund's adjuvant.

5.2.10 Evaluation of humoral immune responses

The blood samples were allowed to clot for 1 hr at 4°C and serum was harvested by centrifugation at 5,000 rpm for 10 min and stored at -20°C, until analyzed. OVA-specific IgG titers were evaluated using ELISA. Briefly, Nunc MaxiSorp flat-bottom 96-well ELISA microplates were coated with 100 μ l of OVA solution (10 μ g/ml) overnight at 4 °C. Next day, plates were washed three times with PBST (0.1 % Tween 20 in PBS pH 7.4) and blocked with 1% BSA solution for 1 hr at 37 °C. Plates were again washed with PBST and 100 μ l of diluted serum (1:10,000) from each mouse was added in duplicate and incubated overnight at 4 °C. The plates were washed with PBST and then incubated with 100 μ l/well of goat anti-mouse HRPO conjugates (1:2000) for 1 hr at 37 °C. The plates were again washed and then 100 μ l/well of TMB substrate was added. Finally, optical density at 650 nm was measured after 15 minute using ELISA Vmax microplate reader (Molecular Devices Corp, CA).

5.2.11 Ex vivo cytokine assay

The spleens from each group of mice were aseptically removed and pooled. Splenocytes were isolated by disrupting the spleens between frosted slides. The red blood cells were lysed using ACK lysis buffer and then cells were washed with serum free RPMI medium. A single cell suspension of splenocytes was prepared by passing through a cell-strainer (70 μm) and count was adjusted to 1×10^7 cells/ml with complete RPMI media. Finally, cells were seeded in 96-well plates at a density of 1×10^6 cells/well. Splenocytes were stimulated with OVA as recall antigen (20 $\mu\text{g/ml}$) in total volume of 200 $\mu\text{l/well}$ and incubated for 96 hr at 37 $^{\circ}\text{C}$ in humidified 5% CO_2 incubator. After incubation, plates were centrifuged and supernatants were collected and stored at -80 $^{\circ}\text{C}$, until analyzed. IL-2, IL-4, IL-10 and IFN- γ levels in culture supernatant were determined using cytokine-specific ELISA according to manufacturer's instructions.

5.2.12 Statistical analysis

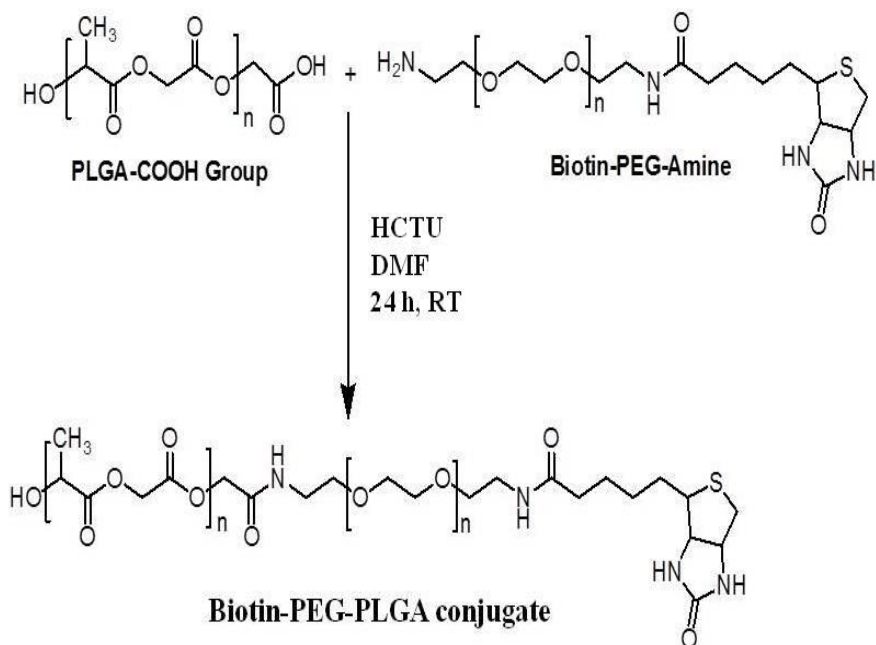
Data are presented as mean \pm standard deviation (SD). Statistical significance of difference was analyzed by one-way ANOVA followed by Tukey's multiple comparison test. Statistical difference is denoted as * $p < 0.05$, ** $p < 0.01$, *** $p < 0.001$ or ns = no significant difference ($p > 0.05$). Data was analyzed using Graphpad Prism, version 5.00 (Graphpad Software Inc., USA).

5.3 Results

5.3.1 Formulation of OVA-encapsulated biotinylated PLGA nanoparticles

Biotin-PEG-PLGA polymer was prepared by conjugating heterobifunctional biotin-PEG2,000-amine to the free carboxylate of PLGA using HCTU as a coupling agent as per previously reported method (**Figure 5.1A**) [16]. The polymer was obtained in 75% yield and was characterized using NMR spectroscopy. The proton NMR of biotin-PEG-PLGA polymer revealed characteristic peak of both PLGA and PEG (**Figure 5.1B**). Peak at 3.5 ppm corresponds to the methylene groups of the PEG backbone, while the peak at 1.48 ppm is attributed to methyl groups of the lactide chain. The multiplets at 5.25 and 4.80 ppm corresponds to the lactic acid CH and the glycolic acid CH₂, respectively.

A



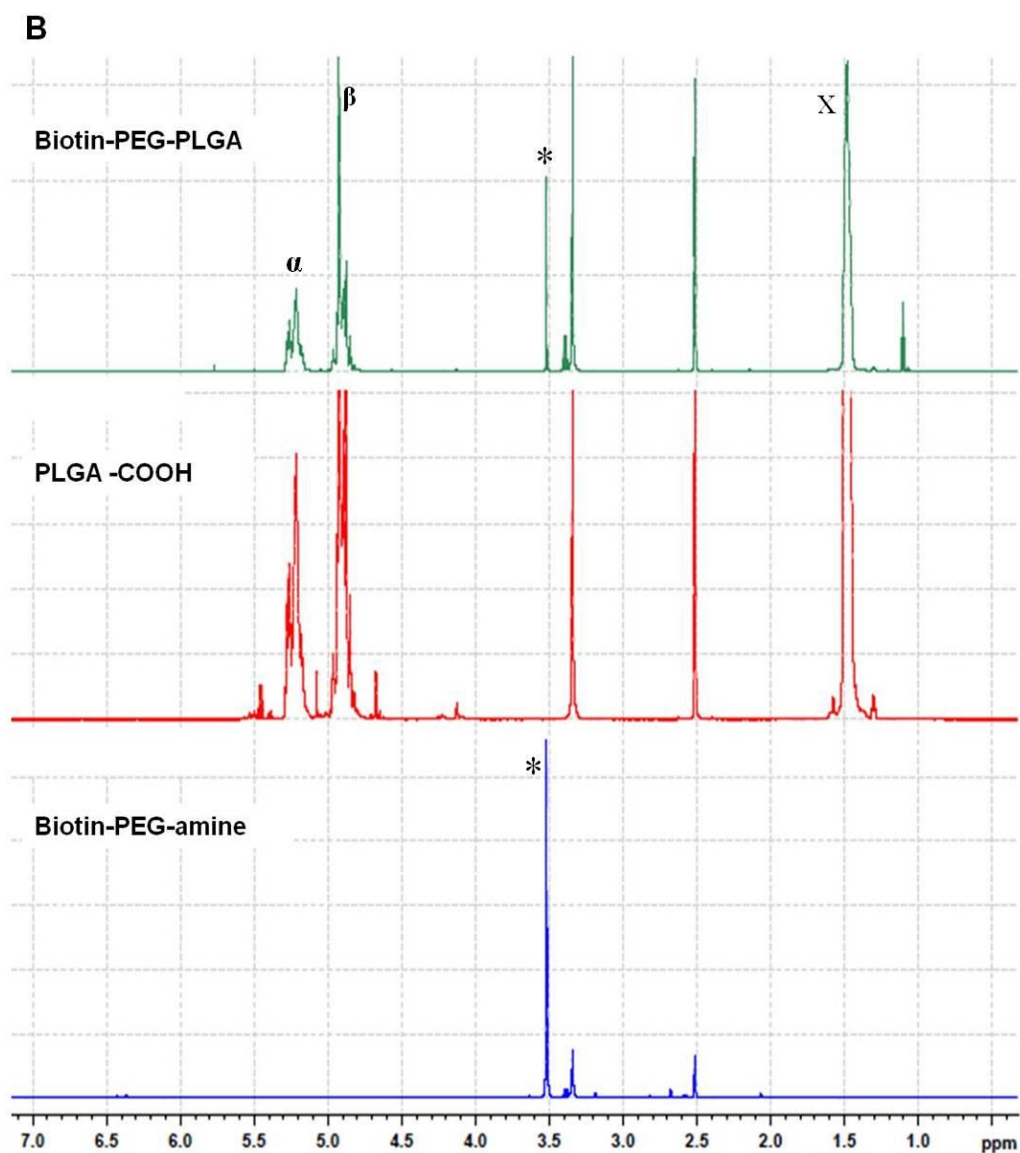


Figure 5.1 Synthesis and characterization of biotin-PEG-PLGA conjugate. Panel A, Synthetic scheme for biotin-PEG-PLGA conjugate. Panel B Proton NMR analysis of biotin-PEG-PLGA, PLGA-COOH and biotin-PEG-amine. Peak at 3.5 ppm (*) corresponds to the methylene groups of the PEG backbone, while the peak at 1.48 ppm (x) is attributed to the methyl groups of the lactide chain. The multiplet at 5.25 ppm (α) and 4.80 ppm (β) corresponds to the lactic acid CH and the glycolic acid CH₂, respectively. Peak at 2.50 ppm is contributed by DMSO-d₆, while peak 3.35 ppm is contributed by water in DMSO.

The double-emulsion solvent evaporation method was used to formulate ovalbumin-encapsulated NPs using native PLGA and biotin functionalized PLGA (**Table 5.2**). The average size of OVA loaded PLGA NPs was found to be 212.1 ± 3.7 nm, slightly more than NPs formulated with biotin-PEG-PLGA (198.5 ± 2.5 nm). With reference to nanoparticles size similar findings have been reported by other research groups using PEG-PLA diblock copolymers [20, 21]. The zeta-potential of NPs formulated with biotin-PEG-PLGA was found to be -23.9 ± 0.5 mV, which is higher than NPs formulated with native PLGA (-31.4 ± 3.2 mV), indicating that COOH groups of polymer have been successfully biotinylated and exposed on the NP surface. The loading efficiency of OVA was increased when biotinylated PLGA was used to formulate NPs, this might be due the presence of hydrophilic PEG chain in PLGA backbone. Based on published results, it is speculated that PEG chains are oriented towards the surface of NPs, thus providing effective surface coverage which results in reduced diffusion of protein towards external aqueous phase [20]. Further, analysis of particle morphology using SEM confirmed that nanoparticles were fairly smooth and spherical in shape (**Fig 5.2A**).

Table 5.2 Physico-chemical characterization of PLGA nanoparticles.

Formulations	Average diameter \pm S.D. (nm)	PDI ^a \pm S.D.	ζ Potential (mV)	OVA loading (μ g/mg)
PLGA NP	212.1 ± 3.7	0.104 ± 0.05	-31.4 ± 3.2	19.2 ± 1.5
Biotinylated PLGA NP	198.5 ± 2.5	0.095 ± 0.07	-23.9 ± 0.5	23.5 ± 2.6

^a Polydispersity index (PDI) of nanoparticle formulations measured by DLS.

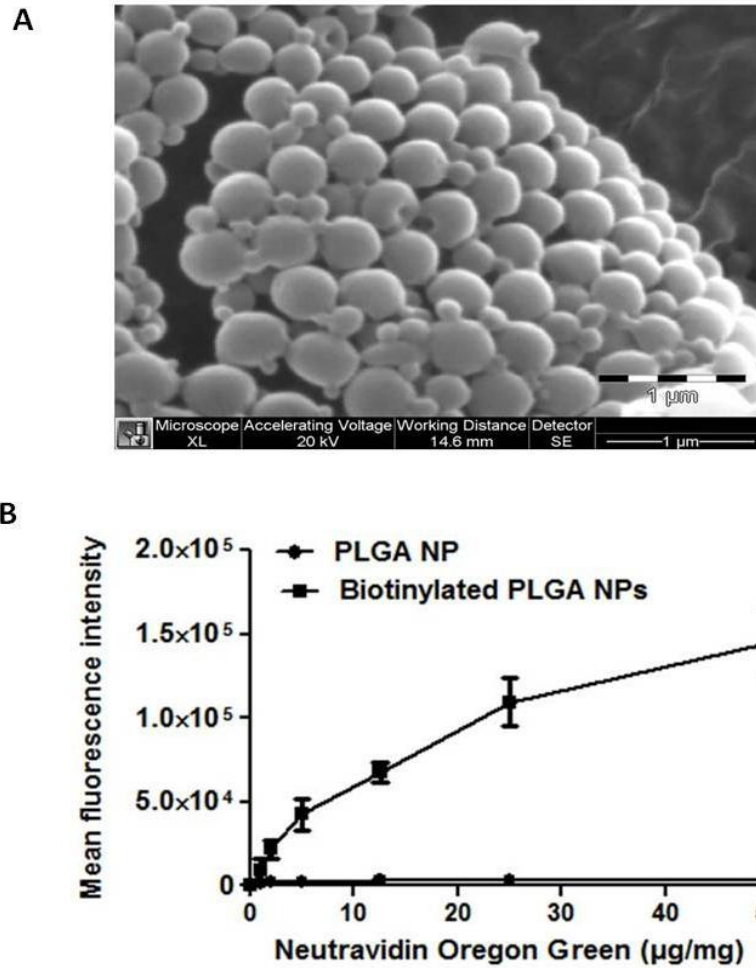


Figure 5.2 Characterization of PLGA nanoparticles. (A) Representative SEM image of PLGA NPs formulated with biotin-PEG-PLGA conjugate. (B) Qualitative analysis of NP surface associated biotin. NPs formulated using biotinylated and non-biotinylated PLGA were incubated with graded amounts of neutravidin Oregon green 488 (NAv) for 15 minutes followed by washing to remove unbound quantity and analyzed using flow cytometry. The binding of NAv contributed to the increase in NP surface associated fluorescence.

To evaluate whether NPs formulated using biotin-PEG-PLGA conjugate display abundant biotin on NP surface, the presence of NP surface associated biotin was verified using qualitative and quantitative methods. For qualitative analysis, the non-biotinylated NPs (prepared using PEG-PLGA copolymer) and biotinylated NPs (prepared using biotin-PEG-PLGA copolymer) were incubated with fluorescent neutravidin (NAv) and after washing the unbound NAv, the NPs were analyzed on flow cytometer. The results of neutravidin binding studies show that there are abundant surface associated biotin molecules providing enough docking sites for the attachment of neutravidin (**Fig 5.2B**).

Comparatively, the efficiency of neutravidin binding was very low on the non-biotinylated NPs and could be merely due to physical adsorption of neutravidin. No drastic increase in the magnitude of mean fluorescence intensity was observed in case of non-biotinylated NPs, even when neutravidin concentration was increased from 1 to 50 $\mu\text{g}/\text{mg}$ of NPs. However, for biotinylated NPs, a proportionate increase in mean fluorescence intensity was observed, when increasing amount of neutravidin (1 to 50 $\mu\text{g}/\text{mg}$ of NP) was used. These results strongly support the conjecture that only the presence of biotin was responsible for effective binding with neutravidin and increase in the fluorescence intensity. Conclusively, neutravidin binding assay confirms that biotin present on NP surface is functionally active.

Quantitative assessment of NP surface associated biotin level was carried out using fluoreporter biotin quantitation assay, which is capable of detecting picomolar quantity of biotin [17, 22]. Using this assay, it was found that biotinylated NPs contained 1176 ± 151 pmol of biotin molecules on 1 mg of nanoparticles. Such a high surface density of biotin on the surface could be attributed to the orientation of PEG chains on NP surface during preparation using double emulsion method.

5.3.2 DEC-205 receptor-mediated uptake of nanoparticles

DCs uptake soluble and particulate materials through different endocytic mechanisms. Here, we analyzed DEC-205 receptor-mediated uptake of bfFp targeted and non-targeted NPs using bone marrow dendritic cells (BMDCs). For uptake studies, TMR-dextran (TMRD) dye loaded biotinylated nanoparticles were used and targeted NPs were formulated by conjugating bfFp for 30 min. Purification of bfFp from periplasmic and cytoplasmic bacterial lysate was done using affinity chromatography as described in chapter 2 [15, 19]. After 1 h incubation of targeted NPs with BMDCs, the TMRD positive cells in CD11c gated population was $60.5 \pm 5\%$, while for non-targeted NPs only $\sim 42 \pm 4\%$ TMRD positive cells were observed. **Figure 5.3A** shows a representative histogram displaying percentage of TMRD positive cells in CD11c⁺ cells from one out of three experiments. Further, blocking of DEC-205 receptor resulted in the decrease of the percent positivity of DCs to $53.5 \pm 7\%$. As shown in **Figure 5.3B**, the cell associated mean fluorescence intensity (MFI) was found to be almost doubled using bfFp targeted NPs compared with non-targeted NPs (***) $p < 0.001$). Further, blocking with soluble anti-DEC-mAb resulted in 25-30% reduction in the MFI. The decrease in percent positivity and MFI indicates that blocking of DEC-205 with soluble ligand can decrease the receptor-mediated uptake of bfFp targeted NPs. However, we found that even non-targeted NPs are efficiently taken up by DCs. These observations can be explained based on the fact that DC are phagocytic cells and possess extraordinary ability to take up particulate materials without specific recognition.

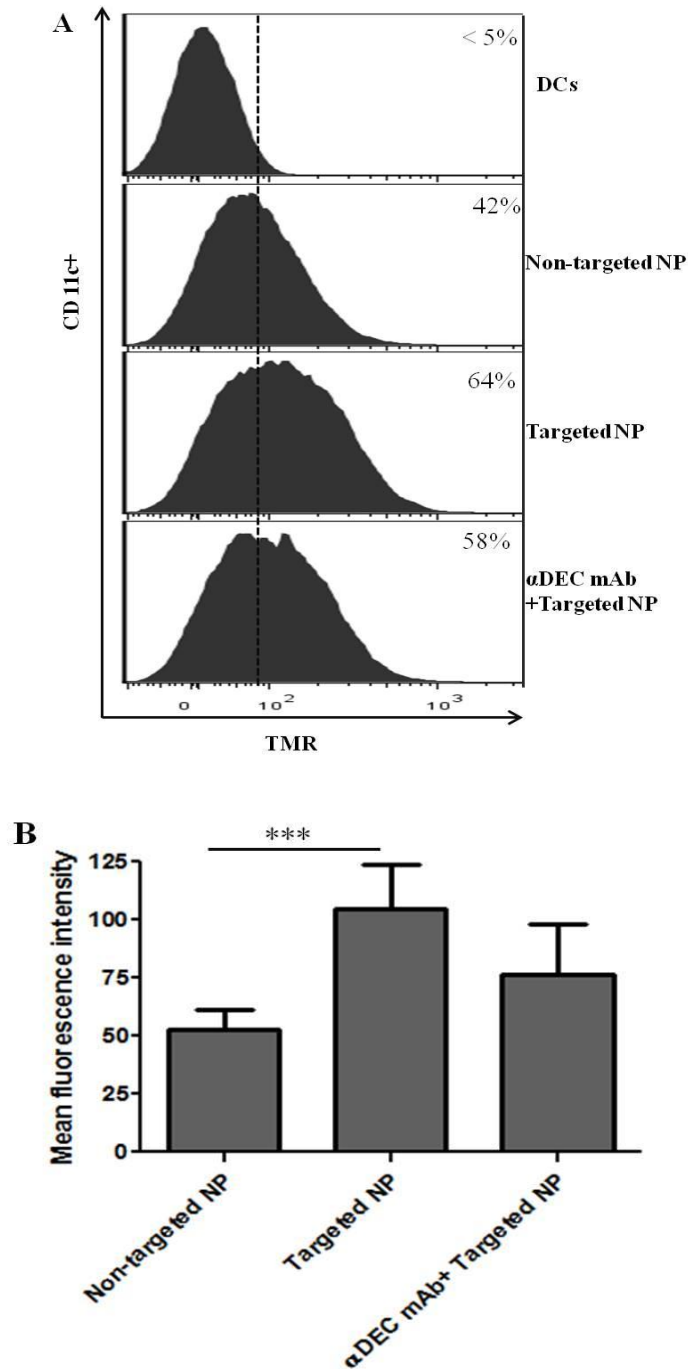


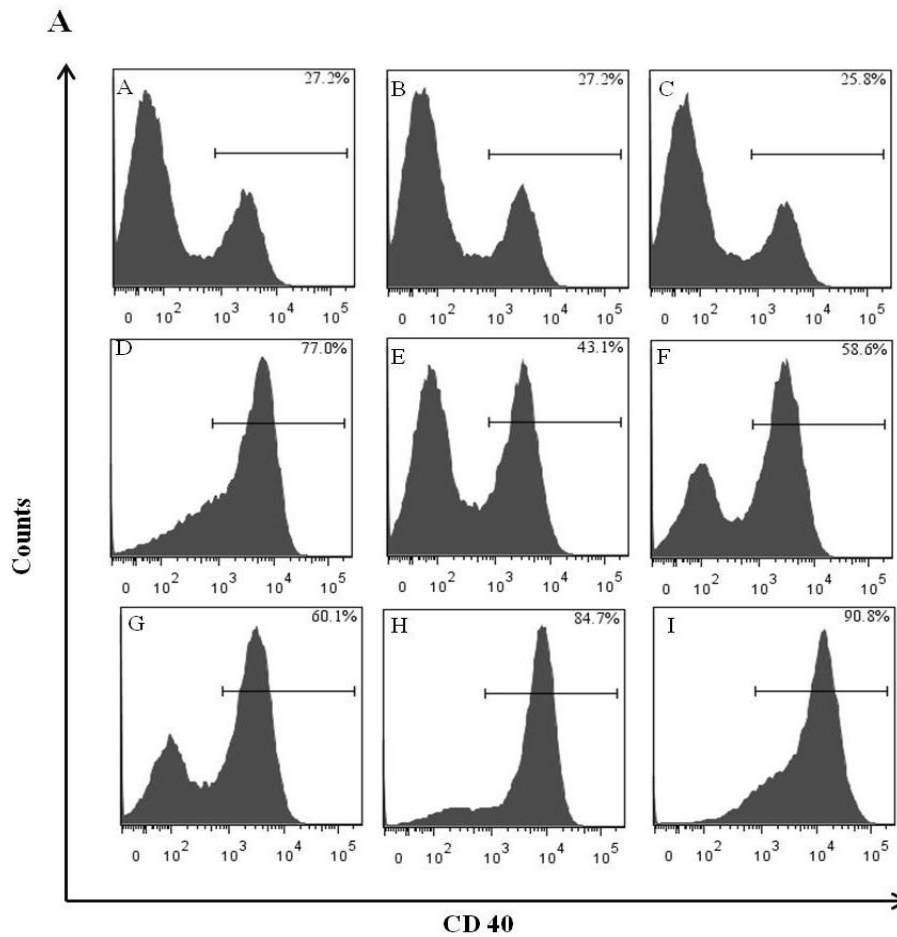
Figure 5.3 Uptake of targeted and non-targeted nanoparticles using flow cytometry. Panel A, BMDCs were incubated with TMRD loaded non-targeted NPs, bfFp functionalized targeted NPs, or bfFp functionalized targeted NPs in the presence of anti-DEC-205 mAb (25 μ g) for 1 hr at 37 $^{\circ}$ C. Cells were washed and stained for CD11c and evaluated by flow cytometry for the uptake of TMRD-NPs in CD11c+ cells. A representative histogram showing percentage of TMRD+ cells

in CD11+ cells from one out of three-independent experiments is shown. Panel B, Mean-fluorescence intensity of TMRD+ cells from different treatment groups was calculated by subtracting fluorescence intensity of non-treated DCs. Data shown are mean \pm S.D of three experiments. Differences in mean fluorescence intensity in different groups were assessed using one-way ANOVA followed by post hoc analysis using Tukey's multiple comparison test. *** denotes statistically significant difference ($P < 0.001$).

5.3.3 Nanoparticle mediated DC maturation and cytokine secretion

To study how the non-targeted and targeted particles influence dendritic cells functions, BMDCs were treated with various formulations and assessed for expression of co-stimulatory molecules and cytokine secretion pattern. To this end, we analyzed the expression of CD40 and CD86 receptors on the DC surface using flow cytometry. The treatment of DC cultures with blank NPs or OVA loaded non-targeted and targeted nanoparticles resulted in modest upregulation of DC associated co-stimulatory molecule CD40 and CD86 compared to non-treated DCs. Further, we found that encapsulation of OVA within NPs slightly increased the expression of both CD40 and CD86 compared to treatment with blank NPs. **Figure 5.4A** shows that following treatment with blank NPs percent positivity of DCs for CD40 was 43%, which increased to ~58 % when OVA loaded NPs were used as a treatment. The results are in agreement with previous studies showing modest upregulation of co-stimulatory molecules, when DCs were treated with antigen loaded PLGA nanoparticles [23, 24]. In contrast, the expression of CD40 and CD86 was significantly increased when anti-CD40 mAb was added either alone or with bfFp targeted NPs to the cultures of DCs (**Fig 5.4A**). Further, treatment of DCs with soluble OVA and bfFp did not alter the expression pattern of CD86 and CD40 compared to non-treated DCs. LPS was used as a positive control and stimulation of DCs with LPS was treated as 100% maturation. Therefore, we compared mean fluorescence intensity of cells relative to LPS treated cells. **Figure 5.4B** shows that there was no significant difference between mean fluorescence intensity, when soluble OVA, bfFp, and NP formulations were

compared with media treated cells. However, anti-CD40 mAb either alone or with targeted NPs appeared to provide significant increase in cell-associated fluorescence intensity. Our data are in accordance with previous findings, showing that CD40 cross-linking with anti-CD40 antibody resulted in considerable upregulation of DC maturation markers [25].



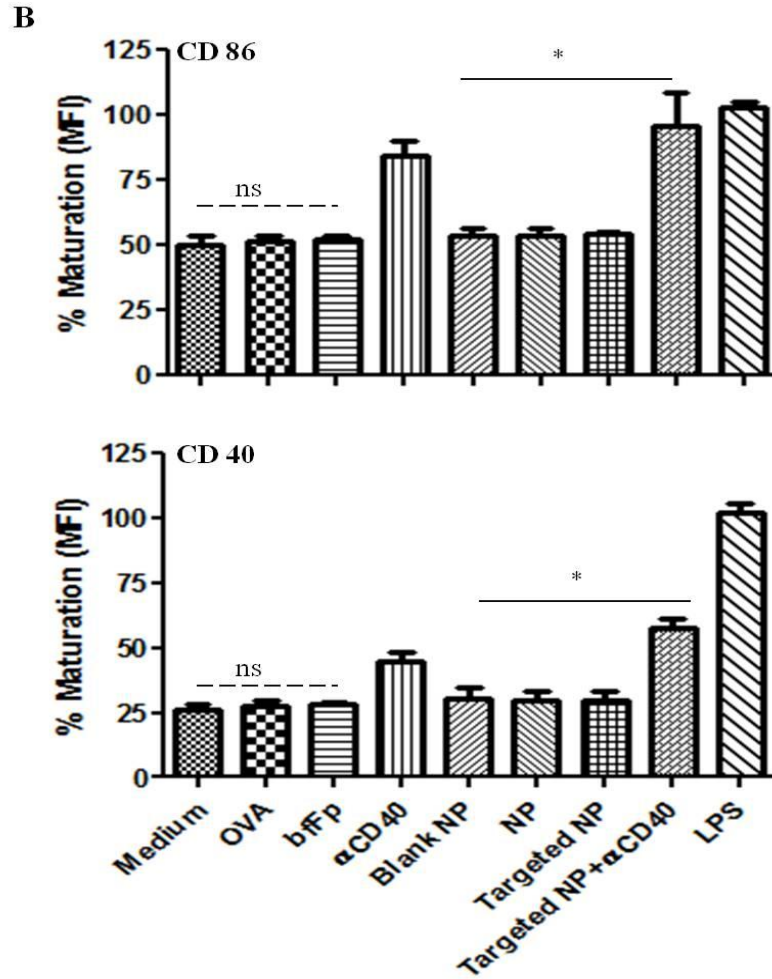


Figure 5.4 Analysis of CD86 and CD40 expression on BMDCs treated with PLGA NPs. BMDCs were treated with blank NP (NP without OVA), NP (OVA loaded NP), targeted NP (NP with bfFp), or targeted NP plus soluble α CD40 mAb for 24 h. Control treatments included soluble OVA, bfFp, and α CD40 mAb. LPS was used as a positive control and media served as a baseline control. After incubation period, cells were harvested and stained for markers. Maturation was assessed by comparing the expression of CD40 and CD86 in CD11c+ DCs. **Panel A** shows a representative example of FACS plots for the expression of CD40 on CD11c+ DCs after treatment with medium (A), OVA (B), bfFp (C), α CD40 mAb (D), blank NP (E), NP (F), targeted NP (G), targeted NP with α CD40 (H) and LPS (I). **Panel B**, relative upregulation of CD86 and CD40 markers by different formulations as described in panel A. The percent MFI of samples relative to LPS was calculated assuming 100% maturation with LPS treatment. Data are representative of three separate experiments. The line above the bars indicates statistically significant difference from targeted NP + α CD40 treatment group (* $P < 0.05$). Dashed line above bars indicate no significant difference between groups (n.s., $P > 0.05$).

To further verify that these results, we evaluated DC activation by analyzing cytokine production. We observed that BMDCs stimulated with targeted NPs along with anti-CD40 antibody, secreted significantly higher levels of IL-12 and IL-6 (**Figure 5.5 A-B**). The IL-12 secretion profile was in good correlation with the expression of maturation markers. Notably, the IL-12 influences the skewing of Th0 cells into Th1 [26], whereas the IL-6 controls this process [27]. We also found that DC treatment with antigen-encapsulated NPs significantly increased IL-12 and IL-6 compared to blank NPs (* $p < 0.05$). Similar outcome has been reported by other studies, which indicates that antigen encapsulation enhances DC stimulatory properties of blank NPs [28, 29]. In contrast, the secretion of IL-10 was found to be significantly higher, when DCs were stimulated with targeted formulation in the absence of anti-CD 40 antibody (**Figure 5.5C**). In agreement with IL-10 secretion, a recent study showed that substantial cross-linking of DEC-205 receptor with anti-DEC-205 antibody decorated NPs, up-regulated the expression of scavenger receptor CD36 on DCs and increased IL-10 production. Furthermore, a strong correlation between extent of DEC-205 cross-linking and IL-10 secretion was observed in the absence of DC activation [29].

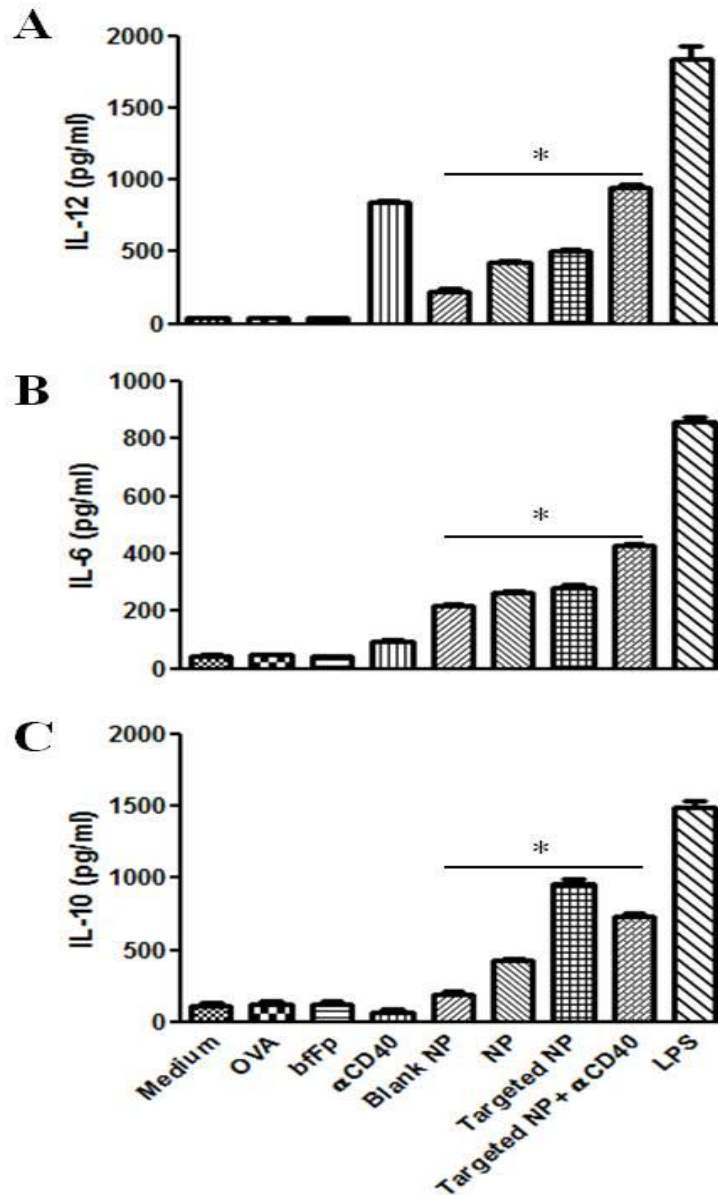


Figure 5.5 In vitro cytokine secretion profile of BMDCs treated with PLGA NPs. BMDCs were treated as described in Figure 5.4 legend. Culture supernatants were assayed in triplicates for the presence of IL-12 (panel A), IL-6 (panel B) or IL-10 (panel C). Cytokine levels (pg/ml) are expressed as mean \pm S.D. Data is representative of two separate experiments. Continuation of the line above the bars indicates statistically significant difference among different treatment groups (*P < 0.05).

5.3.4 Enhanced IgG and IgG isotype responses in the presence of costimulatory anti-CD40 mAb

To further investigate whether the bfFp based DC targeting will improve the immunogenicity of nanoencapsulated antigen, an immunization study was performed. Mice were immunized with OVA encapsulated particles (NP), NPs functionalized with bfFp (targeted NP) or targeted NPs in the presence of anti-CD40 mAb (Table 5.1). As controls, mice were immunized with similar amount of OVA in CFA or in saline.

Ten-days after secondary immunization, mice were euthanized and serum was isolated to evaluate antigen-specific antibody responses. The presence of OVA-specific total IgG, and IgG subclasses (IgG1, IgG2b and IgG2c) in the serum was analyzed by ELISA (**Figure 5.6**). OVA-specific IgG level in non-targeted and targeted nanoparticulate formulations was found to be significantly higher than that obtained with soluble OVA (* $p < 0.05$). However, no significant difference in IgG titer was observed between non-targeted and targeted nanoparticulate formulations (ns, $p > 0.05$). Moreover, administration of targeted formulations together with anti-CD40 maturation stimuli elicited significantly higher OVA-specific IgG titers compared to targeted and non-targeted formulation (* $p < 0.05$). It is evident from these results that, DEC-205 targeted delivery of nanoencapsulated antigen benefit from presence of DC maturation stimuli. These findings are in good agreement with previous observations showing that DEC-205 targeting together with DC activation augmented antigen-specific humoral and cellular responses [30]. Further, we evaluated whether antibody responses obtained with non-targeted nanoparticles could benefit from adjuvant effect of anti-CD40 antibody. To address this question, a separate set of experiment was performed and mice were immunized with surface biotinylated OVA-encapsulated PLGA nanoparticles with anti-CD40 mAb. To avoid adsorption of antibody on particle surface, anti-CD40 antibody was mixed and formulations were injected immediately. We observed that inclusion of anti-CD40 along with non-targeted formulations enhanced serum IgG titers. However, IgG titer of these

formulations was significantly lower than group of mice immunized with targeted formulations together with anti-CD40 mAb (data not shown). IgG isotype class switching from IgG1 to IgG2b and IgG2c plays an important role in the shift of immune of response from Th2 to Th1. Similar to total IgG profile, no significant difference in IgG subclass titers was observed between targeted and non-targeted NPs (Figure 5.6).

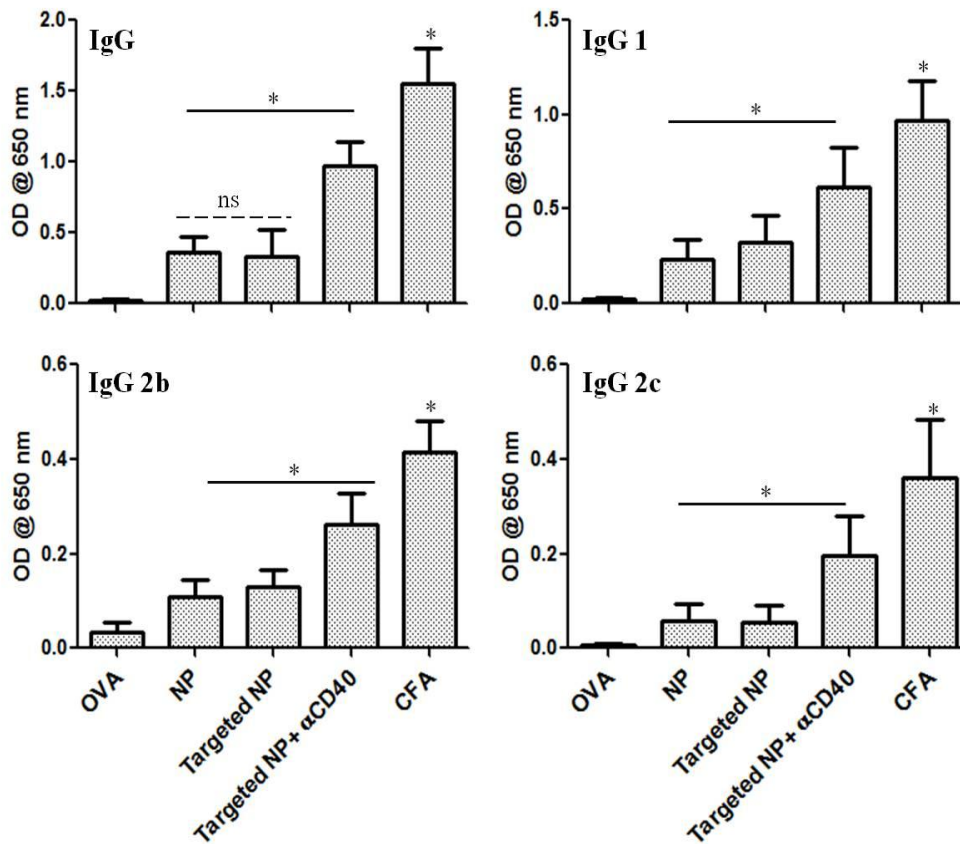


Figure 5.6 Analysis of OVA-specific IgG response. Groups of five mice were immunized by s.c. injection with various formulations containing OVA (20 μ g) on day 0 and 21. Ten days after booster-dose, mice were euthanized and serum was collected following cardiac puncture. Serum samples were diluted (1:10,000) with PBS and analyzed for the presence of OVA specific total IgG or IgG isotypes (IgG1, IgG2b and IgG2c) using ELISA. Data are presented as group mean \pm S.D. Continuous line indicates statistically significant difference (* $P < 0.05$), while ns indicates nonsignificant difference between groups (ns, $P > 0.05$). * indicates significant difference of CFA group from other groups (* $P < 0.05$).

However, the administration of targeted NPs along with soluble DC maturation stimuli provided higher levels of IgG2b and IgG2c compared with targeted and non-targeted formulations (* $p < 0.05$). Notably, OVA specific IgG1 titer were slightly higher for group of mice immunized with targeted NPs compared to non-targeted NPs. The mice immunized with CFA emulsified OVA provoked significantly higher total IgG and IgG isotypes compared to targeted NPs together with anti-CD40 mAb (($*p < 0.05$). Despite using the DC maturation stimuli, the titers of targeted formulations remained lower than that of CFA group. The possible reason could be due to the use of soluble anti-CD40 mAb as maturation stimuli. The scavenging of soluble anti-CD40 mAb by the cells other than DCs might have prevented activation of particular DC, which has taken targeted NP formulation.

5.3.5 Induction of ex-vivo cytokines

The effect of DC targeted and non-targeted formulations on cellular immunity was evaluated based on the production of Th1 (IFN- γ , IL-2) and Th2 (IL-4 and IL-10) cytokines using ovalbumin as a recall antigen to stimulate splenocytes. The ability of lymphocytes to produce IFN- γ describes a Th1 phenotype, while the production of IL-4 is associated with a Th2 phenotype. In agreement with the IgG isotypes, the IFN- γ levels were found to be highest for CFA group followed by bfFp targeted NP administered with anti-CD40 mAb. As shown in **Figure 5.7**, the IFN- γ levels of targeted formulation administered with maturation stimuli was significantly higher than that of non-targeted or targeted formulations (* $p < 0.05$). This trend was also found to be applicable for the IL-2 production. The Th2 cytokine profile reveals that there was no significant difference in IL-4 production between targeted or targeted formulations administered with DC maturation stimuli (ns, $p > 0.05$). However, splenocytes of mice treated with targeted NPs induced higher levels of IL-10 secretion compared with targeted NPs in the presence of anti-CD40 mAb (* $p < 0.05$). These results are in accordance with the previous work showing that DEC-205 targeting in the absence of DC maturation stimuli results in antigen-specific tolerance [31, 32] .

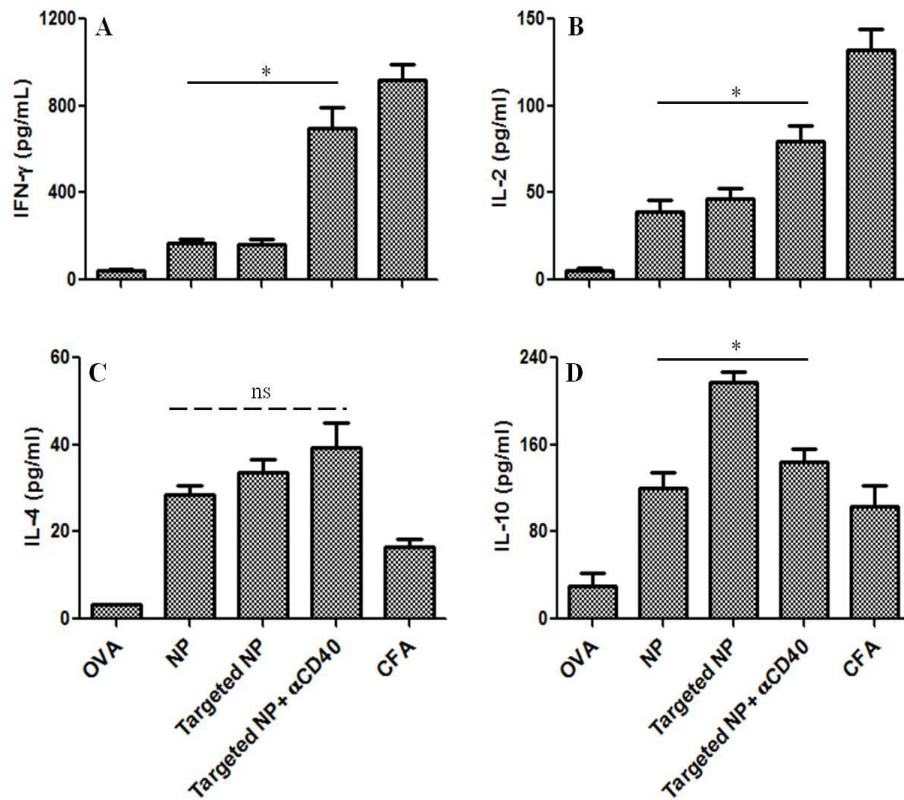


Figure 5.7 OVA-specific ex-vivo cytokine secretion profile. Splenocytes obtained from groups of five mice immunized with vaccine formulations were pooled and single-cell suspensions were seeded in 96-well plates at the density of 1×10^6 /well. Cultures were stimulated with OVA for 96 hr and production of Th1 cytokines IFN- γ (A) and IL-2 (B), and Th2 cytokines IL-4 (C) and IL-10 (D) were analyzed by cytokine-specific ELISA. Data represent mean \pm SD of triplicate cultures. Dashed line above bars indicate no significant difference between groups (ns, $P > 0.05$). Continuous line above the bars indicates statistically significant difference ($*P < 0.05$).

5.4 Discussion

The PLGA is a biocompatible and biodegradable US FDA approved polymer that has been approved for clinical applications. Micro and nanoparticles composed of PLGA have been extensively investigated to improve immunogenicity of encapsulated vaccine antigens, such as proteins, peptides, plasmid and DNA [3, 10]. The antigens delivered using PLGA based micro/nano particles are preferentially taken up by phagocytic cells and more efficiently cross-presented than soluble antigens. Additionally, PLGA based delivery systems facilitate co-delivery of multiple vaccine components and protect them from degradation. Recent studies have shown that antibody-mediated targeting of PLGA nanoparticle based vaccines to dendritic cells can improve immunogenicity of encapsulated antigens [12-14].

Despite extensive use of PLGA as a vaccine carrier, to our knowledge, only a few studies have reported antibody-based DC targeted vaccines. Different strategies to design antibody-targeted PLGA vaccines are still emerging. Here we report a simple and versatile strategy to formulate DC targeted PLGA nanoparticles for the delivery of model antigen, OVA. To achieve this, we employed recombinant bifunctional fusion protein (bfFp) as a DC targeting vector in combination with biotinylated PLGA NPs that encapsulate the antigen. Earlier, we demonstrated that bfFp based DC targeting of plasmid DNA loaded biotinylated chitosan nanoparticles enhanced SARS-nucleocapsid antigen specific immune responses via nasal and intramuscular route [19]. Here we extended studies to design DC targeted PLGA nanoparticle based vaccines for protein antigen.

Accordingly, the presence of NP surface associated biotin is required for proper attachment of bfFp through core-streptavidin arm. To ensure this, we used biotin-PEG-PLGA polymer for nanoparticle preparation and antigen-loaded biotinylated NPs could be formulated without any post-formulation modifications. Pegylated PLGA was employed as PEG is US FDA approved hydrophilic and non-toxic molecule used to impart 'stealth' properties to nanoparticle formulations [33]. The surface associated PEG chains sterically stabilize the nanoparticles, mitigate

opsonization and thus prevent non-specific interactions with the cells. Additionally, due to high flexibility, PEG spacers have been found to enhance the accessible range of PEG-tethered ligand binding [13]. Binding of neutravidin (NAv) and bfFp to biotinylated NPs confirmed the presence of functional biotin on NP surface. Subsequently, bfFp conjugation to NPs enhanced the magnitude of in vitro uptake by almost two-fold, and the uptake of targeted NPs was reduced when DEC-205 receptor was blocked with anti-DEC-205 antibody. These results confirmed DEC-205 receptor-mediated uptake of targeted NPs. Similar to our results, Kwon et al. have shown that anti-DEC-205 antibody targeted acid degradable particles are preferentially taken up by DCs [34]. A recently published study also observed that anti-DEC-205 F(ab')₂ fragment based targeted delivery of PLGA NPs enhanced binding to mouse DCs [14].

Further, we studied how bfFp modification of NPs influenced the outcome of DC functions. To address this, we analyzed DC maturation and secretion of cytokines. Our results show that targeted as well as non-targeted formulations do not alter expression of DC maturation markers. These results are in agreement with a recent report showing that no significant difference in the expression of DC maturation markers was noticed following treatment with anti-DEC-205 antibody targeted or non-targeted PLGA NPs [29]. However, we found that expression of CD86 and CD40 was significantly upregulated, when anti-CD40 mAb was included with targeted NPs. Cytokine secretion pattern of DCs influence the outcome of immune responses. We noticed that DC maturation was associated with secretion of Th1 pro-inflammatory cytokines such as IL-12 and IL-6. Notably, IL-12 is produced by mature DCs and plays a key role in shaping cell-mediated immune responses. In contrast, cross-linking of DEC-205 receptor in the absence of DC activation induced secretion of anti-inflammatory cytokine IL-10, which is known to induce immunosuppression and de novo induction of regulatory T cells [35]. To this end, our results from immunization experiments demonstrate that DEC-205 targeting without DC maturation do not improve antigen-specific IgG titers. However, targeted formulations with costimulatory

anti-CD40 mAb provoked significantly higher IgG responses (Fig. 6). It has been demonstrated that delivery of antigen and adjuvants using non-targeted PLGA NPs provoked robust IgG responses against influenza antigens [36]. In this context, it would be worthy to analyze whether bfFp based DC targeting of nanoparticle encapsulated antigen and adjuvant will further improve antibody responses. Furthermore, a recent study has shown that DC targeted delivery of nanoparticle co-encapsulated adjuvant allowed for almost 100-fold reduction in the dose, compared to the use of adjuvant in soluble form [14].

Ex vivo analysis of cytokine responses showed that splenocytes from a group of mice immunized with CFA and targeted NPs with DC activation preferentially secreted Th1 biased cytokines (IFN- γ and IL-2). Supporting to these results, a previous study has reported that DEC-205 targeted delivery of ovalbumin encapsulated acid-degradable microparticles enhanced antigen-specific IFN- γ secreting CD8⁺ T cells and cytotoxic T lymphocyte-mediated lysis of target cells [34]. In contrast, splenocytes of mice immunized with targeted formulations in the absence of DC maturation stimuli produced higher levels of IL-10. The IL-10 is immunosuppressive cytokine and prevents functional activation of DCs and renders them tolerogenic. These results are parallel to conjecture that DEC-205 targeted antigen delivery in the absence of DC maturation induces peripheral tolerance and production of T regulatory cells [31, 32].

In another study, DC targeting of tumor antigen carrying liposomes was achieved using a single chain antibody against mouse DEC-205 [37]. However, only targeted formulations carrying adjuvant and antigens showed protective immunity against highly metastatic murine melanoma (B16-OVA) model. Advantageously, the scFv fragments are devoid of non-specific interactions with Fc receptors, which is commonly faced drawback when full-length antibody molecules are used. Moreover, the scFv and bfFp based DC targeting vectors can be produced in large-quantities using bacterial expression systems, proving to be cost-effective alternative to full-length antibodies.

The results of the present study demonstrate that targeted delivery of biodegradable particulate vaccines benefit from bfFp based DEC-205 targeting. The bfFp based NP delivery system has several advantages, namely (i) it can be applied to deliver one or more antigens with or without adjuvants, (ii) bfFp attachment precludes any post-formulation modification of antigen-loaded nanoparticles, a step that can have deleterious effect on antigen, (iii) the vaccine (NP) components such as PLGA and PEG are approved for clinical applications, and (iv) lastly, the use of bFfp with biotinylated NPs highlights the importance of easy-to-use two-component based vaccine formulations, which can be prepared by simple mixing of DC targeting ligand with nanoparticles before injection. The approach described here is simple and versatile and can be used for targeting multiple vaccine components to the dendritic cells.

5.5 References

- [1] Reddy ST, van der Vlies AJ, Simeoni E, Angeli V, Randolph GJ, O'Neil CP, et al. Exploiting lymphatic transport and complement activation in nanoparticle vaccines. *Nat Biotech* 2007;25:1159-64.
- [2] Johansen P, Martínez Gómez JM, Gander B. Development of synthetic biodegradable microparticulate vaccines: a roller coaster story. *Expert Rev Vaccines* 2007;6:471-4.
- [3] De Temmerman M-L, Rejman J, Demeester J, Irvine DJ, Gander B, De Smedt SC. Particulate vaccines: on the quest for optimal delivery and immune response. *Drug Discov Today* 2011;16:569-82.
- [4] Jain S, O'Hagan DT, Singh M. The long-term potential of biodegradable poly(lactide-co-glycolide) microparticles as the next-generation vaccine adjuvant. *Expert Rev Vaccines* 2011;10:1731-42.
- [5] Moon JJ, Suh H, Polhemus ME, Ockenhouse CF, Yadava A, Irvine DJ. Antigen-displaying lipid-enveloped PLGA nanoparticles as delivery agents for a *Plasmodium vivax* malaria vaccine. *PLoS ONE* 2012;7:e31472.
- [6] Mohanan D, Slütter B, Henriksen-Lacey M, Jiskoot W, Bouwstra JA, Perrie Y, et al. Administration routes affect the quality of immune responses: A cross-sectional evaluation of particulate antigen-delivery systems. *J Control Release* 2010;147:342-9.
- [7] Thomas C, Rawat A, Hope-Weeks L, Ahsan F. Aerosolized PLA and PLGA Nanoparticles Enhance Humoral, Mucosal and Cytokine Responses to Hepatitis B Vaccine. *Mol Pharm* 2010;8:405-15.
- [8] Goforth R, Salem A, Zhu X, Miles S, Zhang X-Q, Lee J, et al. Immune stimulatory antigen loaded particles combined with depletion of regulatory T-cells induce potent tumor specific immunity in a mouse model of melanoma. *Cancer Immunol Immunother* 2009;58:517-30.
- [9] Pandit S, Cevher E, Zariwala MG, Somavarapu S, Alpar HO. Enhancement of immune response of HBsAg loaded poly (L-lactic acid) microspheres against

Hepatitis B through incorporation of alum and chitosan. *J Microencapsul* 2007;24:539-52.

[10] Jiang W, Gupta RK, Deshpande MC, Schwendeman SP. Biodegradable poly(lactic-co-glycolic acid) microparticles for injectable delivery of vaccine antigens. *Adv Drug Deliv Rev* 2005;57:391-410.

[11] Hamdy S, Haddadi A, Hung RW, Lavasanifar A. Targeting dendritic cells with nano-particulate PLGA cancer vaccine formulations. *Adv Drug Deliv Rev* 2011;63:943-55.

[12] Cruz LJ, Tacke PJ, Fokkink R, Joosten B, Stuart MC, Albericio F, et al. Targeted PLGA nano- but not microparticles specifically deliver antigen to human dendritic cells via DC-SIGN in vitro. *J Control Release* 2010;144:118-26.

[13] Cruz LJ, Tacke PJ, Fokkink R, Figdor CG. The influence of PEG chain length and targeting moiety on antibody-mediated delivery of nanoparticle vaccines to human dendritic cells. *Biomaterials* 2011;32:6791-803.

[14] Tacke PJ, Zeelenberg IS, Cruz LJ, van Hout-Kuijter MA, van de Glind G, Fokkink RG, et al. Targeted delivery of TLR ligands to human and mouse dendritic cells strongly enhances adjuvanticity. *Blood* 2011;118:6836-44.

[15] Wang WW, Das D, Suresh MR. A versatile bifunctional dendritic cell targeting vaccine vector. *Mol Pharm* 2009;6:158-72.

[16] Basu S, Harfouche R, Soni S, Chimote G, Mashelkar RA, Sengupta S. Nanoparticle-mediated targeting of MAPK signaling predisposes tumor to chemotherapy. *Proc Natl Acad Sci USA* 2009; 106(19):7957-61.

[17] Weiss B, Schneider M, Muys L, Taetz S, Neumann D, Schaefer UF, et al. Coupling of biotin-(poly(ethylene glycol))amine to poly(D,L-lactide-co-glycolide) nanoparticles for versatile surface modification. *Bioconjug Chem* 2007;18:1087-94.

[18] Lutz MB, Kukutsch N, Ogilvie ALJ, Röβner S, Koch F, Romani N, et al. An advanced culture method for generating large quantities of highly pure dendritic cells from mouse bone marrow. *J Immunol Methods* 1999;223:77-92.

- [19] Raghuwanshi D, Mishra V, Das D, Kaur K, Suresh MR. Dendritic Cell Targeted Chitosan Nanoparticles for Nasal DNA Immunization against SARS CoV Nucleocapsid Protein. *Mol Pharm* 2012;9:946-56.
- [20] Shan X, Liu C, Yuan Y, Xu F, Tao X, Sheng Y, et al. In vitro macrophage uptake and in vivo biodistribution of long-circulation nanoparticles with poly(ethylene-glycol)-modified PLA (BAB type) triblock copolymer. *Colloid Surf B Biointerfaces* 2009;72:303-11.
- [21] Essa S, Rabanel JM, Hildgen P. Characterization of rhodamine loaded PEG-g-PLA nanoparticles (NPs): Effect of poly(ethylene glycol) grafting density. *Int J Pharm.*2011;411:178-87.
- [22] Patil Y, Sadhukha T, Ma L, Panyam J. Nanoparticle-mediated simultaneous and targeted delivery of paclitaxel and tariquidar overcomes tumor drug resistance. *J Control Release* 2009;136:21-9.
- [23] Elamanchili P, Diwan M, Cao M, Samuel J. Characterization of poly(d,l-lactic-co-glycolic acid) based nanoparticulate system for enhanced delivery of antigens to dendritic cells. *Vaccine* 2004;22:2406-12.
- [24] Zhang Z, Tongchusak S, Mizukami Y, Kang YJ, Ioji T, Touma M, et al. Induction of anti-tumor cytotoxic T cell responses through PLGA-nanoparticle mediated antigen delivery. *Biomaterials* 2011;32:3666-78.
- [25] Demangel C, Palendira U, Feng CG, Heath AW, Bean AGD, Britton WJ. Stimulation of Dendritic Cells via CD40 Enhances Immune Responses to Mycobacterium tuberculosis Infection. *Infect Immun* 2001;69:2456-61.
- [26] Macatonia S, Hosken N, Litton M, Vieira P, Hsieh C, Culpepper J, et al. Dendritic cells produce IL-12 and direct the development of Th1 cells from naive CD4+ T cells. *J Immunol* 1995;154:5071-9.
- [27] Diehl S, Rincón M. The two faces of IL-6 on Th1/Th2 differentiation. *Mol Immunol* 2002;39:531-6.
- [28] Clawson C, Huang C-T, Futralan D, Martin Seible D, Saenz R, Larsson M, et al. Delivery of a peptide via poly(d,l-lactic-co-glycolic) acid nanoparticles enhances its dendritic cell-stimulatory capacity. *Nanomed* 2010;6:651-61.

- [29] Bandyopadhyay A, Fine RL, Demento S, Bockenstedt LK, Fahmy TM. The impact of nanoparticle ligand density on dendritic-cell targeted vaccines. *Biomaterials* 2011;32:3094-105.
- [30] Boscardin SB, Hafalla JCR, Masilamani RF, Kamphorst AO, Zebroski HA, Rai U, et al. Antigen targeting to dendritic cells elicits long-lived T cell help for antibody responses. *J Exp Med* 2006;203:599-606.
- [31] Hawiger D, Inaba K, Dorsett Y, Guo M, Mahnke K, Rivera M, et al. Dendritic cells induce peripheral T cell unresponsiveness under steady state conditions in vivo. *J Exp Med* 2001;194:769-80.
- [32] Bonifaz L, Bonnyay D, Mahnke K, Rivera M, Nussenzweig MC, Steinman RM. Efficient targeting of protein antigen to the dendritic cell receptor DEC-205 in the steady state leads to antigen presentation on major histocompatibility complex class I products and peripheral CD8+ T cell tolerance. *J Exp Med* 2002;196:1627-38.
- [33] Owens Iii DE, Peppas NA. Opsonization, biodistribution, and pharmacokinetics of polymeric nanoparticles. *Int J Pharm* 2006;307:93-102.
- [34] Kwon YJ, James E, Shastri N, Fréchet JMJ. In vivo targeting of dendritic cells for activation of cellular immunity using vaccine carriers based on pH-responsive microparticles. *Proc Natl Acad Sci U S A* 2005;102:18264-8.
- [35] Mahnke K, Bedke T, Enk AH. Regulatory conversation between antigen presenting cells and regulatory T cells enhance immune suppression. *Cell Immunol* 2007;250:1-13.
- [36] Kasturi SP, Skountzou I, Albrecht RA, Koutsonanos D, Hua T, Nakaya HI, et al. Programming the magnitude and persistence of antibody responses with innate immunity. *Nature* 2011;470:543-7.
- [37] van Broekhoven CL, Parish CR, Demangel C, Britton WJ, Altin JG. Targeting dendritic cells with antigen-containing liposomes: a highly effective procedure for induction of antitumor immunity and for tumor immunotherapy. *Cancer Res* 2004;64:4357-65.

Chapter 6: General discussion, conclusions, and future directions

6.1 General discussion

During the past decade, new generation vaccines, particularly those based on the recombinant proteins and DNA, have emerged as viable substitutes to traditional vaccines [1]. These subunit antigens allow rational design of vaccines that are likely less reactogenic than traditional vaccines, but their application potential remains limited due to poor immunogenicity profile. Numerous approaches have been explored to enhance the magnitude of immune response to these subunit vaccines [2]. In this perspective, recent preclinical and clinical studies demonstrate that subunit vaccines can be improved using selective delivery of antigens to DCs in combination with optimum delivery system and adjuvant(s) [3, 4].

The realization that DCs are critical for initiation and control of innate and adaptive immune responses, gave rise to the exploration of a number of strategies for DC-selective antigen delivery. Several studies using mouse models and non-human primates have shown the efficiency and efficacy of *in vivo* DC targeted delivery of antigens [5]. To achieve DC-selective targeted delivery of antigens, different DC-associated receptors are under extensive evaluation with special interest to C-type lectin receptors (CRLs). Area of antibody-mediated antigen targeting to DCs through CRLs has been pioneered by late Nobel laureate Dr. Ralph Steinman and his colleagues. In this regard, first and so far most extensive studied CLR for antigen targeting is DEC-205 (CD205). *In vivo* targeting of the DC DEC-205 receptor has been shown to provide protective immune responses to host against viral, cancer and autoimmune diseases [3]. Furthermore, clinical trials of DEC-205-targeted vaccines are currently underway to determine safety and proof-of-principle. Recently, a fusion protein consisting of a fully human anti-DEC-205 monoclonal antibody linked to the tumor-associated antigen (TAA) NY-ESO-1 with potential immunostimulating and antineoplastic activities has entered clinical trials [6]. The NY-ESO-1 was selected as a target antigen as it is expressed in a wide variety of cancer cells and thus can help in developing therapeutics against multiple cancers.

Current DEC-205 targeting strategies are based on the use of full-length antibodies chemically or genetically conjugated with vaccine antigens. Chemical conjugation of antigens to antibodies is very sensitive process with almost no control over site-specific conjugation and thus poor stoichiometry. To overcome these limitations, genetic fusion approach was developed. In this method, antigen is genetically fused to C-terminal of heavy chain of antibody and expressed as a recombinant fusion protein using mammalian expression system. However, fusion proteins are large molecules that pose numerous challenges in the formulation, manufacturing, process development and stability. Furthermore, a new antibody fusion protein is required for each antigen (protein or peptide), which is often time-consuming and costly.

In this context, the Suresh laboratory has developed a recombinant bifunctional fusion protein (bfFp) vector for realizing DC-targeted delivery of any class of biotinylated antigens [7]. BfFp is comprised of a single chain antibody (scFv) that recognizes DEC-205 receptor of DC, fused with a core-streptavidin domain capable of binding to biotinylated antigens. In vivo DC-targeted delivery of a diverse group of biotinylated antigens (e.g. proteins, peptides, glycolipids, DNA) with bfFp in conjunction with as DC-maturation stimuli (anti-CD40 mAb) provided augmented cellular and humoral responses [7]. BfFp vector has several advantages such as it lacks Fc domain avoiding non-specific interactions, allows targeting of any biotinylated antigen and manufacture in prokaryotic expression system which is economical and consistent. Nevertheless, bfFp based DC-targeting approach has limited antigen-carrying capacity, as well as it exposes targeted antigens to enzymatic degradation and lacks sustained antigen-release profile to boost immune responses.

Therefore, our **main goal** was to formulate an effective strategy that can combine antigen-carrying capacity of nanoparticulate vaccine delivery systems and specific targeting ability of bfFp to DCs. In this work, we attempted to formulate bfFp based DC-targeted nanoparticulate delivery system for plasmid DNA and model protein antigen, OVA.

In the first part of this work (**chapters 2 and 3**), we selected plasmid DNA encoding for SARS CoV N protein (pVAXN) and avian influenza H5N1-HA (pCAG α -HA) as vaccine antigens. SARS and influenza viruses are transmitted through mucosal routes, including respiratory route, therefore, an effective mucosal vaccine is regarded as an ideal preventive measure in case of a pandemic outbreak. The choice of nasal route was also based on the abundance of DEC-205 receptor expressing DCs in the respiratory tract [8, 9]. These respiratory tract DC subsets can be targeted with bfFp functionalized nanoparticles using non-invasive approach. To achieve, nasal delivery of SARS CoV N protein and H5N1 HA DNA vaccines, chitosan was selected as a carrier due to its polycationic nature and mucoadhesive properties. Plasmid DNA (pVAXN or pCAG-HA) loaded biotinylated chitosan nanoparticles were prepared using complex coacervation method and formulated particles were in adequate size range, to allow efficient uptake by DCs. Nanoparticles displayed high encapsulation efficiency and protected encapsulated DNA against nuclease digestion. For in vivo immune response studies in mice, these DNA loaded nanoparticles were appended with bfFp and instilled by intranasal route and intramuscular route. pVAXN was used at 5 μ g per dose, while pCAG α -HA was used at 10 μ g per dose. A time-dependent analysis of systemic SARS CoV N protein and HA specific profile showed that intranasal delivery of unformulated DNA or merely nanoencapsulated DNA did not induce any IgG response, however, bfFp based targeting resulted in improved IgG responses. Furthermore, intranasal administration of bfFp targeted NPs together with anti-CD40 mAb as DC maturation stimuli resulted in significantly higher IgG responses compared to unformulated DNA administered by intramuscular route. Most promising results were obtained for IgA responses when intranasal and intramuscular routes were compared. SARS CoV N protein and HA specific IgA titers were substantially higher, when bfFp targeting and anti-CD40 were used with vaccine formulations. Nasal administration of these formulations also provoked secretion of IFN- γ , when splenocytes were ex vivo

stimulated with antigens; however, levels were significantly lower than those obtained following intramuscular immunization.

Despite using equal amounts of DNA dose via the intranasal or intramuscular route, the intramuscular route provided higher systemic IgG and cellular immune responses. The better outcome of immune responses following intramuscular route can be explained based on certain features. First, complete bioavailability of intramuscularly administered DNA compared with the intranasally administered DNA can be cleared quickly due to harsh environment at mucosal surfaces [10]. Additionally, following the intramuscular immunization, myocytes can serve as antigen-storage factory, while acting as antigen-presenting cells along with muscle-resident DCs, and thus provide better immune responses [11, 12].

Conclusively, our data from **chapters 2 and 3** indicates that intranasal delivery of nanoencapsulated DNA formulations benefit from active targeting and presence of DC maturation stimuli. Given the dose of DNA employed in our studies this strategy could be a vital lead towards formulating a DC targeted low-dose vaccine using non-invasive means. As both SARS and H5N1 viruses require biosafety level 3 and 4 facilities, respectively, we were not able to conduct virus challenge experiments. Nevertheless, the strategy described herein warrants further evaluation in virus challenge studies, as a recent finding has shown that intranasal delivery of even 10 μ g dose of polyethylenimine (PEI) formulated H5N1 HA DNA was sufficient to provide full protection against parental strain and partial cross-protection against highly pathogenic strain [13]. In case of H5N1 influenza viruses, the cross-protective immunity is correlated with mucosal IgA, which is not induced following systemic immunization. In our studies, intranasal administration of DC targeted formulations induced IgA responses at mucosal sites; therefore, we speculate that when tested in virus challenge model these formulations should provide expected outcome.

It is worth mentioning that despite HA-specific IgG titers obtained with our formulations, no detectable hemagglutination inhibition (HI) titers were recorded (HI assay was performed in Dr. Darwyn Kobasa's Lab at National Microbiology

Laboratory, Winnipeg). However, previous studies from Kobasa's group and other researchers have demonstrated that complete protection in different animal species including mice, ferrets and chickens against H5N1 infection was frequently observed in the absence of detectable HI titers before virus challenge with a HA DNA vaccine [14-16].

Our next goal was to formulate a fusion DNA construct (pDECN) that encodes for anti-DEC-205 scFv and SARS CoV N protein genes (**chapter 4**). We envisioned that when delivered intramuscularly, this DNA construct will result in expression and secretion of anti-DEC-scFv-SARS CoV N protein (DECN protein) from transfected myocytes. The secreted fusion protein would be taken up by DCs via DEC-205 receptor-mediated endocytosis. Expression of DECN protein was verified using Western blot analysis and expressed protein was found to be secreted from transfected cells. In vitro DC binding studies were performed to determine DC binding ability of DECN fusion protein. Results show that DECN fusion protein indeed binds with murine DC2.4 cell line that expresses DEC-205 receptor. Next we formulated pVAXN and pDECN loaded chitosan nanoparticle to analyze the immune response in mice. These results demonstrate that introduction of anti-DEC-205 scFv into pVAXN DNA construct led to improved efficacy of DNA vaccine and pDECN construct consistently provided significantly higher IgG titers compared to pVAXN. Moreover, splenocytes of mice vaccinated with pDECN formulations also resulted in secretion of Th1 cytokines (IFN- γ and IL-2), which were higher than those obtained with pVAXN formulations. Furthermore, the magnitude of immune responses obtained with nanoparticle delivered pDECN and pVAXN formulations was improved when anti-CD40 antibody was co-administered as DC maturation stimuli.

This strategy can be applied as an alternate to antibody based DC-targeted vaccines, which require time-consuming optimization and protein production. Furthermore, the DC targeted fusion DNA based vaccines can be promptly engineered and produced on a large-scale, and thus can serve as valuable tools in case of possible SARS CoV or other pandemic and bioterrorism threats to

minimize the extent of damage. Nevertheless, for our experimental work we used high molecular weight chitosan as a carrier for intramuscular delivery of pDECN plasmid DNA. Recent studies have shown that the expression of plasmid DNA can be improved using oligomeric chitosan, which allows easy dissociation of DNA from polyplexes [17, 18]. Alternatively, it will be worth to analyze the performance of pDECN based DC-targeted DNA vaccine with that of widely used and potent DNA carriers such as polyethyleneimine [19]. Additionally, it will be worth comparing the two strategies of DC targeted DNA vaccines for reducing the dose of antigen, and altering the duration as well as the quality of antigen-specific immune responses using different routes of administration.

An efficient DC-targeted delivery system for model protein antigen, ovalbumin (OVA) was also explored (**chapter 5**). PLGA was selected as a carrier due to its widespread use and clinical utility. PLGA nanoparticles have been extensively used as vaccine delivery system for a number of protein antigens. However, only a few studies have attempted designing antibody-targeted PLGA NPs for selective delivery of antigens to DCs [20-23]. Nevertheless, DCs preferentially uptake PLGA NPs and the magnitude of immune responses can be improved by antibody functionalization of these NPs. These studies applied sophisticated chemistry to attach DC-receptor specific antibodies and process was carried out after antigen encapsulation (post-formulation) within NPs.

In our approach, DC-selective targeting of OVA-loaded biotinylated PLGA NPs was accomplished with the help of bfFp. To provide adequate biotin moieties on NP surface, which can serve as docking sites for bfFp, we employed biotin-PEG_(2,000)-PLGA conjugate for NP formulation. Moreover, the use of biotinylated PEG as a spacer allowed abundant exposure of biotin on NPs. In addition PEG can also help to stabilize NP and mitigate non-specific interactions.

In vitro DC uptake studies of bfFp targeted and non-targeted NPs demonstrate that bfFp based targeting indeed improved uptake by one-fold. Uptake of targeted NPs was reduced, when DCs were pre-incubated with soluble ligand (anti-DEC-205 mAb), further indicate that higher uptake of targeted NPs was mediated by

DEC-205 receptor-mediated endocytosis. Next we evaluated how bfFp functionalization of NPs alter the functions of DCs by analyzing expression of DC maturation markers (CD86 and CD40) and functional analysis by estimating in vitro cytokines (IL-12, IL-6 and IL-10). Our results these experiments indicate that bfFp functionalization do not alter expression levels of DC maturation markers (CD86 and CD40) compared to non-targeted NPs, unless anti-CD40 mAb was used as maturation stimuli. In vitro evaluation of DC cytokine profile revealed that IL-12 and IL-6 secretion was significantly higher, when DCs were stimulated with anti-CD40 mAb together with bfFp targeted NPs. In contrast, IL-10 secretion levels were found to be significantly higher when bfFp targeted NPs were used, indicating that cross-linking of DEC-205 receptor in absence of any maturation stimuli, provoked anti-inflammatory cytokine secretion consistent with a recent finding [23].

Finally, we evaluated the in vivo performance of non-targeted and targeted NP with or without anti-CD40 mAb and compared with model adjuvant Complete Freund's adjuvant (CFA). The outcome of our studies suggests that targeted NPs in conjunction with anti-CD40 mAb resulted in significantly enhanced OVA-specific IgG titer, compared to merely targeted or non-targeted NPs. While no difference in IgG titers was found between targeted and non-targeted NP formulations. To study the cellular immune response, we analyzed ex vivo cytokine secretion profile of splenocytes using OVA as recall antigen. Our results suggest that targeted NPs in conjunction with anti-CD40 mAb provoked Th1 biased cytokine secretion and significantly higher levels of IFN- γ and IL-2 were obtained. These results are consistent with in vitro cytokine profile and suggest that anti-CD40 mAb render secretion of pro-inflammatory cytokines (IL-12 and IL-6), which is turn skew immune response to Th1 phenotype.

The strategy of bfFp based DC targeted delivery of protein antigen explored here is straight forward and simple in design. It will be interesting to compare the PLGA NPs with soluble anti-DEC-205 antibody-antigen conjugates/fusion protein based DC targeted vaccines. Furthermore, based on the available literature the

antibody-antigen conjugates/fusion protein based vaccines have been shown to promptly localize in draining lymph nodes and resulting in targeting of lymph node resident DCs [24, 25]. Additionally, it can be speculated that soluble antibody-antigen conjugates/fusion protein might provoke prompt immune response as administered antigen is promptly available.

Alternatively, the bfFp targeted chitosan can also be employed as a substitute for PLGA NPs. Although, PLGA NPs are shown to be preferentially taken up by DCs and provide sustained antigen-release profile [26], the chitosan NPs can be of immense potential, in case of non-invasive DC targeted delivery of protein antigens due to their mucoadhesive nature and ability to open tight junctions that could facilitate antigen delivery to nasal-resident DCs[27].

6.2 Conclusions

In this study we report on the development of nanoparticle based DC targeted vaccine delivery systems for DNA and protein antigen:

1. We have successfully developed a DC-targeted chitosan nanoparticle formulation for delivery of DNA vaccines against SARS CoV and avian influenza (H5N1) virus. Our results suggest that DC-targeted delivery of DNA, through non-invasive intranasal route can be a feasible strategy for designing low-dose vaccine, which can provide mucosal as well as systemic immunity.
2. We have also developed a fusion DNA vaccine construct for in-situ DC targeted delivery encoded vaccine antigen. This approach can bypass the need to formulate active DC targeted vaccines, and can provide a viable alternative to conventional antibody based DC targeted vaccine.
3. Finally, we also developed a simple approach for DC-targeted delivery of model protein antigen using PLGA nanoparticles. Using this approach a ready-to-use two-component DC-targeted PLGA nanoparticle can be formulated without involving post-formulation step. The promising outcome of bfFp functionalized DC targeted PLGA nanoparticles support its use as a versatile vaccine delivery system for the design of monovalent or polyvalent vaccines.

6.3 Future directions

Several studies have shown that the chitosan based gene delivery systems serve as efficient carriers for DNA vaccines [28-30]. However, some recent studies have shown that efficacy of DNA delivery can be enhanced by using low-molecular weight oligomeric chitosan derivatives in place of high molecular weight derivatives [31, 32]. It has been demonstrated that the application of low-molecular weight oligomeric chitosan allows easy dissociation of DNA from complexes and results in higher transfection efficiency [33]. In addition to this, the physiological stability of chitosan nanoparticles was found to be improved by decorating these nanoparticles with low-molecular weight PEG derivatives [34]. Furthermore, based on published reports the functionalization of chitosan nanoparticles with low-molecular weight PEG was shown to impart mucus-penetrating properties and thus can provide a better mucosal delivery system [34, 35]. In contrast to these findings, a limitation of our studies is application of high molecular weight chitosan as a DNA delivery vehicle. Therefore, in this context it is imperative to evaluate bfFp based DC-targeted delivery of DNA vaccines using low-molecular weight oligomeric chitosan, and to analyze influence of PEG-functionalization on the performance of nanoparticle formulated using oligomeric chitosan derivatives.

As an alternative to chitosan, polyethylenimine (PEI) can also be used as DNA carrier, since it is known to serve as gold-standard polymer for gene delivery [36]. Furthermore, recent studies have demonstrated that PEI can improve nasal delivery of DNA vaccines and thus augment the magnitude of antigen-specific immune responses [13, 37]. Furthermore, given the enormous potential of PEI based DNA delivery systems, it would be worth analyzing whether, bfFp based DEC-205 targeted delivery of PEI encapsulated DNA vaccine can improve their potency and quality of immune responses. To our knowledge there is no documented literature, demonstrating comparative evaluation of chitosan and PEI for nasal DNA vaccine delivery warranting direct comparison of PEI and chitosan for DC-targeted delivery of DNA vaccines.

Based on the data presented here, it is evident that immune responses following DEC-205 targeted delivery of nanoparticle encapsulated antigens can be drastically improved in the presence of a DC maturation stimulus. Therefore, in our studies we used soluble anti-CD40 mAb as a DC maturation stimulus. The application of soluble anti-CD40 mAb along with DC targeted nanoparticles could be a limitation as after administration the soluble antibody can be mopped by cells other than DC. Cells like macrophages and B cells are shown to express CD40 receptor and can uptake soluble anti-CD40 mAb [38]. The possible scavenging of soluble anti-CD40 ligand might prevent adequate maturation of a particular DC, which has taken up targeted antigen. Therefore, to overcome this limitation and as a viable substitute to anti-CD40 mAb, toll-like receptor ligand(s) (TLR) can be co-encapsulated with antigens in nanoparticles. Several studies have demonstrated co-delivery or coadministration of TLR ligands and antigen in PLGA nanoparticles serves as an effective vaccine delivery approach for improving immune responses [39, 40]. Furthermore, bfFp based DC targeting of co-encapsulated antigen and adjuvant can also help in reducing the dose of antigen as well as adjuvant.

Based on the application of TLR ligands as DC maturation stimuli in anti-DEC-205 mAb-antigen conjugate and fusion protein based approach, a number of TLR ligands can be used. Specifically, TLR3 ligand such as poly I:C, TLR9 ligand bacterial CpG and TLR4 ligand such as monophosphoryl lipid A can be used as viable substitute for anti-CD40 mAb [24, 41, 42]. The choice of most suitable TLR ligand will depend on the expression pattern of DEC-205 receptor and TLR ligand on particular DC subset. Therefore, it will be particularly interesting to use TLR3 ligand poly I:C in place of anti-CD40 mAb, as both DEC-205 receptor and TLR3 has been co-expressed by mouse and human DC subsets [21, 43].

6.4 References

- [1] Ulmer JB, Valley U, Rappuoli R. Vaccine manufacturing: challenges and solutions. *Nat Biotech* 2006;24:1377-83.
- [2] Rappuoli R. Bridging the knowledge gaps in vaccine design. *Nat Biotech* 2007;25:1361-6.
- [3] Trumpfheller C, Longhi MP, Caskey M, Idoyaga J, Bozzacco L, Keler T, et al. Dendritic cell-targeted protein vaccines: a novel approach to induce T-cell immunity. *J Inter Med* 2012;271:183-92.
- [4] Joshi MD, Unger WJ, Storm G, van Kooyk Y, Mastrobattista E. Targeting tumor antigens to dendritic cells using particulate carriers. *J Control Release* 2012;161:25-37.
- [5] Tacke PJ, Figdor CG. Targeted antigen delivery and activation of dendritic cells in vivo: Steps towards cost effective vaccines. *Semin Immunol* 2011;23:12-20.
- [6] Tsuji T, Matsuzaki J, Kelly MP, Ramakrishna V, Vitale L, He L-Z, et al. Antibody-targeted NY-ESO-1 to mannose receptor or DEC-205 in vitro elicits dual human CD8+ and CD4+ T cell responses with broad antigen specificity. *J Immunol* 2011;186:1218-27.
- [7] Wang WW, Das D, Suresh MR. A versatile bifunctional dendritic cell targeting vaccine vector. *Mol Pharm* 2008;6:158-72.
- [8] Langlois RA, Legge KL. Respiratory dendritic cells: mediators of tolerance and immunity. *Immunol Res* 2007;39:128-45.
- [9] Blank F, Stumbles P, Von Garnier C. Opportunities and challenges of the pulmonary route for vaccination. *Expert Opin Drug Deliv* 2011;8:547-63.
- [10] Neutra MR, Kozlowski PA. Mucosal vaccines: the promise and the challenge. *Nat Rev Immunol* 2006;6:148-58.
- [11] Coban C, Koyama S, Takeshita F, Akira S, Ishii KJ. Molecular and cellular mechanisms of DNA vaccines. *Hum Vaccines* 2008;4:453-7.

- [12] Shirota H, Petrenko L, Hong C, Klinman DM. Potential of transfected muscle cells to contribute to DNA vaccine immunogenicity. *J Immunol* 2007;179:329-36.
- [13] Torrieri-Dramard L, Lambrecht B, Ferreira HL, Van Den Berg T, Klatzmann D, Bellier B. Intranasal DNA vaccination induces potent mucosal and systemic immune responses and cross-protective immunity against influenza viruses. *Mol Ther* 2011;19:602-11.
- [14] Patel A, Tran K, Gray M, Li Y, Ao Z, Yao X, et al. Evaluation of conserved and variable influenza antigens for immunization against different isolates of H5N1 viruses. *Vaccine* 2009;27:3083-9.
- [15] Rao S, Kong WP, Wei CJ, Yang ZY, Nason M, Styles D, et al. Multivalent HA DNA vaccination protects against highly pathogenic H5N1 avian influenza infection in chickens and mice. *PLoS ONE* 2008;3(6):e2432.
- [16] Lipatov AS, Hoffmann E, Salomon R, Yen HL, Webster RG. Cross-protectiveness and immunogenicity of influenza A/Duck/Singapore/3/ 97(H5) vaccines against infection with A/Vietnam/1203/04(H5N1) virus in ferrets. *J Infect Dis* 2006;194:1040-3.
- [17] Lavertu M, Méthot S, Tran-Khanh N, Buschmann MD. High efficiency gene transfer using chitosan/DNA nanoparticles with specific combinations of molecular weight and degree of deacetylation. *Biomaterials* 2006;27:4815-24.
- [18] Strand SP, Lelu S, Reitan NK, de Lange Davies C, Artursson P, Vårum KM. Molecular design of chitosan gene delivery systems with an optimized balance between polyplex stability and polyplex unpacking. *Biomaterials* 2010;31:975-87.
- [19] Akinc A, Thomas M, Klivanov AM, Langer R. Exploring polyethylenimine-mediated DNA transfection and the proton sponge hypothesis. *J Gene Med* 2005;7:657-63.
- [20] Cruz LJ, Tacke PJ, Fokkink R, Figdor CG. The influence of PEG chain length and targeting moiety on antibody-mediated delivery of nanoparticle vaccines to human dendritic cells. *Biomaterials* 2011;32:6791-803.

- [21] Tacke PJ, Zeelenberg IS, Cruz LJ, van Hout-Kuijter MA, van de Glind G, Fokkink RG, et al. Targeted delivery of TLR ligands to human and mouse dendritic cells strongly enhances adjuvanticity. *Blood* 2011;118:6836-44.
- [22] Cruz LJ, Tacke PJ, Fokkink R, Joosten B, Stuart MC, Albericio F, et al. Targeted PLGA nano- but not microparticles specifically deliver antigen to human dendritic cells via DC-SIGN in vitro. *J Control Release* 2010;144:118-26.
- [23] Bandyopadhyay A, Fine RL, Demento S, Bockenstedt LK, Fahmy TM. The impact of nanoparticle ligand density on dendritic-cell targeted vaccines. *Biomaterials* 2011;32:3094-105.
- [24] Johnson TS, Mahnke K, Storn V, Schönfeld K, Ring S, Nettelbeck DM, et al. Inhibition of melanoma growth by targeting of antigen to dendritic cells via an anti-DEC-205 single-chain fragment variable molecule. *Clin Cancer Res* 2008;14:8169-77.
- [25] Flacher V, Tripp CH, Haid B, Kissenpfennig A, Malissen B, Stoitzner P, et al. Skin langerin+ dendritic cells transport intradermally injected anti-DEC-205 antibodies but are not essential for subsequent cytotoxic CD8+ T cell responses. *J Immunol* 2012;188:2146-55.
- [26] Newman KD, Elamanchili P, Kwon GS, Samuel J. Uptake of poly(D,L-lactic-co-glycolic acid) microspheres by antigen-presenting cells in vivo. *J Biomed Mater Res* 2002;60:480-6.
- [27] Kang ML, Cho CS, Yoo HS. Application of chitosan microspheres for nasal delivery of vaccines. *Biotechnol Adv* 2009;27:857-65.
- [28] Khatri K, Goyal AK, Gupta PN, Mishra N, Vyas SP. Plasmid DNA loaded chitosan nanoparticles for nasal mucosal immunization against hepatitis B. *Int J Pharm* 2008;354:235-41.
- [29] Kumar M, Mohapatra SS, Behera AK, Lockey RF, Zhang J, Bhullar G, et al. Intranasal gene transfer by chitosan-DNA nanospheres protects BALB/c mice against acute respiratory syncytial virus infection. *Hum Gene Ther* 2002;13:1415-25.

- [30] Iqbal M, Lin W, Jabbal-Gill I, Davis SS, Steward MW, Illum L. Nasal delivery of chitosan-DNA plasmid expressing epitopes of respiratory syncytial virus (RSV) induces protective CTL responses in BALB/c mice. *Vaccine* 2003;21:1478-85.
- [31] Vila A, Sánchez A, Janes K, Behrens I, Kissel T, Jato JLV, et al. Low molecular weight chitosan nanoparticles as new carriers for nasal vaccine delivery in mice. *Eur J Pharm Biopharm* 2004;57:123-31.
- [32] Yang X, Yuan X, Cai D, Wang S, Zong L. Low molecular weight chitosan in DNA vaccine delivery via mucosa. *Int J Pharm* 2009;375:123-32.
- [33] Köping-Höggård M, Vårum KM, Issa M, Danielsen S, Christensen BE, Stokke BT, et al. Improved chitosan-mediated gene delivery based on easily dissociated chitosan polyplexes of highly defined chitosan oligomers. *Gene Ther* 2004;11:1441-52.
- [34] Casettari L, Vilasaliu D, Mantovani G, Howdle SM, Stolnik S, Illum L. Effect of PEGylation on the toxicity and permeability enhancement of chitosan. *Biomacromolecules* 2010;11:2854-65.
- [35] Wang YY, Lai SK, Suk JS, Pace A, Cone R, Hanes J. Addressing the PEG mucoadhesivity paradox to engineer nanoparticles that "slip" through the human mucus barrier. *Angew Chem Int Ed Engl* 2008;47:9726-9.
- [36] Hsu CYM, Uludağ H. Nucleic-acid based gene therapeutics: Delivery challenges and modular design of nonviral gene carriers and expression cassettes to overcome intracellular barriers for sustained targeted expression. *J Drug Target* 2012;20:301-28.
- [37] Shim BS, Park SM, Quan JS, Jere D, Chu H, Song MK, et al. Intranasal immunization with plasmid DNA encoding spike protein of SARS-coronavirus/polyethylenimine nanoparticles elicits antigen-specific humoral and cellular immune responses. *BMC Immunol* 2010;11:65.
- [38] van Kooten C, Banchereau J. CD40-CD40 ligand. *J Leukoc Biol* 2000;67:2-17.

- [39] Hamdy S, Molavi O, Ma Z, Haddadi A, Alshamsan A, Gobti Z, et al. Co-delivery of cancer-associated antigen and Toll-like receptor 4 ligand in PLGA nanoparticles induces potent CD8⁺ T cell-mediated anti-tumor immunity. *Vaccine* 2008;26:5046-57.
- [40] Kasturi SP, Skountzou I, Albrecht RA, Koutsonanos D, Hua T, Nakaya HI, et al. Programming the magnitude and persistence of antibody responses with innate immunity. *Nature* 2011;470:543-7.
- [41] Pantel A, Cheong C, Dandamudi D, Shrestha E, Mehandru S, Brane L, et al. A new synthetic TLR4 agonist, GLA, allows dendritic cells targeted with antigen to elicit Th1 T-cell immunity in vivo. *Eur J Immunol* 2012;42:101-9.
- [42] Idoyaga J, Lubkin A, Fiorese C, Lahoud MH, Caminschi I, Huang Y, et al. Comparable T helper 1 (Th1) and CD8 T-cell immunity by targeting HIV gag p24 to CD8 dendritic cells within antibodies to Langerin, DEC205, and Clec9A. *Proc Natl Acad Sci USA* 2011;108:2384-9.
- [43] Tel J, Benitez-Ribas D, Hoosemans S, Cambi A, Adema GJ, Figdor CG, et al. DEC-205 mediates antigen uptake and presentation by both resting and activated human plasmacytoid dendritic cells. *Eur J Immunol* 2011;41:1014-23.